The Characterisation of a Lactate Biosensor for Real-Time Neurochemical Monitoring of L-Lactate

A thesis submitted by

Keane McNamee B.Sc. (Hons.)

This report is submitted in fulfilment of the Requirements for the M.Sc. Degree in Chemistry

Maynooth University Department of Chemistry

Maynooth University

Date: October 2023

Supervisor: Prof John P. Lowry

Head of Department: Prof. Denise Rooney

Declaration

This thesis has not been submitted before, in whole or in part, to this or any other University for any degree, and except where otherwise stated, is the original work of the author.

Signed: 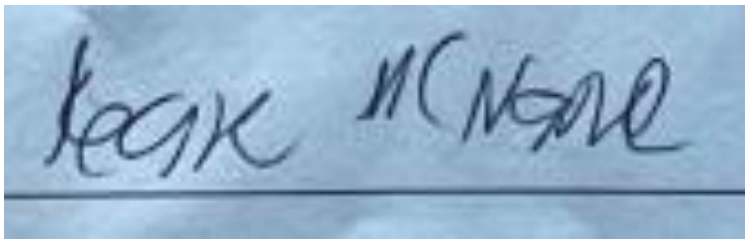

Keane McNamee

Acknowledgements

I'd like to thank my supervisor Prof. John Lowry for the opportunity to carry out such interesting and unique research and for all your support over the last 2 years . I'd also like to thank Michelle Doran and Michelle Sands for all their help and support too.

The other postgraduates in the group, Caitlin, and Chloe, thank you for all the laughs and for listening to my constant moaning. Alongside everyone else in the department who are all lovely and made working in the department a joy.

Finally, a massive thanks to my Mam and Dad without who's support I'd have not been able to make it this far never mind finish, and Milo for keeping me sane with all the walks.

Abstract

The aim of this project was to characterise a first-generation polymer enzyme composite (PEC) biosensor utilising lactate oxidase for the real-time neurochemical monitoring of lactate. Lactate, which was originally thought to be nothing but a mere waste product of anaerobic respiration, has gained recognition as a cell signalling molecule and playing a significant role in long term potentiation. It has been postulated that lactate may act as a primary energy substrate following glutamatergic transmission and this idea is foundation of the astrocyte lactate neuron shuttle hypothesis (ALNSH) which was proposed by Pellerin and Magistretti in 1994. This theory states that following glutamatergic transmission lactate is exported from astrocytes to neurons where it is used for oxidative phosphorylation. Lactate has also shown promise as a biomarker for sleep and lactate dysregulation in the brain has been shown to be a feature of schizophrenia and autism spectrum disorder. Electrochemical PEC biosensors used for the monitoring of other neuro metabolites such as glucose and pyruvate have been previously developed and characterised by members of the Lowry research group. A PEC lactate biosensor has also been previously developed, so the core components (cross-linking/stabilising agents and enzyme), layering strategies and drying times have been optimised to provide a sensitive sensor that now required to be characterised *in vitro* and *in vivo.* Tests included verifying the sensors signal over the range of temperatures and pHs it would encounter. As the brain is a harsh environment with low [O_2] compared to benchtop conditions, oxygen dependence tests were performed to ensure the signal given on benchtop conditions was representative of what will be seen at vivo oxygen concentrations. Biocompatibility tests were performed to ensure minimal signal loss from electrode poisons, surface modifying agents and surfactants. Finally, interference testing was done to ensure minimal signal contribution from electroactive reducing agents, electrocatalysts, and endogenous electroactive interferents e.g. ascorbic acid. In summary, it showed appropriate sensitivity (0.242 ± 0.014 nA/μM) and excellent stability/biocompatibility with no significant decrease in sensitivity following ex-vivo storage in rodent brain tissue (14 days) or 28 days in dry storage. Interference from endogenous electroactive interferents was minimal with extracellular concentrations typically being ~3% of the 350 μM L-lactate response. Changes in molecular oxygen (the natural enzyme mediator) over the normal range found in brain tissue (40-80 μM) had minimal effect on the L-lactate signal for concentrations of 350 and 500 μM (K_MO_2 of 39.4 ± 17.5 μM and 40.4 ± 16.1 μM respectively). Alongside this a low μM limited of detection (0.153 ±

0.098), was calculated with a slower than expected response time of *ca.* 18 seconds, combined with no effect of pH and temperature changes over physiologically relevant ranges (7.2-7,6 and 34-40 °C respectively), collectively suggest this composite biosensor has the ability to reliably monitor L-lactate in the brain. The sensor was then implanted into the striatum of freely moving rats where it demonstrated stable recording over several weeks and reliable detection of physiological changes in L-lactate. The sensors' ability to provide a reliable signal with changes in [O_2] was proven, following this changes in L-lactate were monitored in response to neuronal activation (tail-pinch). Future work will focus on pharmacological interventions and the effect these have on extracellular fluid levels of lactate, which will hopefully aide in our understanding of how these interventions affect brain metabolism.

Abbreviations

- 3,4-Dihydroxyphenylacetic acid (DOPAC)
- 5-Hydroxyindoleacetic Acid (5-HIAA)
- 5-Hydroxytrypramine (5-HT) [Serotonin]
- Alzheimer's Disease (AD)
- Ascorbic Acid (AA)
- Astrocyte-Lactate-Neuron Shuttle Hypothesis (ALNSH)
- Blood Brain Barrier (BBB)
- Bovine Serum Albumin (BSA)
- Bovine Serum Albumin: Glutaraldehyde(BSA:GA)
- Carbon Paste Electrode (CPE)
- Cellulose Acetate (CA)
- Constant Potential Amperometry (CPA)
- Cyclic Voltammetry (CV)
- Dehydroascorbic Acid (DHAA)
- Dialdehyde Starch (DAS)
- Differential Pulse Amperometry (DPA)
- Excitatory Amino Acid Transporters (EAATs)
- Extracellular Fluid (ECF)
- Flavin mononucleotide (FMN)
- functional Magnetic Resonance Imaging (fMRI)
- Glucose transporter (GLUT)
- Glutaraldehyde (GA)
- Homovanallic acid (HVA)
- Intraperitoneal injection (i.p.)
- *In Vivo* Voltammetry (IVV)
- Iridium (Ir)
- Lactate Dehydrogenase (LDH)
- Lactate Oxidase (LOx)
- Limit Of Detection (LOD)

- Linear Region Slope (rLRS)
- Maximum Velocity (V_{MAX})
- Micheale's Menten Constant (K_M)
- Microdialysis (MD)
- Monocarboxylate Transporter (MCT)
- Nuclear Resonance Imaging (NMR)
- Ortho-phenylenediamine(*o*PD)
- Phosphate Buffered Saline (PBS)
- Platinum (Pt)
- Polyethylenimine (PEI)
- Phenylenediamine (PPD)
- Polymer Enzyme Composite (PEC)
- Poly-*ortho*-phenylenediamine (P*o*PD)
- Position Emission Topography (PET)
- Response Time (RT)
- Saturated Calomel Electrode (SEC)
- Standard Error of the Mean (SEM)
- Styrene (Sty)
- Traumatic Bain Injury (TBI)
- Tricarboxylic Acid Cycle (TCA)

Contents

Chapter 1 – Introduction

Chapter 1 – Introduction

This chapter outlines why lactate is of interest for real-time neurochemical monitoring and how this is achieved using a polymer-enzyme composite (PEC) L-lactate biosensor which, will be referred to as biosensor throughout. As the enzyme lactate oxidase (LOx) is selective for L-lactate, and D-lactate is not found in the ECF of the mammalian brain, L-lactate and lactate are used interchangeably throughout.

1.1 Introduction

The focus of this work was to characterise a biosensor that can reliably monitor lactate in the mammalian brain. The sensor had been previously developed by a member of the Lowry research group[1] building on expertise regarding the core components (cross-linking/stabilising agents), drying times and layering strategies, which have been gained through the development of PEC biosensor for other neurochemicals[1-5]. The sensor was characterised *in-vitro* to ensure signal integrity across various physiological conditions that may be experienced in the brain. This was followed by *in–vivo* studies designed to test signal integrity. It is hoped that in the future the sensor will be used for the chronic real-time neurochemical monitoring of lactate and will potentially illuminate lactate's role in brain metabolism.

The brain is a complex organ comprised of a wide array of cell types each with their own unique role in the variety of essential functions performed by the brain, such as: memory formation, sleep, mood, regulating heart rate and muscle contraction[6]. With the brain having high metabolic demands being ~2 % by mass of the body mass in an adult human while, accounting for 25 % of the energy consumption during rest[7]. All functions in the brain are controlled by neurochemicals, the most studied of which are neurotransmitters and energy metabolites, due to their clinical relevance with disruption to brain energy metabolism leading to altered cell function, neuroplasticity, and brain circuits in schizophrenia[8-12]. The most well-known and studied neurotransmitter is dopamine due to its role in mood disorders[13] and in Alzheimer's and Parkinson's disease[14].

Over the past 80 years there has been significant research aimed at improving our understanding of the role(s) these neurochemicals play in brain function and metabolism using analytical techniques. Beginning in the 50's with the detection of serotonin using fluorometric methods[15]. Since then, a wide array of techniques have been developed for neurochemical monitoring from non-invasive methods including functional magnetic resonance imaging (fMRI)[16], position emission topography[17] and spectroscopic methods such as NMR[18] to invasive techniques such as optical biosensors[19], microdialysis[20] and *in-vivo* voltammetry[21,22]. The wide array of techniques used to monitor neurochemicals from different areas highlights the complexity of accomplishing such a task in the brain.

The biggest challenge posed when trying to understand brain function is the brains signalling and controlling strategies. These processes are both electrical and chemical in nature, so both chemical and electrical changes in the extracellular fluid (ECF) influence the brains behaviour. The brain ECF is also a complex and hostile environment consisting of neurotransmitters, metabolites, ions, electroactive substances, and electrode poisons (proteins).

The brain consists of two main types of cells: neurons and glial cells. Neurons are the cells responsible for receiving and sending messages through the use of neurotransmitters; there are ~100 billion neurons in the mature human brian[23]. These neurons are enveloped by glial cells which provide electrical insulation via the production of myelin sheats[24] and metabolic support for neurons[25]. The activation of a neuron involves the presence of a stimulus which causes an electrical response primarily due to changes in Na^+ and Cl^- ions. This is known as an action potential, which passes along the axon to the nerve endings which release neurotransmitter(s) upon electrical stimulation. These neurotransmitters are released into the synaptic cleft where they travel to adjacent nerve cells via diffusion where they can excite or inhibit these neurons causing a response. This is the cellular basis by which every process in the brain is carried out and is the reason why neurotransmitters are of immense importance in the field of neuroscience.

1.2. Neurochemical analysis

As neurochemicals play such a significant role in the regulation of the brain a lot of work has been done in order to understand their role in physiological functions. As mentioned in Section 1.1 the analysis of neurochemicals dates back to the 1950's with the detection of serotonin using fluorometric methods[15]. The first Clarke electrode being developed in the same decade for the detection of O_2[26], this laid the foundation for the first biosensor for the detection of glucose developed by Clarke and Lyons in 1962[27]. With the first biosensor for neurochemical monitoring being developed by Clarke and Lyons in 1965[28]. A wide variety of electrochemical techniques have been employed for neurochemical analysis since Clarke and his electrode, e.g., constant potential amperometry (CPA)[29,30], cyclic voltammetry (CV)[31] and differential pulse voltammetry[32]. The advantages of electrochemical methods for neurochemical monitoring are their low cost, low detection limits[2,33] and excellent spaciotemporal resolution[34]. While the disadvantages are loss of sensitivity due to enzyme degradation, electrode fouling and interference due to endogenous species in the brain. To overcome this polymer layers have been added to electrodes, e.g. poly-*ortho*-phenylenediamine (P*o*PD)[35,36], polypyrrole[37] and poly(ester-sulfonic acid)[38]. Finally, the sensors must be small enough to ensure minimal tissue damage[39].

While the development of biosensors for neurochemical monitoring was occurring a new method for sampling *in-vivo* extracellular fluid was developed in 1960s by Bito *et al*[40]. This was microdialysis (MD) and is an *ex-situ* technique where a dialysis catheter is inserted into the tissue of interest, and a solution is constantly perfused causing molecules to diffuse along their concentration gradient through the semi-permeable membrane of the catheter. The collected perfusate can then be analysed *ex-vivo* using a variety of techniques including ultra high-performance liquid chromatography[41], mass-spectrometry[42] and enzyme assays[43]. MD offers the benefits of high sensitivity and selectivity as the sample is analysed by well-established methods such as those mentioned previously however, this comes at the cost of low temporal resolution[44]. The semipermeable membranes used have a large surface area (typical length of 1-4 mm and a diameter of 400 μm) limiting the spatial resolution of MD[45]. Some neurochemicals e.g., monoamines degrade rapidly at room temperature following collection limiting the recovery rate

of MD[46]. There have been recent advances in recent years to improve the poor temporospatial resolution of these systems with the development of push-pull sampling methods[47,48].

Optical methods, i.e., those that are based on the samples reaction to electromagnetic radiation, are another powerful tool that have been used for neurochemical monitoring, with the use of near infra-red spectroscopy to detect brain oxygenation first reported in 1977[49]. Then in the 1980's optical fibre-based sensors started to be used for *in-vivo* monitoring NADH redox states in awake rodents[50]. A new and particularly interesting class of optical sensor are genetically encoded sensors; these are devices that rely on genetically encoded proteins to evaluate physiological events. Genetically encoded sensors have been developed for the monitoring of simultaneous dopamine and Ca^{2+} release *in-vivo*[51] and norepinephrine[52]. Like electrochemical sensors, optical devices have excellent spatiotemporal resolution, with the bonus of being minimally or non-invasive techniques. However, they suffer from only being able to monitor where the light can penetrate the tissue, instability, and often require complex analysis methods.

1.3. Lactate

Lactate is a three-carbon organic acid (Figure.1.1.). Lactate's role in human physiology has been complex and controversial with lactate originally thought to be nothing but a waste product of anaerobic respiration[53]. However, in recent years its role has been revealed to be more complex and controversial as highlighted in several recent publications[54,55]. Lactate may have a role in cancer biology, as in some cases lactate is the primary product of glycolysis in cancer cell lines, a phenomenon called the Warburg effect[56]. It also has a role in muscle energy metabolism[57]. Finally, lactate is also reported to play a role in many complex neurological processes such as memory formation[58], synaptic plasticity[59] and as a potential treatment for traumatic brain injury[60]**.** Lactate's intricate role in the brain is only further highlighted by is potential involvement in the Astrocyte Lactate Neuron Shuttle Hypothesis (ALNSH) as proposed by Magistretti and Pellerin[61], which states that neurons use lactate as a fuel in an activity dependent manner which is mediated by glutamate.

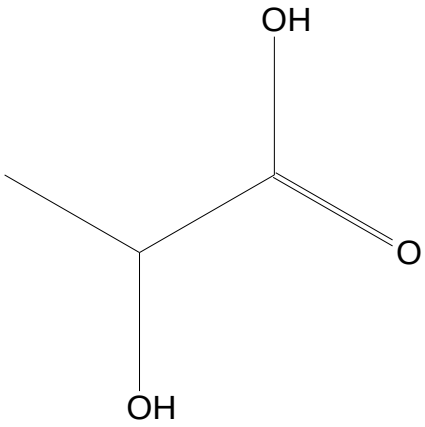

Figure 1.1. Structure of Lactate.

1.3.1. The astrocyte lactate neuron shuttle hypothesis.

The ALNSH has been controversial since its conception[62] as it questions the source of fuel for neurons during periods of synaptic activation. This fuel was originally thought to be solely glucose[63], until the proposal of the ALNSH by Pellerin and Magistertti[61] , based on the observation that lactate is released by astrocytes in an activity dependent manner and taken up by neurons following glutamate uptake by the astrocytes as shown in Figure.1.2. There has been indirect evidence for this theory based on the distribution of Lactate Dehydrogenase (LDH) isoforms, an enzyme responsible for the interconversion of lactate to pyruvate. LDH_5 is mostly found on astrocytes and LDH_1 is more common on neurons. LDH_5 is an isoform that has a high affinity for pyruvate therefore favouring the conversion of pyruvate to lactate. While LHD_1 has a high affinity for lactate[64], which results in the enzyme causing an accumulation of pyruvate. This provides support to the idea that lactate is exported from astrocytes to neurons where it is converted to pyruvate. With pyruvate being able to be used as a metabolic fuel by being metabolised via the tricarboxylic acid cycle (TCA). The distribution of Monocarboxylate Transporters (MCT), which are a family of proton-linked plasma membrane transporters that carry molecules with one carboxylate group across biological membranes[65], has also provided support for the ALNSH[66]. MCT1 is localised mainly in astrocytes in the adult brain, while MCT2 is regularly found on neurons. This distribution of MCTs provides *in-vivo* support for the ALNSH as MCT2 is thought to be the MCT with a higher affinity for lactate and pyruvate suggesting that the expression of this MCT is mainly on tissue that will use monocarboxylates for metabolic fuel[67]. The fact that there have been cell cultures where neurons have been able to survive on lactate alone also suggests that lactate is a sufficient fuel for neurons[68]. There have also been experiments showing that inhibiting

glutamate uptake, which causes glutamate accumulation, results in increased lactate which provides more support for the ALNSH[69].

However, there has also been evidence suggesting that the ALNSH does not exist, such as the idea that the increase in lactate associated with neuronal activation may just be neurons releasing lactate following its metabolism from glucose. Additionally, arguments against the ALNSH have been made based on the abundance of glucose transporters in the brain, and the even distribution of glucose between intra and extracellular compartments[70]. There is also evidence that both astrocytes and neurons release lactate[71], but astrocytes produce more lactate which would agree with findings that neurons have a higher rate of glucose oxidation than astrocytes[71]. As such, the role of lactate in brain energy metabolism remains quite controversial. However, despite the lack of consensus, it is becoming increasingly accepted that synaptic activity is at least partly fueled by the transfer of metabolites from astrocytes to neurons, and that L-lactate, traditionally assumed to be a waste product of energy metabolism, is likely to be one of these metabolites with a particularly important role in maintaining neuronal viability. In order to understand the role of disrupted metabolism in diseases such as AD (*see* below), we need to know the unique inter-relationship of the different metabolites in the brain. Also, supporting proof for the ANLS has predominantly come from *in vitro* preparations, e.g., cell cultures and brain slices. Thus, the application of the lactate biosensor characterised in this work, in chronic *in vivo* studies, may make a significant contribution to our understanding of lactate and its role(s) in the brain.

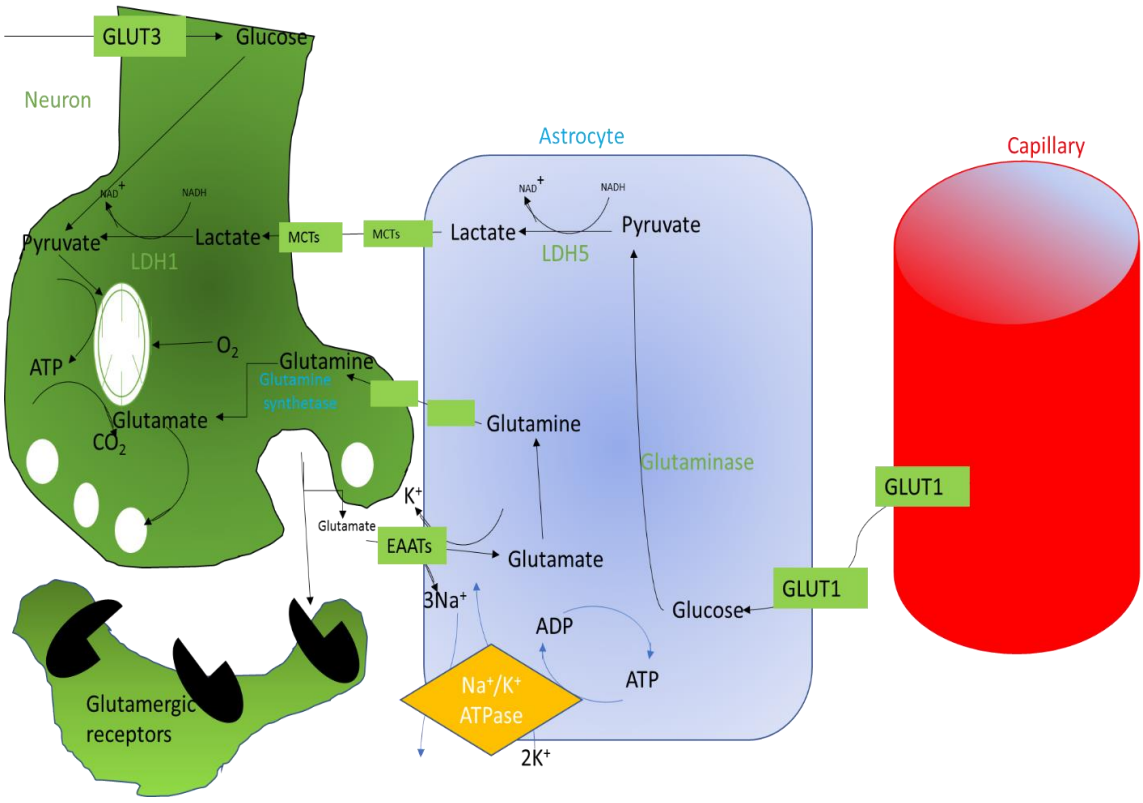

Figure 1.2. Schematic representation of the ALNSH. Glucose transporter (GLUT), Monocarboxylate transporter (MCT), Lactate dehydrogenase (LDH), Excitatory Amino Acid Transporters (EAATs). Glucose is converted into lactate in the astrocyte where following glutamatergic activation it is transported from the astrocyte to the neuron where it is converted to pyruvate and enters the TCA cycle providing ATP for neurons.

1.3.2. Lactate and its potential roles in neurological and psychiatric disorders

The brain is an organ with incredibly high energetic demands, taking up only 2 % of our overall weight but using approximately 20 % of all calories consumed[72]. Given these incredibly high energetic demands, and the potential of lactate having a role as an energy metabolite, it makes an ideal molecule to investigate as being a potential biomarker for neurological and psychiatric disorders, for example, metabolic dysfunction has been shown to be a key contributor to the pathology of Alzheimer's Disease (AD) with impaired mitochondrial function and glycolytic pathways being implicated[73]. Several groups have reported increased levels of lactate in patients

with AD[74,75]. These associated changes in lactate concentration in the brains of AD have been linked with the altered mitochondrial dysfunction and there may be a relationship between the severity of the disease and the levels of lactate. Lactate has also been implicated in the pathology of schizophrenia where its presence has also been related to mitochondrial dysfunction[76]. However, schizophrenia also has decreased brain pH as part of its pathology[77] and lactate is thought to be one of the molecules that contributes to this decrease. Furthermore, the accumulation of lactate has been shown to alter neuronal activity[78]. Thus, a better understanding of the involvement of lactate in neurological disorders will potentially aide how we not only diagnose but treat these disorders.

1.4. Monitoring lactate

Due to the controversial and complex range of functions lactate has been implicated in in the past several years, monitoring lactate in the brain has been of interest. The principal method of monitoring lactate has been microdialysis (MD), with MD being used to monitor basal levels of lactate in the striatum of freely-moving rats[79]. There have also been many reports of MD being used to probe the effects of stress on the ECF concentration of lactate. With stressors such as handling[80], tail pinch[81] and immobilisation[82] being probed for their effects on lactate levels. As through the ALNSH there is thought to be a relationship between lactate and glutamate this has been investigated using MD[83,84]. Uehara *et al.* investigated the effects of diazepam on the effects of lactate[85], the effects of volatile anaesthetics on ECF lactate concentrations have been investigated by Klien *et al*.[86] and the levels of lactate following TBI have been probed[87].

There have been several reports of lactate biosensors developed for neurochemical monitoring. Wilson *et al.* developed a lactate biosensor[88] by replacing glucose oxidase from a previously developed sensor[89] resulting in a lactate biosensor which was implanted into the dentate gyrus of an anesthetized rat, where changes in lactate following electrical stimulation were monitored. There have been lactate biosensors fabricated based on Prussian blue modified carbon fibre electrodes[35] . A ceramic-based multisite array microelectrode has been developed for the detection of lactate has been reported by Gerhardt *et al.*[90]. Carbon fibre electrodes have been modified with LOx and used differential normal pulse voltammetry by Cespugilo *et al.*[91] and have been used to investigate lactate and its relationship with sleep-wake states[92]. Amperometric lactate biosensor

have been coupled with electroencephalogram electrodes by Petillo *et al.*[93] to investigate the potential of using lactate as a biomarker for sleep. Platinized carbon fibre microelectrodes have been developed by Barbosa *et al.*[94] where lactate and glucose biosensors were coupled to investigate neurometabolism. Lactate biosensors have been coupled with microdialysis allowing the drawbacks of microdialysis regarding temporal resolution to be overcome, and enabling lactates role in TBI to be probed[95]. However, chronic long-term lactate minoring in a freely-moving animal has yet to be achieved, the goal of this work is to characterise a lactate biosensor for this type of recording.

1.5. Summary

The human brain is a complex organ highlighted by the variety of techniques that have been developed to elucidate some of the electrical and chemical process that control our behaviour. An understanding of these process is not only of a medical importance but economic importance with the cost of poor mental health being estimated to reach $6 trillion come 2030[96]. This is evident by the variety of fields of study associated with the brain such as psychology (the study of mind and behaviour), neurophysiology (the study of healthy brain activity), neurology (a medical approach to studying the brain, its disorders, and their pathology) and finally psychiatry (the medical approach to study mental illness). The use of microelectrode systems and biosensors is advantageous for *in-vivo* neurochemical monitoring due to their small size providing minimal tissue damage, and high spaciotemporal resolution allowing real-time analyte concentrations to be related to behaviours.

This thesis describes the characterisation of an electrochemical sensor for the real time neurochemical monitoring of lactate based on a polymer-enzyme composite design. This chapter (Chapter 1) has introduced the area of neurochemical monitoring and explained why monitoring lactate is of interest. Chapter 2 presents a more in-depth and thorough discussion of the theory relevant to the work presented in the thesis. Chapter 3 contains details of the experimental methodologies employed during the characterisation of the lactate biosensor. Chapter 4 describes the *in-vitro* characterisation of the lactate biosensor testing signal integrity for implantation into

the brain. Chapter 5 describes the characterisation of the lactate biosensor *in-vivo*. Finally, Chapter 6 is an overall conclusion to this body of work.

1.6. References

(1) Bolger, F. B. The in-vitro and in-vivo characterisation and application of real-time sensor and biosensor for neurochemical studies of brain metabolism PhD, Maynooth University, Maynooth **2007**.

(2) Bermingham, K. P.; Doran, M. M.; Bolger, F. B.; Lowry, J. P. Design optimisation and characterisation of an amperometric glutamate oxidase-based composite biosensor for neurotransmitter l-glutamic acid. Analytica Chimica Acta **2022**, 1224, 340205.

(3) Doran, M. M.; Finnerty, N. J.; Lowry, J. P. In–Vitro Development and Characterisation of a Superoxide Dismutase-Based Biosensor. Chemistry Select **2017**, 2 (14), 4157-4164.

(4) O'Riordan, S. L.; Lowry, J. P. In vivo characterisation of a catalase-based biosensor for real-time electrochemical monitoring of brain hydrogen peroxide in freely-moving animals. Analytical Methods **2017**, 9 (8), 1253-1264.

(5) Baker, K. L.; Bolger, F. B.; Lowry, J. P. Development of a microelectrochemical biosensor for the real-time detection of choline. Sensors and Actuators B: Chemical **2017**, 243, 412-420.

(6) Raiteri, L.; Raiteri, M.; Bonanno, G. Coexistence and function of different neurotransmitter transporters in the plasma membrane of CNS neurons. Progress in Neurobiology **2002**, 68 (4), 287-309.

(7) Siesjö, B. K. Brain Energy Metabolism; Weily, **1978**.

(8) Fišar, Z. Biological hypotheses, risk factors, and biomarkers of schizophrenia. Progress in Neuro-Psychopharmacology and Biological Psychiatry **2023**, 120.

(9) Ni, P.; Ma, Y.; Chung, S. Mitochondrial dysfunction in psychiatric disorders. Schizophrenia Research **2022**.

(10) Duarte, J. M. N.; Xin, L. Magnetic Resonance Spectroscopy in Schizophrenia: Evidence for Glutamatergic Dysfunction and Impaired Energy Metabolism. Neurochemical Research **2019**, 44 (1), 102-116.

(11) Sullivan, C. R.; O'Donovan, S. M.; Mc Cullumsmith, R. E.; Ramsey, A. Defects in Bioenergetic Coupling in Schizophrenia. Biological Psychiatry **2018**, 83 (9), 739-750.

(12) Fizíková, I.; Dragašek, J.; Račay, P. Mitochondrial Dysfunction, Altered Mitochondrial Oxygen, and Energy Metabolism Associated with the Pathogenesis of Schizophrenia. International Journal of Molecular Sciences **2023**, 24 (9), 7991.

(13) Radwan, B.; Liu, H.; Chaudhury, D. The role of dopamine in mood disorders and the associated changes in circadian rhythms and sleep-wake cycle. Brain Research **2019**, 1713, 42-51.

((14) Venton, J,; Wrightman,; R.M. Psychoanalytical Electrochemistry: Dopamine and Behavior. Analytical Chemistry **2003**, 75 (19), 414 A-421 A.

(15) Bogdanski, D. F.; Pletscher, A.; Brodie, B. B.; Undefined, S. Identification and assay of serotonin in brain. Journal of Pharmacology and Experimental Therapeutics **1956**, 117 (1), 82-88.

(16) Wei, H.; Frey, A. M.; Jasanoff, A. Molecular fMRI of neurochemical signalling. Journal of Neuroscience Methods **2021**, 364, 109372.

(17) Placzek, M. S.; Zhao, W.; Wey, H.-Y.; Morin, T. M.; Hooker, J. M. PET Neurochemical Imaging Modes. Seminars in Nuclear Medicine **2016**.

(18) Bachelard, H.; Badar-Goffer, R. NMR Spectroscopy in Neurochemistry. Journal of Neurochemistry **1993**, 61 (2), 412-419.

(19) Dey, S.; Dolci, M.; Zijlstra, P. Single-Molecule Optical Biosensing: Recent Advances and Future Challenges. American Chemical Society Physical Chemistry Australia **2023**, 3 (2), 143-156.

(20) Petit-Pierre, G.; Colin, P.; Laurer, E.; Déglon, J.; Bertsch, A.; Thomas, A.; Schneider, B. L.; Renaud, P. In vivo neurochemical measurements in cerebral tissues using a droplet-based monitoring system. Nature Communications **2017**, 8 (1), 1239.

(21) Stamford, J. A. - In Vivo Voltammetry. In Methods in Neurosciences, Conn, P. M. Ed.; Vol. 4; Academic Press, **1991**; pp 127-142.

(22) Brown, F. O.; Finnerty, N. J.; Bolger, F. B.; Millar, J.; Lowry, J. P. Calibration of NO sensors for in-vivo voltammetry: laboratory synthesis of NO and the use of UV-visible spectroscopy for determining stock concentrations. Analytical and Bioanalytical Chemistry **2005**, 381 (4), 964-971.

(23) Pakkenberg, B.; Gundersen, H. J. Neocortical neuron number in humans: effect of sex and age. Journal Comparative Neurology **1997**, 384 (2), 312-320.

(24) Traiffort, E.; Kassoussi, A.; Zahaf, A.; Laouarem, Y. Astrocytes and Microglia as Major Players of Myelin Production in Normal and Pathological Conditions. Frontiers in Cellular Neuroscience **2020**, 14, Review.

(25) Jha, M. K.; Morrison, B. M. Glia-neuron energy metabolism in health and diseases: New insights into the role of nervous system metabolic transporters. Experimental Neurology **2018**, 309, 23-31.

(26) Leland C. Clark, J.; Wolf, R.; Granger, D.; Taylor, Z. Continuous Recording of Blood Oxygen Tensions by Polarography. Journal of Applied Physiology **1953**, 6 (3), 189-193.

(27) Clark Jr., L. C.; Lyons, C. Electrode systems for continuous monitoring in cardiovascular surgery. Annals of the New York Academy of Sciences **1962**, 102 (1), 29-45.

(28) Clark, L. C., Jr.; Lyons, C. Studies of a glassy carbon electrode for brain polarography with observations on the effect of carbonic anhydrase inhibition. The Alabama Journal Medical Sciences **1965**, 2 (4), 353-359.

(29) Lowry, J. P.; Fillenz, M. Real-time monitoring of brain energy metabolism in vivo using microelectrochemical sensors: the effects of anesthesia. Bioelectrochemistry **2001**, 54 (1), 39-47.

(30) Baker, K. L.; Bolger, F. B.; Doran, M. M.; Lowry, J. P. Characterisation of a Platinum-based Electrochemical Biosensor for Real-time Neurochemical Analysis of Choline. Electroanalysis **2019**, 31 (1), 129-136.

(31) Rafi, H.; Zestos, A. G. Multiplexing neurochemical detection with carbon fiber multielectrode arrays using fast-scan cyclic voltammetry. Analytical and Bioanalytical Chemistry **2021**, 413 (27), 6715-6726.

(32) Luo, Y.; Zhang, L.; Liu, W.; Yu, Y.; Tian, Y. A Single Biosensor for Evaluating the Levels of Copper Ion and L-Cysteine in a Live Rat Brain with Alzheimer's Disease. Angewandte Chemie International Edition English **2015**, 54 (47), 14053-14056.

(33) Hanrahan, G.; Patil, D. G.; Wang, J. Electrochemical sensors for environmental monitoring: design, development and applications. Journal of Environmental Monitoring **2004**, 6 (8), 657-664.

(34) Venton, B. J.; Cao, Q. Fundamentals of fast-scan cyclic voltammetry for dopamine detection. Analyst **2020**, 145 (4), 1158-1168.

(35) Salazar, P.; Martin, M.; O'Neill, R. D.; Roche, R.; Gonzalez-Mora, J. L. Biosensors Based On Prussian Blue Modified Carbon Fibers Electrodes for Monitoring Lactate in The Extracellular Space of Brain Tissue. International Journal of Electrochemical Science **2012**, 7 (7), 5910-5926.

(36) Lowry, J. P.; O'Neill, R. D. Partial characterization in vitro of glucose oxidase-modified poly(phenylenediamine)-coated electrodes for neurochemical analysis in vivo. Electroanalysis **1994**, 6 (5-6), 369-379.

(37) Tolosa, V. M.; Wassum, K. M.; Maidment, N. T.; Monbouquette, H. G. Electrochemically deposited iridium oxide reference electrode integrated with an electroenzymatic glutamate sensor on a multi-electrode array microprobe. Biosensors and Bioelectronics **2013**, 42, 256-260.

(38) Lielpetere, A.; Jayakumar, K.; Leech, D.; Schuhmann, W. Cross-Linkable Polymer-Based Multi-layers for Protecting Electrochemical Glucose Biosensors against Uric Acid, Ascorbic Acid, and Biofouling Interferences. American Chemical Sciences Sensors **2023**, 8 (4), 1756-1765.

(39) Adams, R. N. Probing brain chemistry with electroanalytical techniques. Analytical Chemistry **1976**, 48.

(40) Bito, L.; Davson, H.; Levin, E.; Murray, M.; Snider, N. The concentrations of free amino acids and other electrolytes in cerebrospinal fluid, in vivo dialysate of brain, and blood plasma of the dog. Journal of Neurochemistry **1966**, 13 (11), 1057-1067.

(41) González, R. R.; Fernández, R. F.; Vidal, J. L.; Frenich, A. G.; Pérez, M. L. Development and validation of an ultra-high performance liquid chromatography-tandem mass-spectrometry (UHPLC-MS/MS) method for the simultaneous determination of neurotransmitters in rat brain samples. Journal of Neuroscience Methods **2011**, 198 (2), 187-194.

(42) Song, P.; Hershey, N. D.; Mabrouk, O. S.; Slaney, T. R.; Kennedy, R. T. Mass spectrometry "sensor" for in vivo acetylcholine monitoring. Analytical Chemistry **2012**, 84 (11), 4659-4664.

(43) Slaney, T. R.; Nie, J.; Hershey, N. D.; Thwar, P. K.; Linderman, J.; Burns, M. A.; Kennedy, R. T. Push-pull perfusion sampling with segmented flow for high temporal and spatial resolution in vivo chemical monitoring. Analytical Chemistry **2011**, 83 (13), 5207-5213.

(44) Su, C. K.; Sun, Y. C.; Tzeng, S. F.; Yang, C. S.; Wang, C. Y.; Yang, M. H. In vivo monitoring of the transfer kinetics of trace elements in animal brains with hyphenated inductively coupled plasma mass spectrometry techniques. Mass Spectrometry Reviews **2010**, 29 (3), 392-424.

(45) Su, C.-K.; Sun, Y.-C.; Tzeng, S.-F.; Yang, C.-S.; Wang, C.-Y.; Yang, M.-H. In vivo monitoring of the transfer kinetics of trace elements in animal brains with hyphenated inductively coupled plasma mass spectrometry techniques. Mass Spectrometry Reviews **2010**, 29 (3), 392-424.

(46) Chefer, V. I.; Thompson, A. C.; Zapata, A.; Shippenberg, T. S. Overview of brain microdialysis. Current Protocols in Neuroscience **2009**, Chapter 7, Unit7.1.

(47) Wotjak, C. T.; Landgraf, R.; Engelmann, M. Listening to neuropeptides by microdialysis: Echoes and new sounds? Pharmacology Biochemistry and Behaviour **2008**, 90 (2), 125-134.

(48) Das, C.; Wang, G.; Sun, Q.; Ledden, B. Multiplexed and fully automated detection of metabolic biomarkers using microdialysis probe. Sensors and Actuators B: Chemical **2017**, 238, 633-640.

(49) Jöbsis, F. F. Noninvasive, infrared monitoring of cerebral and myocardial oxygen sufficiency and circulatory parameters. Science **1977**, 198 (4323), 1264-1267.

(50) Mayevsky, A. Brain NADH redox state monitored in vivo by fiber optic surface fluorometry. Brain Research Reviews **1984**, 7 (1), 49-68.

(51) Sun, F.; Zhou, J.; Dai, B.; Qian, T.; Zeng, J.; Li, X.; Zhuo, Y.; Zhang, Y.; Wang, Y.; Qian, C.; et al. Next-generation GRAB sensors for monitoring dopaminergic activity in vivo. Nature Methods **2020**, 17 (11), 1156-1166.

(52) Patriarchi, T.; Cho, J. R.; Merten, K.; Howe, M. W.; Marley, A.; Xiong, W.-H.; Folk, R. W.; Broussard, G. J.; Liang, R.; Jang, M. J.; et al. Ultrafast neuronal imaging of dopamine dynamics with designed genetically encoded sensors. Science **2018**, 360.

(53) Jorfeldt, L.; Juhlin-Dannfelt, A.; Karlsson, J. Lactate release in relation to tissue lactate in human skeletal muscle during exercise. Journal of Applied Physiology Respiratory Environmental and Exercise Physiology **1978**, 44 (3), 350-352.

(54) Brooks, G. A.; Arevalo, J. A.; Osmond, A. D.; Leija, R. G.; Curl, C. C.; Tovar, A. P. Lactate in contemporary biology: a phoenix risen. The Journal of Physiology **2022**, 600 (5), 1229-1251.

(55) Rabinowitz, J. D.; Enerbäck, S. Lactate: the ugly duckling of energy metabolism. Nature Metabolism **2020**, 2 (7), 566-571.

(56) Liberti, M. V.; Locasale, J. W. The Warburg Effect: How Does it Benefit Cancer Cells? Trends in Biochemical Science **2016**, 41 (3), 211-218.

(57) Lindinger, M. I. Combating muscle fatigue: extracellular lactic acidosis and catecholamines. The Journal of Physiology **2007**, 581 (Pt 2), 419.

(58) Suzuki, A.; Stern, S. A.; Bozdagi, O.; Huntley, G. W.; Walker, R. H.; Magistretti, P. J.; Alberini, C. M. Astrocyte-neuron lactate transport is required for long-term memory formation. Cell **2011**, 144 (5), 810-823.

(59) Bueschke, N.; Amaral-Silva, L.; Hu, M.; Santin, J. M. Lactate ions induce synaptic plasticity to enhance output from the central respiratory network. The Journal of Physiology **2021**, 599 (24), 5485-5504.

(60) Brooks, G. A.; Martin, N. A. Cerebral metabolism following traumatic brain injury: new discoveries with implications for treatment. Frontiers in Neuroscience **2014**, 8, 408.

(61) Pellerin, L.; Magistretti, P. J. Glutamate uptake into astrocytes stimulates aerobic glycolysis: a mechanism coupling neuronal activity to glucose utilization. Proceedings of the National Academy of Sciences **1994**, 91 (22), 10625-10629.

(62) Chih, C. P.; Roberts, E. L., Jr. Energy substrates for neurons during neural activity: a critical review of the astrocyte-neuron lactate shuttle hypothesis. Journal of Cerebral Blood Flow Metabolism **2003**, 23 (11), 1263-1281.

(63) Chih, C.-P.; Roberts, E. L. Energy Substrates for Neurons during Neural Activity: A Critical Review of the Astrocyte-Neuron Lactate Shuttle Hypothesis. Journal of Cerebral Blood Flow & Metabolism **2003**, 23 (11), 1263-1281.

(64) Laughton, J. D.; Charnay, Y.; Belloir, B.; Pellerin, L.; Magistretti, P. J.; Bouras, C. Differential messenger RNA distribution of lactate dehydrogenase LDH-1 and LDH-5 isoforms in the rat brain. Neuroscience **2000**, 96 (3), 619-625.

(65) Felmlee, M. A.; Jones, R. S.; Rodriguez-Cruz, V.; Follman, K. E.; Morris, M. E. Monocarboxylate Transporters (SLC16): Function, Regulation, and Role in Health and Disease. Pharmacological Reviews **2020**, 72 (2), 466-485.

(66) Pellerin, L.; Pellegri, G.; Bittar, P. G.; Charnay, Y.; Bouras, C.; Martin, J. L.; Stella, N.; Magistretti, P. J. Evidence supporting the existence of an activity-dependent astrocyte-neuron lactate shuttle. Developmental Neuroscience **1998**, 20 (4-5), 291-299.

(67) Halestrap, A. P.; Wilson, M. C. The monocarboxylate transporter family—Role and regulation. International Union Biochemistry Molecular Biochemistry Life **2012**, 64 (2), 109-119.

(68) Mc, I. H. Substances which support respiration and metabolic response to electrical impulses in human cerebral tissues. Journal of Neurology, Neurosurgery and Psychiatry **1953**, 16 (4), 257-266.

(69) Demestre, M.; Boutelle, M.; Fillenz, M. Stimulated release of lactate in freely moving rats is dependent on the uptake of glutamate. Journal of Physiology **1997**, 499 (Pt 3), 825-832.

(70) Vannucci, S. J.; Maher, F.; Simpson, I. A. Glucose transporter proteins in brain: delivery of glucose to neurons and glia. Glia **1997**, 21 (1), 2-21.

(71) Itoh, Y.; Esaki, T.; Shimoji, K.; Cook, M.; Law, M. J.; Kaufman, E.; Sokoloff, L. Dichloroacetate effects on glucose and lactate oxidation by neurons and astroglia in vitro and on glucose utilization by brain in vivo. Proceedings of the National Academy of Sciences **2003**, 100 (8), 4879-4884.

(72) Raichle, M. E.; Gusnard, D. A. Appraising the brain's energy budget. Proceedings of the National Academy of Sciences **2002**, 99 (16), 10237-10239.

(73) Cunnane, S.; Nugent, S.; Roy, M.; Courchesne-Loyer, A.; Croteau, E.; Tremblay, S.; Castellano, A.; Pifferi, F.; Bocti, C.; Paquet, N.; et al. Brain fuel metabolism, aging, and Alzheimer's disease. Nutrition **2011**.

(74) Liguori, C.; Stefani, A.; Sancesario, G.; Sancesario, G. M.; Marciani, M. G.; Pierantozzi, M. CSF lactate levels, τ proteins, cognitive decline: a dynamic relationship in Alzheimer's disease. Journal of Neurology, Neurosurgery and Psychiatry **2015**, 86 (6), 655-659

(75) Redjems-Bennani, N.; Jeandel, C.; Lefebvre, E.; Blain, H.; Vidailhet, M.; Guéant, J. L. Abnormal substrate levels that depend upon mitochondrial function in cerebrospinal fluid from Alzheimer patients. Gerontology **1998**, 44 (5), 300-304.

(76) Sullivan, C. R.; Mielnik, C. A.; Funk, A.; O'Donovan, S. M.; Bentea, E.; Pletnikov, M.; Ramsey, A. J.; Wen, Z.; Rowland, L. M.; Mc Cullumsmith, R. E. Measurement of lactate levels in postmortem brain, iPSCs, and animal models of schizophrenia. Scientific Reports **2019**, 9 (1), 5087.

(77) Park, H. J.; Choi, I.; Leem, K. H. Decreased Brain pH and Pathophysiology in Schizophrenia. International Journal Molecular Science **2021**, 22 (16)

(78) Kuang, H.; Duong, A.; Jeong, H.; Zachos, K.; Andreazza, A. C. Lactate in bipolar disorder: A systematic review and meta-analysis. Psychiatry and Clinical Neuroscience **2018**, 72 (8), 546-555.

(79) Kuhr, W. G.; Korf, J. Extracellular lactic acid as an indicator of brain metabolism: continuous on-line measurement in conscious, freely moving rats with intrastriatal dialysis. Journal Cerebral Blood Flow and Metabolism **1988**, 8 (1), 130-137.

(80) Schasfoort, E. M.; De Bruin, L. A.; Korf, J. Mild stress stimulates rat hippocampal glucose utilization transiently via NMDA receptors, as assessed by lactography. Brain Research **1988**, 475 (1), 58-63.

(81) Fellows, L. K.; Boutelle, M. G.; Fillenz, M. Physiological stimulation increases nonoxidative glucose metabolism in the brain of the freely moving rat. Journal Neurochemistry **1993**, 60 (4), 1258-1263.

(82) Uehara, T.; Kurata, K.; Sumiyoshi, T.; Kurachi, M. Immobilization stress-induced increment of lactate metabolism in the basolateral amygdaloid nucleus is attenuated by diazepam in the rat. European Journal of Pharmacology **2003**, 459 (2-3), 211-215.

(83) Demestre, M.; Boutelle, M.; Fillenz, M. Stimulated release of lactate in freely moving rats is dependent on the uptake of glutamate. The Journal of Physiology **1997**, 499 (3), 825-832.

(84) Ronald Zielke, H.; Zielke, C. L.; Baab, P. J. Direct measurement of oxidative metabolism in the living brain by microdialysis: a review. Journal of Neurochemistry **2009**, 109 (s1), 24-29.

(85) Uehara, T.; Sumiyoshi, T.; Matsuoka, T.; Tanaka, K.; Tsunoda, M.; Itoh, H.; Kurachi, M. Enhancement of lactate metabolism in the basolateral amygdala by physical and psychological stress: role of benzodiazepine receptors. Brain Research **2005**, 1065 (1-2), 86-91.

(86) Horn, T.; Klein, J. Lactate levels in the brain are elevated upon exposure to volatile anesthetics: a microdialysis study. Neurochemistry International **2010**, 57 (8), 940-947.

(87) Jalloh, I.; Helmy, A.; Shannon, R. J.; Gallagher, C. N.; Menon, D. K.; Carpenter, K. L.; Hutchinson, P. J. Lactate uptake by the injured human brain: evidence from an arteriovenous gradient and cerebral microdialysis study. Journal of Neurotrauma **2013**, 30 (24), 2031-2037.

(88) Hu, Y.; Zhang, Y.; Wilson, G. S. A needle-type enzyme-based lactate sensor for in vivo monitoring. Analytica Chimica Acta **1993**, 281 (3), 503-511.

(89) Hu, Y.; Wilson, G. S. Rapid changes in local extracellular rat brain glucose observed with an in vivo glucose sensor. Journal of Neurochemistry **1997**, 68 (4), 1745-1752.

(90) Burmeister, J. J.; Palmer, M.; Gerhardt, G. A. L-lactate measures in brain tissue with ceramic-based multisite microelectrodes. Biosensors and Bioelectronics **2005**, 20 (9), 1772-1779.

(91) Shram, N. F.; Netchiporouk, L. I.; Martelet, C.; Jaffrezic-Renault, N.; Bonnet, C.; Cespuglio, R. In vivo voltammetric detection of rat brain lactate with carbon fiber microelectrodes coated with lactate oxidase. Analytical Chemistry **1998**, 70 (13), 2618-2622.

(92) Shram, N.; Netchiporouk, L.; Cespuglio, R. Lactate in the brain of the freely moving rat: voltammetric monitoring of the changes related to the sleep-wake states. European Journal of Neuroscience **2002**, 16 (3), 461-466.

(93) Naylor, E.; Aillon, D. V.; Barrett, B. S.; Wilson, G. S.; Johnson, D. A.; Johnson, D. A.; Harmon, H. P.; Gabbert, S.; Petillo, P. A. Lactate as a biomarker for sleep. Sleep **2012**, 35 (9), 1209-1222.

(94) Fernandes, E.; Ledo, A.; Barbosa, R. M. Design and Evaluation of a Lactate Microbiosensor: Toward Multianalyte Monitoring of Neurometabolic Markers In Vivo in the Brain. Molecules **2022**, 27 (2).

(95) Zimphango, C.; Alimagham, F. C.; Carpenter, K. L. H.; Hutchinson, P. J.; Hutter, T. Monitoring Neurochemistry in Traumatic Brain Injury Patients Using Microdialysis Integrated with Biosensors: A Review. Metabolites **2022**, 12 (5).

(96) Arias, D. S., S.; Verguet, S. Quantifying the Global Burden of Mental Disorders and Their Economic Value. eClinicalMedicine **2022**, 54, 101675.

Chapter 2 - Theory

Chapter 2. Theory

2.1. How to monitor lactate?

Lactate has been monitored in biological systems since the 1930s[1] using the Friedman method as described by W.H Owles[2]. Since then, lactate has come to be appreciated as more than a waste metabolite of anaerobic respiration and has gained significant interest from the scientific community. During the course of this work a biosensor was characterised and used to monitor lactate in real-time with good spaciotemporal resolution allowing concentration changes to be linked to behaviours.

Biosensors are a technology that was first developed in 1962 by Clark and Lyons[3], who designed a glucose biosensor. Glucose being non-electroactive can't be directly monitored using electrochemical methods. However, oxidase enzymes consume O_2 and produce H_2O_2, both of which can be monitored at an electrode and are proportional to the amount of glucose in the system. As glucose is such an important energy metabolite, this system has been significantly modified and developed from its initial conception, leading to the refinement of biosensors for glucose[4,5] , and the development of other biosensors to monitor a wide range of important analytes such as glutamate[6,7] ,choline[8] and D-serine[9,10]. There are some key features which are common amongst biosensors, which can be seen in Figure 2.1. The bioreceptor, the transducer, the signal processor, and the display. The bioreceptor, which is also referred to as the biomolecular recognition element, is the part of the sensor that specifically recognises the analyte. Enzymes, antibodies, oligonucleotides, and nucleic acids[11] can be used as the bioreceptor. Throughout the course of this work, the bioreceptor is the enzyme Lactate Oxidase (LOx). The transducer is what turns the event at the biorecognition element into a measurable signal. In the case of this work, the transducer is a Pt working electrode monitoring the production of H_2O_2 as a biproduct of the oxidation of lactate to pyruvate see Equation 2.4. The transducer then converts the signal from the biosensor into a readable form. Finally, the display is where the output of the data from the biosensor is shown.

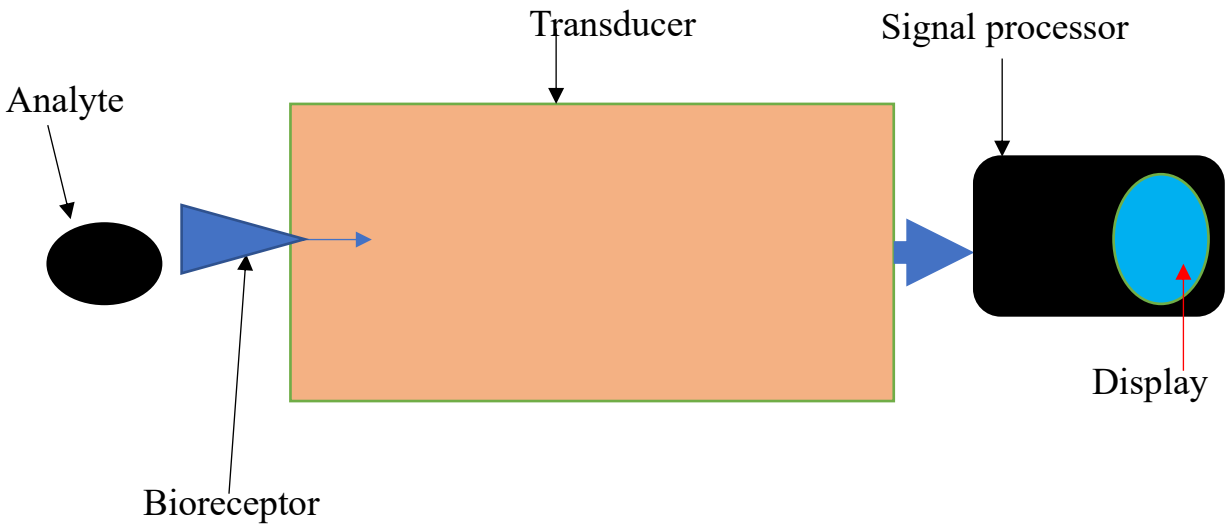

Figure 2.1 Components of a biosensor.

2.2. Enzyme immobilisation

Most first-generation biosensors (biosensors that monitor the production of H_2O_2 or consumption of O_2), comparable to the one described in this work, can be defined as devices that measure the concentration of analytes and/or products of enzymatic reactions that diffuse to the transducer surface and generate a response[12]. To achieve the time scale required to relate sensor signals to behaviour[13,14] the enzyme is usually immobilised directly onto the surface of the transducer. Many different methods exist for the immobilisation of enzymes (Figure 2.2), a detailed description of these methods can be found in Sassolas *et. al.*[15] and Nugyen *et al.*[16] In short, entrapment/encapsulation involves immobilising the enzyme in a three-dimensional matrix and has been done previously for lactate sensors[17,18]. Adsorption represents the easiest method of immobilising an enzyme and involves attaching the enzyme to a solid support. Covalent attachment involves attaching the enzyme to a polymeric support through interactions via functional groups that aren't necessary for the catalytic activity of the enzyme. Crosslinking is achieved when a bifunctional group such as glutaraldehyde is used to form strong bonds between enzymes. A drawback of this is that sometimes these functional groups are harsh and can denature the enzyme. To minimize this an inert protein such as bovine serum albumin is used in the process of crosslinking to prevent the harsh bifunctional molecules reducing the enzyme activity too much. Finally, affinity seeks to create a bond between an activated support and specific groups of the protein's sequence e.g., histidine residues. Each method of immobilisation comes with its own

benefits and drawbacks regarding strength of adsorption and effect on enzyme activity, and some methods such as covalent attachment or crosslinking can affect the 3D structure of the enzyme. Multiple techniques can be used in tandem to play off each other's strengths and weaknesses. During the course of this work, adsorption, encapsulation, alongside crosslinking were used together to provide an extremely sensitive and stable sensor see Section 3.5 for a more detailed description on the construction of the lactate biosensor.

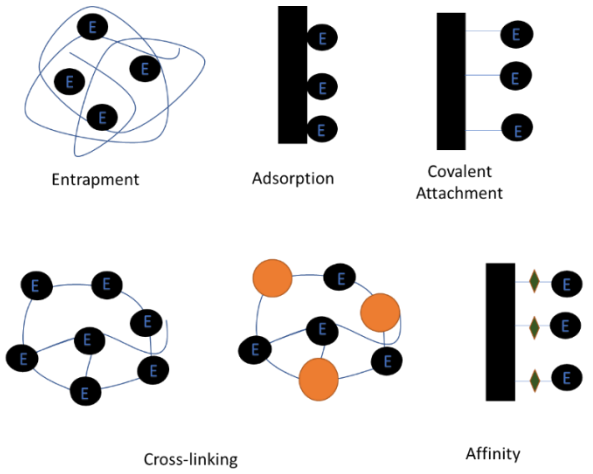

Figure 2.2. Different methods of enzyme immobilisation. Black dots are the enzyme molecule and orange dots are inert protein molecules.

2.3. Electroanalysis

Electroanalysis is a branch of analytical chemistry that uses electrochemical methods to give quantitative and or qualitative data regarding a chosen analyte. As the transducers used in the reported experiments are electrochemical in nature (Pt working electrode), a knowledge of electrochemistry is required to fully appreciate the biosensors used in this work. There are three common types of electroanalysis employed for the monitoring of neurochemicals: 1) Conductimetric 2) Potentiometric 3) Amperometry[19].

Throughout the course of this experimental work a three-electrode system was used. The components of this system are were as follows: 1) The working electrode – this is where the electrochemical reaction of interest occurs; 2) The reference electrode - its purpose is to provide a

stable potential which the working electrode can base its potential from; and 3) The auxiliary/counter electrode - which can act either as the sink (oxidation) or the source (reduction) of electrodes transported to or from the species in solution, as shown in (Equation 2.1), where O is the species being oxidised and R is the reduced species:

$$O + ne^- \longrightarrow R.$$

$$R \longrightarrow O + ne^-$$

Equation 2.1. General equation for redox reaction.

Conductometric methods involve measuring the conductivity of an analyte by measuring its ability to carry an electrical current between two electrodes. Potentiometry alters the potential applied to the electrochemical system and monitoring of the resulting current. There are many distinct kinds of amperometry depending on how the potential is altered throughout the course of the experiment. It is generally used if the redox potential of the analyte is known. A fixed potential is applied to the electrode and the resulting current produced is proportional to the concentration of the analyte. The three most commonly used amperometric methods are differential pulse amperometry (DPA), chronoamperometry and finally, the electrochemical method used throughout this body of work, constant potential amperometry (CPA). In CPA, the electrode is held at a potential sufficient to allow the oxidation or reduction of the analyte of interest, hence the currents are limited by mass transport. For hydrogen peroxide this potential is +700 mV vs. the saturated calomel electrode (SCE).

2.4. Microelectrodes

Since the Ralph Adams pioneering work in the field of electrochemical analysis of the[20] it has been recognied that microelectrodes would have distinct advantages such as minimising tissue damage and providing localised real-time chemical information[21]. Microelectrodes are defined as electrodes with a tip having dimensions in the order of a micrometre. The most common geometries for microelectrodes include disc and cylinder electrodes. Cylinder electrodes with

surface length of 2 mm and a diameter of 0.125 mm (*see* Figure 2.3) were employed throughout the course of this work unless stated otherwise.

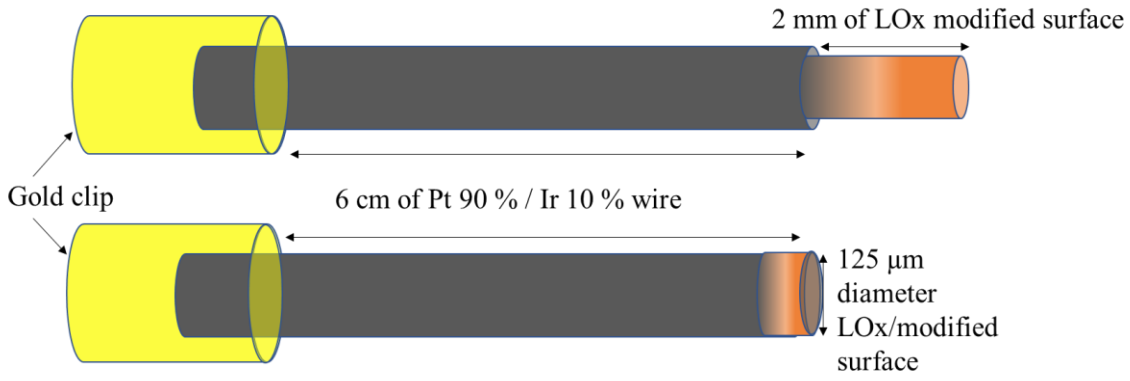

Figure 2.3. Schematic of a cylinder (top) and disc(bottom) microelectrode for monitoring lactate.

2.5. Enzymology

Enzymes are biological catalysts, which are substances that change the rate of a chemical reaction without themselves being consumed in the reaction. The molecule that binds to an enzyme is the substrate and the molecule that is transformed by the enzyme is the product. Enzymes tend to have a high specificity to their given substrate which is integral for biosensor function[22]. The general equation for an enzymatic reaction is given by:

$$\text{Substrate} \xrightarrow{\text{Enzyme}} \text{Product}$$

Equation 2.2. General enzymatic reaction.

The specificity of an enzyme comes from the shape of its active site. The active site is the region of the enzyme where the substrate binds in a specific manner. This specificity is caused by interactions between the analyte and the residue groups of the amino acids that constitute the proteins make-up. As these interactions are integral to the functioning of the enzyme, factors that can influence these interactions, such as pH and temperature, can influence the rate of the

enzymatic reaction. Some proteins also require a cofactor to function. A cofactor is a non-protein compound required for the enzyme to perform its catalytic role. Oxygen is a common co-factor for oxidase enzymes, which are most often used for biosensors. Furthermore, this can introduce the problem of oxygen dependence. As these oxidase enzymes need O_2 to be able to complete their enzymatic reaction. This isn't a problem under normal laboratory benchtop conditions as the atmospheric concentration of O_2 is large at ~240 μM[7]. However, brain ECF concentrations of oxygen are significantly lower varying from 40-80 μM[23,24]. The enzyme used in the course of this work, LOx, also required flavin mononucleotide (FMN) for its function[25], because without FMN the enzymes active site couldn't be reduced back to its original form rendering it useless. The hydrogen peroxide electrochemically monitored is produced by the oxidation of the FMN according to Equation 2.3. The hydrogen peroxide generated by the enzymatic reaction is then monitored (oxidized) at the surface of the electrode according to Equation 2.4.

$$E_{FMN} + \text{Lactate} \longrightarrow \text{Pyruvate} + E_{FMNH_2}$$

$$E_{FMNH_2} + O_2 \longrightarrow H_2O_2 + E_{FMN}$$

Equation 2.3. Overall enzymatic reaction scheme for LOx.

$$H_2O_2 \longrightarrow O_2 + 2\,H^+ + 2\,e^-$$

Equation 2.4. Oxidation of hydrogen peroxide at an electrode surface at +700 mV vs. SCE.

2.5.1 Enzyme kinetics

Due to the ultra-thin nature of the poly-*ortho*-phenylenediamine (P*o*PD) layer being 10-30 nm in thickness[26], this results in a sensor that isn't diffusion limited. This allows Michaelis-Menten kinetics[26] to be employed as a simple and accessible way to determine enzyme efficiency without the need for more complex analysis. The basic principles of Michaelis-Menten kinetics are described below. The reaction between an enzyme and its substrate can be expressed as given in

Equation 2.5, where S is the substrate, E is the enzyme, P is the product, and K_1, K_{-1} and K_2 are rate constants.

$$E + S \underset{K^{-1}}{\overset{K^{1}}{\rightleftharpoons}} ES \xrightarrow{K^{2}} E + P$$

Equation 2.5. General enzymatic reaction.

The two-substrate form of the Michaelis−Menten equation for the rate of reaction (V) of an enzymatic reaction, is shown in Equation 2.6, where V_{MAX} is the maximum reaction velocity and K_M is the Michaelis-Menten constant both of which can be seen in Figure 2.4. A typical example of the two-substrate form of Michaelis-Menten kinetics is shown in Equation 2.6 where S is the enzymes substrate in this case lactate and O_2 representing the co substrate which is O_2.

$$V = \frac{VMAX}{1} + \frac{KM(S)}{[S]} + \frac{K<(O2)}{[O2]} \quad (2.6)$$

If the co-substrates concentration is large, then Equation 2.6 can be simplified to give the Michaelis-Menten equation given in Equation 2.7.

$$V = \frac{VMAX}{1} + KM\frac{(S)}{[S].} \quad (2.7)$$

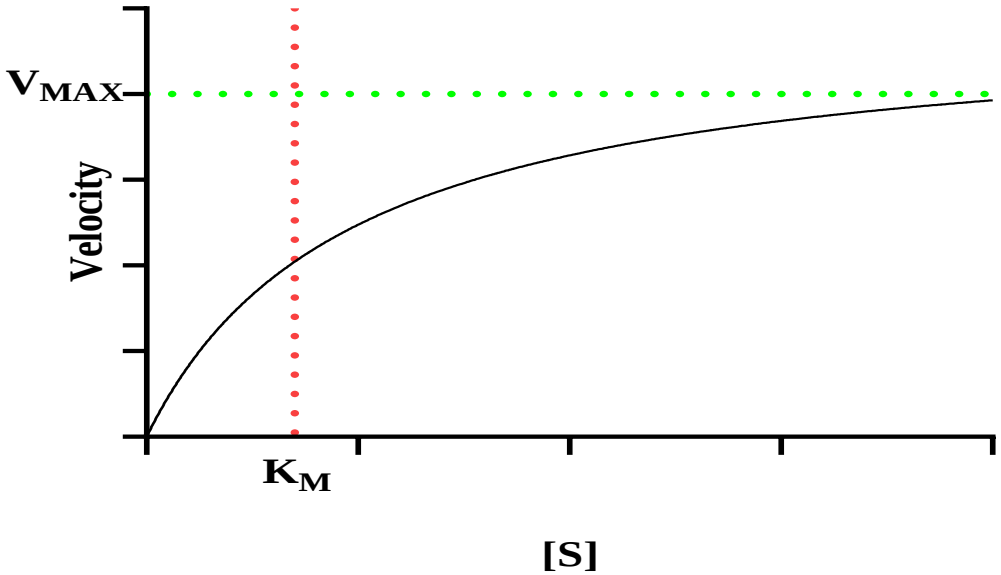

Figure 2.4. Graph of reaction rate (velocity) against substrate concentration [S] for a given enzyme concentration [E] for a single substrate enzyme catalysed reaction from the Michaelis-Menten equation (see Equation 2.7).

This represents the rate of reaction of the enzyme which is also proportional to the amount of H_2O_2 produced, as can be seen by Equation 2.3. As the developed composite biosensor expresses the concentration of analyte in terms of current it is also useful to express the rate of the enzymatic reaction in terms of current (I) (*see* Equation 2.8). This is done by multiplying both sides of Equation 2.7. by AzαF, where α is the fraction of the flux of H_2O_2 oxidized by the electrode, A is the electrodes surface area, z is the number of electrons taking place in the reaction and F is Faraday's constant. This can then be divided by the electrode's surface area to give current density (J, *see* Equation 2.9.) which is a useful parameter for comparing sensors of different geometries.

$$\mathrm{I} = \frac{\mathrm{IMAX}}{1} + \frac{\mathrm{KM(S)}}{[\mathrm{S}]} \quad (2.8)$$

$$\mathrm{J} = \frac{\mathrm{JMAX}}{1} + \frac{\mathrm{KM(S)}}{[\mathrm{S}]} \quad (2.9)$$

Not all calibrations used throughout this work fit Michaelis-Menten kinetics, some calibrations fit better to Hill-type kinetics, a phenomenon first observed by Archibald Vivian Hill in 1910[27]. This model describes enzymes which work based on a cooperative binding model, i.e., the binding sites or the macromolecule (protein in this case) is non-linear[28] resulting in a sigmoidal shaped graph, as opposed to the rectangular hyperbole shaped observed in Michaelis-Menten kinetics. The Hill equation is shown in Equation 2.10. Where V_{MAX} and K_M are as previously described and α is the hill coefficient which describes the cooperativity of the substrate binding the enzyme.

$$\mathrm{y} = \frac{\mathrm{VMAX}}{(1+\mathrm{KM}/[\mathrm{S}])\hat{}\alpha} \quad (2.10)$$

2.6. Microdialysis (MD)

Similar to *in vivo* voltammetry, MD is an invasive technique, i.e. it involves implanting a probe into the brain. This probe is then used to sample a variety of neurochemicals. The first use of MD *in vivo* was in the 1960s using dogs[29]. MD is based on the principles of dialysis; a MD probe consists of a semi-permeable membrane that allows for the free diffusion of water and small solutes (10-30 kDa cut off)[30] is inserted into the brain of a living organism. This probe is perfused with artificial cerebrospinal fluid (aCSF) which is made to mimic the ionic composition of the brain. It

is typically perfused at a rate of 2 µL/min. The perfusate reaches equilibrium with the ECF by bidirectional diffusion, where osmosis is the primary driving force of the equilibrium. The perfusate is then analysed *ex-vivo* for multiple analytes using analytical methods such as ultra-high performance liquid chromatography[31], mass-spectrometry[32] and enzyme assays[33].

While the latter is a significant advantages of MD, the technique is also associated with a range of disadvantages such as the large surface area of the MD probe limiting its resolution[34], chemicals (e.g., monoamines) degrade rapidly at room temperature limiting the recovery rate[35]. Additionally, the large probe size could cause tissue trauma resulting in damage to the BBB[36, 37] and fibrosis[38], or the probe may clog as a result of gliosis[39].

2.7. Biosensor performance factors

For a more detailed and through discussion and derivation of the performance factors that will be discussed in this section, please see O'Neill *et al.*[40]. The apparent Michaelis-Menten constant (K_M) (*see* Figure 5.2.) measures the affinity the enzyme has for the substrate. K_M is defined as half the V_{MAX} and is a key factor as it defines the sensitivity or Linear Region Slope (rLRS) according to Equation 2.11:

$$\text{rLRS} = ½\ \text{KM} \quad (2.11)$$

The rLRS is a crucial factor as for real time neurochemical monitoring the *in-vivo* concentrations of the analyte of interest should fall into this range for accurate measurement. Enzymes for the biosensors used throughout the course of this work were attached to the surface of the sensor via dip adsorption (*see* Section 3.5.4). This means it is hard to gauge the concentration of enzyme at the surface of the sensor. However, the concentration of enzyme on the sensors surface can be estimated using $[E]_{act}$ which is defined in Equation 2.12, with J_{MAX} being the maximum current obtained at the biosensor and Slope(H_2O_2) being the slope.

$$[\text{E}]\text{act} = \text{JMAX}/\text{Slope}(\text{H2O2}) \quad (2.12)$$

The main challenge with electrochemical monitoring in the brain is the presence of electroactive species which can interfere with the target signal. The most abundant of these in the brain is

ascorbic acid (AA) with an extracellular fluid concentration of approximately 400 μM[41]. This is why the P*o*PD polymer layer is employed as it has been shown to facilitate interference rejection. The polymer undergoes a unique "self-blocking" process which has been previously described[42, 43]. In short, AA and or the products of its oxidation, clog the pores in the polymer layer resulting in the response to AA at concentrations over 100 μM being negligible. Due to the nature of the behaviour of the P*o*PD layer's response to AA I_{LIM} is used alongside I_{MAX}[40]. I_{LIM} is the current value at the plateau region which typically occurs at concentrations around 1,000 μM and provides an insight into the blocking ability of the polymer layer. I_{MAX} is the maximum current response observed during an AA calibration on P*o*PD electrodes the concentration at which I_{MAX} occurs is a good indication of the appropriate application of the biosensor.

2.8. References

(1) Owles, W. H. Alterations in the lactic acid content of the blood as a result of light exercise, and associated changes in the co(2)-combining power of the blood and in the alveolar CO_2 pressure. Journal of Physiology **1930**, 69 (2), 214-237.

(2) Kendall, T. E. F. a. A. I. The determination of Lactic Acid. The Journal of Biological Chemistry 1928.

(3) Clark Jr., L. C.; Lyons, C. Electrode systems for continuous monitoring in cardiovascular surgery. Annals of the New York Academy of Sciences **1962**, 102 (1), 29-45.

(4) Aloraefy, M.; Pfefer, T. J.; Ramella-Roman, J. C.; Sapsford, K. E. In vitro evaluation of fluorescence glucose biosensor response. Sensors (Basel) **2014**, 14 (7), 12127-12148.

(5) Lowry, J. P.; O'Neill, R. D.; Boutelle, M. G.; Fillenz, M. Continuous Monitoring of Extracellular Glucose Concentrations in the Striatum of Freely Moving Rats with an Implanted Glucose Biosensor. Journal of Neurochemistry **1998**, 70 (1), 391-396.

(6) McLamore, E. S.; Mohanty, S.; Shi, J.; Claussen, J.; Jedlicka, S. S.; Rickus, J. L.; Porterfield, D. M. A self-referencing glutamate biosensor for measuring real time neuronal glutamate flux. Journal of Neuroscience Methods **2010**, 189 (1), 14-22.

(7) Bermingham, K. P.; Doran, M. M.; Bolger, F. B.; Lowry, J. P. Design optimisation and characterisation of an amperometric glutamate oxidase-based composite biosensor for neurotransmitter l-glutamic acid. Analytica Chimica Acta **2022**, 1224, 340205.

(8) Baker, K. L.; Bolger, F. B.; Lowry, J. P. A microelectrochemical biosensor for real-time in vivo monitoring of brain extracellular choline. Analyst **2015**, 140 (11), 3738-3745.

(9) Zain, Z. M.; O'Neill, R. D.; Lowry, J. P.; Pierce, K. W.; Tricklebank, M.; Dewa, A.; Ghani, S. A. Development of an implantable d-serine biosensor for in vivo monitoring using mammalian d-amino acid oxidase on a poly (o-phenylenediamine) and Nafion-modified platinum–iridium disk electrode. Biosensors and Bioelectronics **2010**, 25 (6), 1454-1459.

(10) Vongsouthi, V.; Whitfield, J. H.; Unichenko, P.; Mitchell, J. A.; Breithausen, B.; Khersonsky, O.; Kremers, L.; Janovjak, H.; Monai, H.; Hirase, H.; et al. A Rationally and Computationally Designed Fluorescent Biosensor for d-Serine. American Chemical Sciences Sensors **2021**, 6 (11), 4193-4205.

(11) Ravina; Kumar, D.; Prasad, M.; Mohan, H. 8 - Biological recognition elements. In Electrochemical Sensors, Maruccio, G., Narang, J. Eds.; Woodhead Publishing, 2022; pp 213-239.

(12) Rocchitta, G.; Spanu, A.; Babudieri, S.; Latte, G.; Madeddu, G.; Galleri, G.; Nuvoli, S.; Bagella, P.; Demartis, M. I.; Fiore, V.; et al. Enzyme Biosensors for Biomedical Applications: Strategies for Safeguarding Analytical Performances in Biological Fluids. Sensors **2016**, 16 (6).

(13) Fillenz, M. In vivo neurochemical monitoring and the study of behaviour. Neuroscience & Biobehavioural Reviews **2005**, 29 (6), 949-962.

(14) O'Neill, R. D.; Lowry, J. P.; Mas, M. Monitoring brain chemistry in vivo: voltametric techniques, sensors, and behavioural applications. Critical Reviews in Neurobiology **1998**, 12 (1-2), 69-127.

(15) Sassolas, A.; Blum, L. J.; Leca-Bouvier, B. D. Immobilization strategies to develop enzymatic biosensors. Biotechnology Advances **2012**, 30 (3), 489-511.

(16) Nguyen, H. H.; Lee, S. H.; Lee, U. J.; Fermin, C. D.; Kim, M. Immobilized Enzymes in Biosensor Applications. Materials **2019**, 12 (1).

(17) Dempsey, E.; Wang, J.; Smyth, M. R. Electropolymerised o-phenylenediamine film as means of immobilising lactate oxidase for a L-lactate biosensor. Talanta **1993**, 40 (3), 445-451.

(18) Li, C. I.; Lin, Y. H.; Shih, C. L.; Tsaur, J. P.; Chau, L. K. Sol-gel encapsulation of lactate dehydrogenase for optical sensing of L-lactate. Biosensors and Bioelectronics **2002**, 17 (4), 323-330.

(19) Xu, C.; Wu, F.; Yu, P.; Mao, L. In Vivo Electrochemical Sensors for Neurochemicals: Recent Update. ACS Sensors **2019**, 4 (12), 3102-3118.

(20) Kissinger, P. T.; Hart, J. B.; Adams, R. N. Voltammetry in brain tissue — a new neurophysiological measurement. Brain Research **1973**, 55 (1), 209-213.

(21) Adams, R. N. Probing brain chemistry with electroanalytical techniques. Analytical Chemistry **1976**, 48 (14), 1126a-1138a.

(22) Grieshaber, D.; MacKenzie, R.; Vörös, J.; Reimhult, E. Electrochemical Biosensors - Sensor Principles and Architectures. Sensors **2008**, 8 (3), 1400-1458.

(23) McMahon, C. P.; O'Neill, R. D. Polymer−Enzyme Composite Biosensor with High Glutamate Sensitivity and Low Oxygen Dependence. Analytical Chemistry **2005**, 77 (4), 1196-1199.

(24) Chatard, C.; Meiller, A.; Marinesco, S. Microelectrode Biosensors for in vivo Analysis of Brain Interstitial Fluid. Electroanalysis **2018**, 30 (6), 977-998.

(25) Yorita, K.; Misaki, H.; Palfey, B. A.; Massey, V. On the interpretation of quantitative structure–function activity relationship data for lactate oxidase. Proceedings of the National Academy of Sciences **2000**, 97 (6), 2480-2485.

(26) Killoran, S. J.; O'Neill, R. D. Characterization of permselective coatings electrosynthesized on Pt–Ir from the three phenylenediamine isomers for biosensor applications. Electrochimica Acta **2008**, 53 (24), 7303-7312.

(27) Hill, A. V. The possible effects of the aggregation of the molecules of haemoglobin on its dissociation curves. Journal of Physiology **1910**, 40, iv-vii.

(28) Stefan, M. I.; Le Novère, N. Cooperative binding. PLOS Computational Biology **2013**, 9.

(29) Bito, L.; Davson, H.; Levin, E.; Murray, M.; Snider, N. The concentrations of free amino acids and other electrolytes in the cerebrospinal fluid, in vivo dialysate of brain, and blood plasma of the dog. Journal of Neurochemistry **1966**, 13 (11), 1057-1067.

(30) Tisdall, M. M.; Smith, M. Cerebral microdialysis: research technique or clinical tool. British Journal of Anaesthesia **2006**, 97 (1), 18-25.

(31) González, R. R.; Fernández, R. F.; Vidal, J. L.; Frenich, A. G.; Pérez, M. L. Development and validation of an ultra-high performance liquid chromatography-tandem mass-spectrometry (UHPLC-MS/MS) method for the simultaneous determination of neurotransmitters in rat brain samples. Journal of Neuroscience Methods **2011**, 198 (2), 187-194.

(32) Song, P.; Hershey, N. D.; Mabrouk, O. S.; Slaney, T. R.; Kennedy, R. T. Mass spectrometry "sensor" for in vivo acetylcholine monitoring. Analytical Chemistry **2012**, 84 (11), 4659-4664.

(33) Slaney, T. R.; Nie, J.; Hershey, N. D.; Thwar, P. K.; Linderman, J.; Burns, M. A.; Kennedy, R. T. Push-pull perfusion sampling with segmented flow for high temporal and spatial resolution in vivo chemical monitoring. Analytical Chemistry **2011**, 83 (13), 5207-5213.

(34) Su, C.-K.; Sun, Y.-C.; Tzeng, S.-F.; Yang, C.-S.; Wang, C.-Y.; Yang, M.-H. In vivo monitoring of the transfer kinetics of trace elements in animal brains with hyphenated inductively coupled plasma mass spectrometry techniques. Mass Spectrometry Reviews **2010**, 29 (3), 392-424.

(35) Chefer, V. I.; Thompson, A. C.; Zapata, A.; Shippenberg, T. S. Overview of brain microdialysis. Current Protocols in Neuroscience **2009**, Chapter 7, Unit7.1.

(36) Umezu, T.; Sano, T.; Hayashi, J.; Shibata, Y. Simultaneous blood and brain microdialysis in a free-moving mouse to test blood-brain barrier permeability of chemicals. Toxicology Reports **2020**, 7, 1542-1550.

(37) Hammarlund-Udenaes, M. In Vivo Approaches to Assessing the Blood–Brain Barrier. In The Blood Brain Barrier (BBB), Fricker, G., Ott, M., Mahringer, A. Eds.; Springer Berlin Heidelberg, 2014; pp 21-48.

(38) Sides, C. R.; Stenken, J. A. Microdialysis sampling techniques applied to studies of the foreign body reaction. European Journal of Pharmaceutical Science **2014**, 57, 74-86.

(39) Jaquins-Gerstl, A.; Michael, A. C. Dexamethasone-Enhanced Microdialysis and Penetration Injury. Frontiers in Bioengineering and Biotechnology **2020**, 8, Review.

(40) O'Neill, R. D.; Rocchitta, G.; McMahon, C. P.; Serra, P. A.; Lowry, J. P. Designing sensitive and selective polymer/enzyme composite biosensors for brain monitoring in vivo. TrAC Trends in Analytical Chemistry **2008**, 27 (1), 78-88.

(41) Miele, M.; Fillenz, M. In vivo determination of extracellular brain ascorbate. Journal of Neuroscience Methods **1996**, 70 (1), 15-19.

(42) Lowry, J. P.; McAteer, K.; El Atrash, S. S.; Duff, A.; O'Neill, R. D. Characterization of Glucose Oxidase-Modified Poly(phenylenediamine)-Coated Electrodes in vitro and in vivo: Homogeneous Interference by Ascorbic Acid in Hydrogen Peroxide Detection. Analytical Chemistry **1994**, 66 (10), 1754-1761.

(43) Sasso, S. V.; Pierce, R. J.; Walla, R.; Yacynych, A. M. Electropolymerized 1,2-diaminobenzene as a means to prevent interferences and fouling and to stabilize immobilized enzyme in electrochemical biosensors. Analytical Chemistry **1990**, 62 (11), 1111-1117.

Chapter 3 - Experimental

3. Experimental

3.1. Introduction

This chapter contains a description of all materials and methods used throughout the course of this work. The core design of this composite biosensor for lactate is based on designs previously published from the group[1,2], utilising styrene to immobilise the enzyme Lactate Oxidase (LOx), LOx has been reported to have high substrate specificity to L-lactate[3] and low specificity for other α-hydroxy acids[4,5], primarily due to conformational variations in the different members of the α-hydroxy acid oxidase family of flavoenzymes[6]. A polyphenylenediamine (PPD) layer is used as an interference rejecting underlayer layer.

3.2. Chemicals and apparatus

3.2.1. Reagents and solutions

The following reagents were used for the preparation of the lactate biosensor. For a more detailed description of the preparation *see* Section 3.5.

Polyethylenimine (PEI,80% ethoxylated), Bovine serum albumin (BSA), Glutaraldehyde (GA), Styrene (Sty), Cellulose acetate (CA), Flavin mononucleotide (FMN), *Ortho*-phenylenediamine(*o*PD), were all obtained from Sigma-Aldrich Ireland Ltd. Dublin, Ireland Lactate Oxidase II (Aerococcus viridians) (LoX) was obtained from Genzyme (Cambridge, MA, USA). HEPES (200 nM) was obtained from cell signalling technology (Danvers, MA, USA).
Poly-dialdehyde starch (Polymeric dialdehyde), more commonly referred to as Dialdehyde starch, was obtained from Biosynth (Thal, Switzerland).

All solutions were made up in double distilled deionised water obtained from a Milli-Q® water purification system supplied by Millipore Ireland BV, Tullagreen, Carrigtwohill, Co. Cork, Ireland. Stock solutions for calibrations were prepared as detailed below. If solutions were not immediately

used following preparation, they were stored at -20 °C. Light sensitive compounds (e.g. dopamine) were made up and stored in amber glassware to minimise decomposition before use.

Ascorbic acid (AA)

AA was made up fresh daily as it can undergo oxidative decomposition. A 0.1 M solution was prepared by dissolving 0.176 g of L-Ascorbic acid (Sigma-Aldrich) in 10 mL.

Hydrogen peroxide (H_2O_2)

A 0.1 M stock solution was prepared by dissolving 225 µL of H_2O_2 (Sigma-Aldrich) in 25 mL.

L-Lactate

A 0.25 M stock solution of L-lactate was prepared by dissolving 0.140 g of sodium-L-lactate (Sigma-Aldrich) in 5 mL.

Stock solutions for interference studies were prepared as follows:

L-Cystine

A 0.001 M stock solution was made by dissolving 0.609 mg of L-cystine (Sigma-Aldrich) in 5 mL.

Dopamine

A 0.001 M stock solution was made by dissolving 0.948 mg of Dopamine (Sigma-Aldrich) in 5mL.

Uric acid

A 0.001 M stock solution was made by dissolving 0.841 mg of Uric Acid (Sigma-Aldrich) in 5 mL.

3,4-Dihydroxyphenylacetic acid (DOPAC)

A 0.001 M stock solution was made by dissolving 0.866 mg of DOPAC (Sigma-Aldrich) in 5 mL.

Homovanallic acid (HVA)

A 0.001 M stock solution was prepared by dissolving 0.911 mg of HVA (Sigma-Aldrich) in 5 mL.

5-Hydroxytrypramine (5-HT) [Serotonin]

A 0.001 M stock solution was prepared by dissolving 0.811 mg of 5-HT (Sigma-Aldrich) in 5 mL.

5-Hydroxyindoleacetic Acid (5-HIAA)

A 0.001 M stock solution was prepared by dissolving 9.56 mg of 5-HIAA (Sigma-Aldrich) in 5 mL.

L-Tyrosine

A .05 M stock solution was prepared by dissolving 45.3 mg of L-tyrosine (Sigma-Aldrich) in 5mL.

L-Tryptophan

Was used as supplied from Sigma-Aldrich.

Glutathione

Was used as supplied from Sigma-Aldrich.

Dehydroascorbic acid (DHAA)

A 0.001 M solution was prepared by dissolving 0.871 mg of DHAA (Sigma-Aldrich) in 5 mL.

Ascorbic acid

Prepared the same as described above.

In vitro experiments were performed in pH 7.4 Phosphate Buffered Saline (PBS). The PBS solution was prepared using PBS tablets purchased from Sigma-Aldrich. The solution was prepared according to the manufacturer's instructions. The pH was then adjusted using sodium phosphate monobasic monohydrate and potassium phosphate dibasic until a pH of 7.4 was reached.

3.2.2. Equipment

Electronic balances

There were two balances used throughout the course of this work, a 5 decimal place balance CP225D from Sartorius®, AG Göttingen Germany, and a 4 decimal place balance Analytical Series from Fisher Scientific Hampton, New Hampshire, United States.

Microscope

The microscope used throughout this work was an Olympus SZ51 (Mason technology Ltd, Dublin).

Micropipettes

For the transfer of small volumes two Gilson pipettes were used, one P200 for volumes between 20-200 µL and a P1000 was used for volumes between 200-1,000 µL.

Water purifier

The double distilled deionised water was provided from a Milli-Q Direct 8 provided by Millipore Ireland BV, Tullagreen, Carrigtwohill, Co. Cork, Ireland.

Electrode wire

All wire for this work was sourced from Advent Research Materials (Advent Research Materials, Suffolk, UK).

pH meter

The pH meter used was an Eutech Instruments pH 510 (Mason technology Ltd, Dublin).

Sonicator

The sonicator used in this work was a FB11002 from Fisher Scientific Ltd.

3.2.3. Instrumentation and Software

In all experiments a custom designed low-noise potentiostat (Biostat IV, ACM Instruments, Cumbria, UK) was used. Data acquisition *in-vitro* was performed using a Dell notebook and either an eDAQ e-Corder (Green-leaf Scientific, Dublin) or a Powerlab 8/30 (ADInstruments Ltd, Oxford, UK) interface system. eDAQ chart (version 5, eDAQ Pty Ltd., NSW 2112, Australia) or LabChart for windows (version 8, ADInstruments Ltd) was used to visualise the raw data from the experiments. Data acquisition for *in-vivo* experiments were performed using an Apple iMac®, a Powerlab 8/30 (ADInstruments Ltd) interface system, and LabChart for IOS (version 8, ADInstruments Ltd).

3.2.4. Data Recording and analysis

LabChart 8 was used to record the data from all constant potential amperometry experiments. Once the raw data was obtained it was transferred to GraphPad Prism 9 (Version 8.2.0; GraphPad Software Inc., CA, USA) for analysis. All data was baseline subtracted (unless otherwise stated) and analysed using Michaelis-Menten equations[7] to calculate the enzyme kinetic parameters, V_{MAX} and K_M. The linear region was defined as $K_M/2$[8] and sensitivity defined as the slope of the line in this linear region which wis obtained via linear regression analysis. The data is expressed as mean ± SEM, where n is the number of sensors used. Statistical significance was determined either using *t*-tests or one-way ANOVA where appropriate. A p value < 0.05 indicates statistical significance.

3.3. The Electrochemical cell

All experiments performedin vitro were carried out in a standard three electrode electrochemical cell (*see* Figure.3.1.) containing 15 mL of PBS at room temperature (ca. 21 °C). The setup consists of an ACM Instruments (Cumbria, UK) four channel Biostat connected to a Saturated Calomel Electrode (SCE) which acts as the reference electrode, and Pt wire which acted as the auxiliary electrode. Then four working electrodes (typically biosensors) were connected and a potential of +700 mV vs. (SCE) was applied to monitor the production of H_2O_2. Calibrations were performed in PBS at a pH pf 7.4 to mimic physiological conditions. A stirring bead was used to ensure homogeneity when analytes were added to the solution.

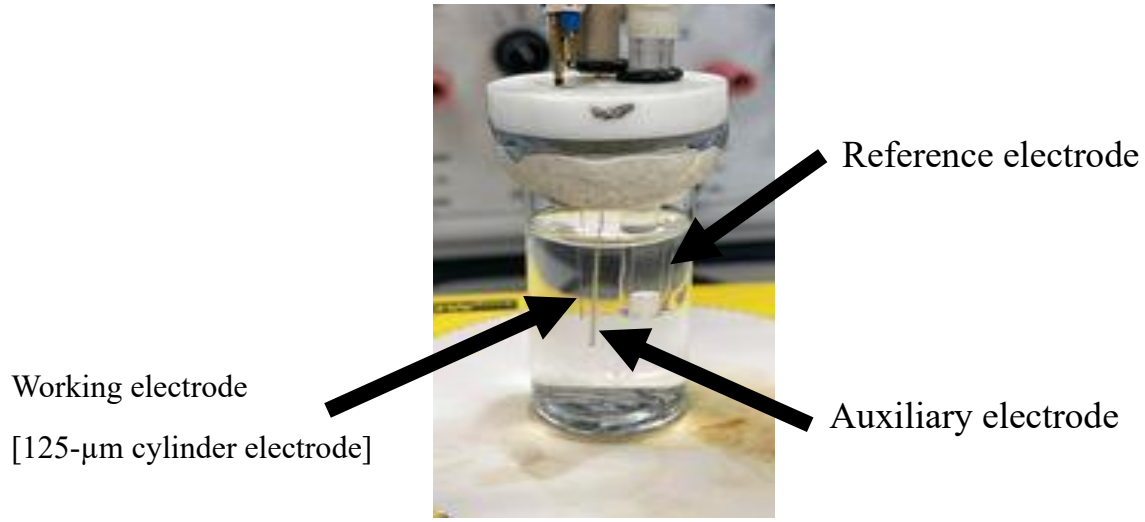

Figure 3.1 Three electrode electrochemical cell.

3.3.1. The bare Pt electrode

Pt cylinder ($Pt_{C)}$) electrodes were constructed using 5 cm lengths of Teflon® coated PT wire (125-µM, bare). Using a new scalpel blade a section of the Teflon® insulation was striped back under a stereo microscope, exposing approximately 2 mm of wire which is soldered into a gold clip, providing both electrical contact and rigidity to allow connection to the potentiostat. The active surface for a disc electrode (*see* Figure 2.3, bottom) is then made by carefully cutting the opposite end of the wire to create a disc surface. Cylinder electrodes (*see* Figure 2.3, top) were prepared by subsequently removing a 2mm portion of the insulation.

3.4. Experimental technique

The electrochemical method employed throughout the course of this work was constant potential amperometry (CPA). In short, a fixed potential is applied to the working electrode, in this case +700mV vs. SCE was used to monitor the production of H_2O_2. The current resulting from the oxidation of H_2O_2 can be related the concentration of lactate in solution.

3.4.1. Calibrations

Prior to beginning the calibrations all electrodes were allowed to reach stead-state current which took three to four hours on average. All calibrations followed the same procedure: an aliquot of the analyte was taken from the stock solution and added to the electrochemical cell, the solution was mixed for approximately 15 seconds, the next aliquot was then added when the current had reached a steady-state.

Ascorbic acid calibration

Aliquots were taken from the 0.1 M stock solution and injected to give the following concentrations:

200, 400, 600, 800, 1000 μM

Lactate calibration

Aliquots were taken from the 0.25 M stock solution of lactate until the following concentrations were reached:

5, 10, 15, 20, 30, 50, 100, 200, 300, 400, 500, 600, 700, 800, 900, 1000, 1500 μM

pH studies

The pH of the PBS solution used as the electrolyte in the electrochemical cell (typically 7.4) was changed using sodium phosphate monobasic monohydrate (to increase the pH to 7.6) and potassium phosphate dibasic (to decrease the pH to 7.2). Calibrations were run as previously described.

Interference studies

Preparation of all stock solutions and their respective concentrations are given in Section 3.2.1. Volumes of each interferent were added to give the concentrations shown in Table 3.1.

Interferent	Concentration (µM)
L-Cystine	4
Dopamine	0.05
uric acid	10
DOPAC	20
HVA	10
Serotonin	0.01
5-HIAA	50
L-Tyrosine	20
L-Tryptophan	20
Glutathione	50
DHAA	100
Ascorbic acid	500

Table.3.1. Showing concentrations (µM) of interferents to be added to cell.

Biocompatibility

All conditions were kept the same as used for the lactate calibrations. Following initial calibration sensors were stored in moist brain tissue for two weeks and then calibrated post storage.

Temperature

Temperature experiments were performed in 10 mL PBS (as opposed to 15 mL) using a jacketed cell (ALS Ltd, IJ Cambria Scientific Ltd, Llanelli, UK). The temperature of the cell (34°, 37° and 40° C) was maintained using a temperature-controlled water bath (Julabo Corio CD-BC4, Fisher Scientific, Dublin, Ireland).

O_2 dependence studies

O_2 dependence studies were performed using a bare Pt oxygen sensor that was previously calibrated at -650 mV vs. SCE. The biosensors were polarised at +700 mV vs. SCE. Initially, under a N_2 atmosphere the desired substrate concentration was achieved by adding an aliquot of stock into the solution, and upon reaching the steady-state response, one of two things was performed depending on the method being performed:

1) Bubbling method: air was slowly added into the electrochemical cell. This was slowly and carefully so as to not to introduce convection into the system and to avoid any of the solution wetting the electrodes. The [O_2] in the cell was determined using the O_2 calibration curve.

2) Injection method: O_2-saturated PBS was used for injections according to Table 2 for a 20 mL cell until the following concentrations were reached: (see Section 4.3).

0, 25, 50, 75, 100, 125 μM

Response time

The response time was defined as the time taken for the biosensor signal at a fixed concentration to rise from 10% to 90% of the maximum amplitude ($t_{10–90\%}$).

3.5. Biosensor construction

All sensors manufactured during this work used Pt wire as the transducer. The active surface was a 2 mm cylinder.

3.5.1. Cylinder electrode construction

The process for manufacturing a 2mm cylinder electrode is detailed in 3.3.1.

3.5.2. The P*o*PD layer

The monomer solution was prepared by dissolving 0.165 g of the *o*PD monomer in 5 mL of N_2 saturated PBS in a 5 mL volumetric that was also N_2 saturated. This is to prevent the oxidation of the monomer to allow a good polymer layer to be formed. Once the monomer was fully dissolved in the PBS, the 2 mm cylinder electrodes were placed in the electrochemical cell and a potential of +700 mV vs SCE was applied for 30 minutes to allow polymer formation.

3.5.3. Solution preparation for lactate biosensor preparation

Styrene

A small solution from the bottle was kept in an Eppendorf tube stored at 4 ^{o}C. Before biosensor construction the solution was allowed to reach room temperature.

1% (w/v) PEI solution

The solution of PEI was prepared by dissolving 0.031 g in 1 mL.

1% GA solution

40 µL of stock GA was dissolved in 1 mL.

1% BSA in 0.1% GA (BSA:GA)

0.01 g of BSA was dissolved in 0.4 mL H_2O. 0.1 mL of 1% GA was then added, and the solution was then made up 1 mL.

2% CA solution

0.02 g of CA was dissolved in a 1 mL solution of acetone and ethanol prepared using a 2:1 ratio of the respective liquids.

10 mM HEPES solution

A 10 mM HEPES solution was prepared by diluting 1 mL of the stock solution (200 mM) in 20 mL.

20 µM FMN solution

0.956 mg of FMN was dissolved in 10 mL H_2O. This yielded a 200 µM stock solution of FMN. 1 mL of this stock was diluted to 10 mL giving the final 20 µM solution of FMN.

Lactate oxidase solution

100 mg of LOx was dissolved in 1 mL of HEPES solution and 115 µL of the FMN solution was added. This was the dipping solution used in construction of the 100 mg LOx PCE biosensor. 1 mg of LOx was dissolved in 1 mL of HEPES solution and 115 µL of the FMN solution was added to prepare the dipping solution used in construction of the 1 mg LOx PCE biosensor.

Dialdehyde starch (DAS)

0.01 g of dialdehyde starch was dissolved in 1 mL H_2O creating a saturated solution.

Dialdehyde starch/GA

For dialdehyde starch/GA solutions the GA was added to a 1mL solution of saturated DAS, to yield the concentrations given in Table 3 and then made up to 1 mL with saturated dialdehyde starch solution.

% GA	Amount of GA added (µL)
0	0
0.01	10
0.05	50
0.075	75
0.1	100

Table 3.2. Volumes of GA required to make up different % solutions in DAS.

3.5.4. Enzyme immobilization by dip adsorption

Bare Pt sensors are prepared according to 3.3.1, once the bare electrode is manufactured various chemical layers are then used to modify the surface of the sensor to facilitate enzyme immobilisation/stabilisation, interference rejection etc. The first of these layers was P*o*PD which was electrochemically deposited onto the sensors surface from a solution of *o*PD monomer (300 mM in N_2 saturated PBS) following the method described in 3.5.2. This layer was allowed to dry for a minimum of 3 hours at room temperature (*ca.* 21 °C) before proceeding with the layering of other reagents using the dip-adsorption method. Briefly, the Pt/P*o*PD electrode were dipped into the immobiliser Sty (*ca.* 0.5 s) into LOx, PEI (1%) and a BSA:GA (1.0:0.1%) mixed solution and with 4 min drying time between each coating until the following design was achieved:

$$\text{Pt-P}o\text{PD-Sty-(LOx-PEI-BSAGA)}_{10}$$

The electrodes are then left to dry for 1 hour at room temperature where the following drying the came process is repeated, however during the last set of dips, following the tenth dip into the BSAGLU solution the sensor is dipped into CA (2%) resulting in the final PEC design:

$$\text{Pt-P}o\text{PD-Sty-(LOx-PEI-BSAGA)}_{10}\text{-Sty-(LOx-PEI-BSAGA)}_{10}\text{-CA}$$

The final sensor design is depicted below in Figure 3.2.below. These sensors were then stored overnight at 4° C before calibration. The only time this wasn't done is for shelf-life studies.

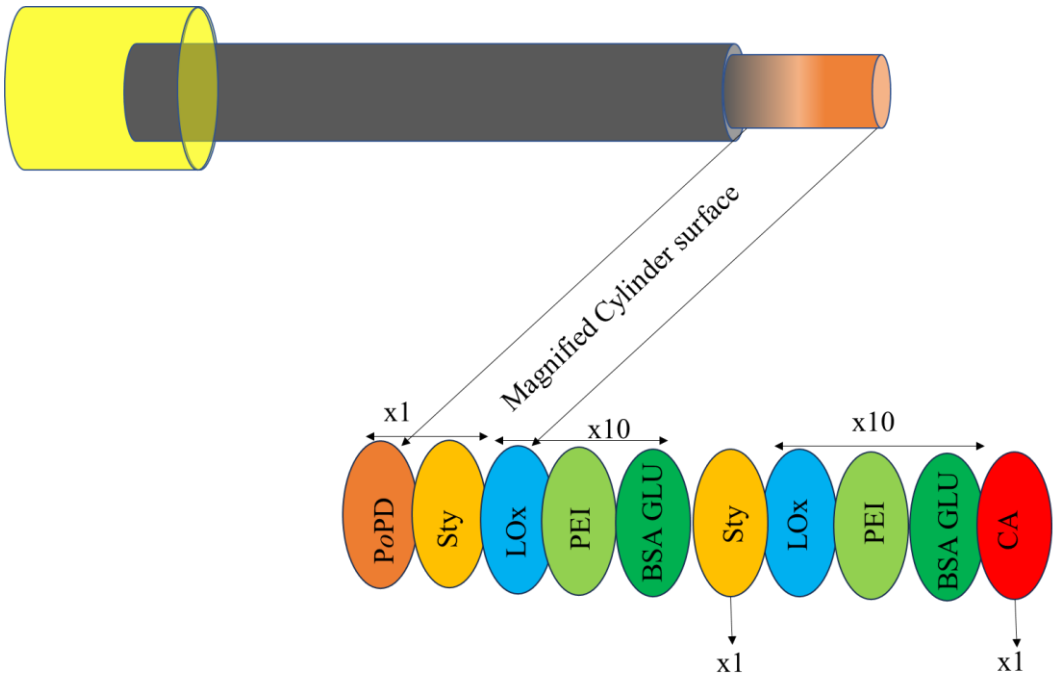

Figure 3.2 Final lactate polymer enzyme composite biosensor showing each layer.

3.5.5. Composite blank sensor

The composite blank sensor was made using the same method described in Section 3.5.4, however BSA was used instead of LOx.

3.6. In-Vivo equipment and solutions

This section details all aspects of the *in-vivo* experiments from the subjects to the equipment and solutions used and handling and surgery. All experiments during the course of this project were carried out with approval from Maynooth University Research Ethics Committee (BSRESC-2017-019) and under the license (B100/2205 and HPRA AE19214/PO19) in accordance with the European Communities regulations 2002 (Irish Statutory Instrument 556/2002 – Amendment of Cruelty to Animals Act 1876) and part 5 of the European Union (Protection of Animals Used for Scientific Purposes) Regulations 2012 (S.I 543 of 2012).

3.6.1. Subjects

The strain of rodent used throughout the course of this experimental work was Wistar (Rattus norvegicus) rats. Male rats were used to reduce the number of factors being included in the analysis and therefore reduce the total numbers of animals being used, and also to facilitate comparison with lactate biosensor data reported by other groups which to-date have all been performed in males. All animals were obtained from Charles River Laboratories International Inc, UK, and typically underwent surgery at around 250-350 g. Prior to surgery the animals were allowed to habituate and were subject to regular handling to help minimise stress. Rats were housed in large plastic bowls with a diameter of approximately 50 cm in a temperature and humidity-controlled room. The temperature was kept between 20-24 °C and humidity was kept between 45 and 65 %. The room was on a 12-hour dark light cycle with lights turning on at 7:00 and off at 19:00. All treatments were given during the light phase. Post-surgery animals were housed individually for no more than four consecutive days. After the four days they housed in groups to ensure appropriate social interaction and good welfare. From arrival to termination food and water was available ad libitum and environmental enrichment was provided.

3.6.2. In-vivo equipment

Anaesthetic set-up

There were multiple components of the set-up:

- The vaporiser used was a Univentor-400 anaesthetic unit.
- The air pump used was a Stellar S30.
- The induction chamber was a 1.4 L chamber.
- A gas routing switch.
- A stereotaxic inhalation mask.

All were provided by AgnThos, Sweeden.

Cables

The six pin flexible cables used were provided by Plastics One Ltd, Virginia, USA.

Stereotaxic frame

The stereotaxic frame was provided by Kopf Instruments Ltd, California, USA (Model 942).

Pulse oximeter

The two pulse oximeters used in this work were a Vet/Ox® (Heska Ltd, Barrie, Canada) and a H100 (Edan Ltd, Shenzhen, China).

Recovery chamber

The recovery chamber used in this work was a Thermacage MK II (Datesand Ltd, Stockport, UK).

Drill

The drill used for this work was a microspeed 317 (Silfradent, Sofia, Italy).

Microdialysis Probes

The microdialysis probes used throughout this project were BR2 (2 mm) brain microdialysis probes supplied from BASi (West Lafayette, IN, USA) .

Microdialysis Pump

The microdialysis pump used for all microdialysis experiments was a CMA 100 Microinjection Pump, supplied by Carnegie Medicine, Stockholm, Sweden.

3.6.3. Surgery

Rats were anesthetised with the volatile anaesthetic Isoflurane using a vaporiser (Univentor) at 4 % until sufficient anaesthetic depth was reached (typically between 3-4 min). The animal was then taken from the chamber where the hair from the centre line of the ears to the front of the eyes was shaved and a subcutaneous injection of buprenorphine (0.05 mg/kg) made up to 1 mL with 0.9 % sterile saline solution. The animal was then placed back in the induction chamber to ensure sufficient depth of anaesthesia before transfer to the stereotaxic frame. The animal was placed in the stereotaxic frame where its mouth was placed in the mouthpiece with an isoflurane flow rate of 2 %. The animal was tested for anaesthetic depth using both the pedal withdrawal reflex and tail pinch. A pulse oximeter is then placed on the animal's foot and the rectal probe was inserted. EMLA cream was then put on the ear bars, and they were inserted ensuring the animal was stable and level. 2 mL of lidocaine was then injected subcutaneously over the skull. The assistant then cleaned and gowned the surgeon to ensure a sterile environment. Once gowned an incision was made and the underneath layer of skin was broken using a cotton swab. Once this was done clamps were added to increase the surgical area. With the use of a marker and forceps bregma was found and marked.

From this mark all stereotaxic co-ordinates were referenced for implantation into the striatum:

Anterior-Posterior: +1

Medial-Lateral: ±2.5

Dorsal-Ventral: -5

Once these coordinates were found they were marked and then bore holes were drilled. Following these 5 other holes were drilled; three for screws for support and the other two for the reference and auxiliary electrodes respectively. Using the stereotaxic frame, the sensors were aligned by eye over the bore hole then using the microscope the sensors were lowered into the hole according to the coordinates given above. This was done on the other side for the second sensor. Then three anchor screws were put into the screw holes, and finally the auxiliary was screwed into place and the reference was placed into the it's hole by eye. A thin layer of cement was used to ensure all implanted electrodes were secured. Once the cement had sufficiently dried the electrodes were

removed from the arms and inserted into the plastic headpiece where they were cemented to ensure sensor stability. Finally, the surgical area was cemented to ensure the headpiece was secure, and that there were no gaps that the animal could get its paws under to remove the headpiece and no wires exposed. The animal was then removed from the stereotaxic frame and placed in a heated recovery chamber.

At the conclusion of each experiment, animals were euthanised with pentobarbital (Euthanimal, 800 mg/kg), decapitated and the head-pedestal was carefully removed. The brain was extracted and stored in 10% buffered formalin solution at 4 °C for future histological processing to confirm sensor placement for publications.

3.6.4. Microdialysis

The surgical procedure detailed in the previous section (3.6.4) was adapted for the implantation of a microdialysis (MD) probe. Each MD probe consisted of two hollow tubes, one inside of the other, allowing unidirectional flow of the perfusion media. A length of the dialysis membrane is exposed with a pore size that allows free diffusion of the solute molecules but not proteins or other macromolecules in the ECF. The MD probes were modified in-house to allow the combined implantation with a biosensor. This technique was particularly suited for the in vivo characterisation of the biosensor. The biosensor modified MD probes were prepared by gluing a pre-calibrated biosensor to the MD probe using epoxy, ensuring that the active area of the biosensor and probe were aligned. The distance between the sensor and MD probe was ca. 1 mm.

3.6.5. In-Vivo Solutions

Normal saline solution

A 0.9% solution of saline was prepared by dissolving 9 g of NaCl in 100 mL.

Lactate solution (for intraperitoneall injection (i.p.))

A solution of lactate was prepared by dissolving 0.169 g of lactate in 1.5 mL normal saline.

Ascorbate solution

Sodium ascorbate (2 g/kg) was dissolved in normal saline.

Artificial Cerebrospinal Fluid (aCSF)

aCSF was prepared by dissolving 8.6 g NaCl (0.15 M), 0.298 g KCl (0.004 M), 0.176 g $CaCl_2$ (0.0016M) and 0.204 g $MgCl_2$ (0.021M) in 1 L H_2O.

Lactate solution (MD)

A 1 mM solution of lactate was prepared for reverse microdialysis by dissolving 1.8 mg of sodium L-lactate in 20 mL aCSF.

3.7. Physiological stimulation

Tail-pinch

Three durations of tail pinch were used: one second, 1.5 minute and 5-minutes. A tweezers was used to administer the 1 s tail pinch. The 1.5- and 5-min experiments were performed by attaching a paperclip 2-3 cm from the tip of the rat's tail for the allotted time frame. This stimuli produces a well characterised behavioural pattern consisting of gnawing, licking earring and a general increase in locomotion[9]. To distract the rat from the paper clip a piece of wood was held in front of the rat's snout to encourage gnawing. Once the clip was on for the required amount of time the paperclip was quickly and carefully removed to minimise the stress on the subject.

3.8 References

(1) Bermingham, K. P.; Doran, M. M.; Bolger, F. B.; Lowry, J. P. Design optimisation and characterisation of an amperometric glutamate oxidase-based composite biosensor for neurotransmitter l-glutamic acid. Analytica Chimica Acta **2022**, 1224, 340205 .

(2) Doran, M. M.; Finnerty, N. J.; Lowry, J. P. In–Vitro Development and Characterisation of a Superoxide Dismutase-Based Biosensor. Chemistry Select **2017**, 2 (14), 4157-4164.

(3) Biryukova, E. N.; Arinbasarova, A. Y.; Medentsev, A. G. L-Lactate Oxidase Systems of Microorganisms. *Microbiology* **2022**, *91* (2), 124-132.

(4) Duncan, J. D.; Wallis, J. O.; Azari, M. R. Purification and properties of Aerococcus viridans lactate oxidase. Biochemical and Biophysical Research Communication **1989**, 164 (2), 919-926.

(5) Yorita, K.; Aki, K.; Ohkuma-Soyejima, T.; Kokubo, T.; Misaki, H.; Massey, V. Conversion of L-Lactate Oxidase to a Long Chain α-Hydroxyacid Oxidase by Site-directed Mutagenesis of Alanine 95 to Glycine. Journal of Biological Chemistry **1996**, 271 (45), 28300-28305.

(6) Stoisser, T.; Brunsteiner, M.; Wilson, D. K.; Nidetzky, B. Conformational flexibility related to enzyme activity: evidence for a dynamic active-site gatekeeper function of Tyr215 in Aerococcus viridans lactate oxidase. Scientific Reports **2016**, *6* (1), 27892.

(7) Leypoldt, J. K.; Gough, D. A. Model of a two-substrate enzyme electrode for glucose. Analytical Chemistry **1984**, 56 (14), 2896-2904.

(8) McMahon, C. P.; Rocchitta, G.; Kirwan, S. M.; Killoran, S. J.; Serra, P. A.; Lowry, J. P.; O'Neill, R. D. Oxygen tolerance of an implantable polymer/enzyme composite glutamate biosensor displaying polycation-enhanced substrate sensitivity. Biosensors and Bioelectronics **2007**, 22 (7), 1466-1473.

(9) Antelman, S. M.; Szechtman, H.; Chin, P.; Fisher, A. E. Tail pinch-induced eating, gnawing, and licking behaviour in rats: Dependence on the nigrostriatal dopamine system. Brain Research **1975**, 99 (2), 319-337.

Chapter 4- In Vitro Lactate

Chapter 4. In-vitro Lactate.

4.1. Biosensor design

This biosensor has been designed by building on experience from the previous development of polymer enzyme composite (PEC) biosensors for several important neurochemicals[1-5], where the core components (crossing-linking/stabilising agents and enzyme), layering strategies, and drying times of the composite design a were optimised to produce sensitive and reliable biosensors. A classical cylinder electrode design was used throughout the course of this work, as previously employed by the Lowry research group[4-8] and other groups for the monitoring of neurochemicals *in vivo*[9-11]. Layering of the core components was achieved by dip-adsorption. The surface modifications to the cylinder are as follows: a layer of poly-*ortho*-phenylenediamine (P*o*PD) is electrodeposited onto the sensor's surface, followed by a layer of Styrene (Sty), then 10 sequential layers of lactate oxidase (LOx), Bovine Serum Albumin/Glutaraldehyde (BSAGA), and Polyethylenimine (PEI), applied consecutively, with a 4-minute drying time between each complete coating sequence. The sensor is then allowed to dry at room temperature for an hour before a second styrene layer is applied followed by another 10 LOx-BSAGA-PEI layers. Finally, a layer of cellulose acetate (CA) is then applied. The resulting Pt-P*o*PD-Sty-$(LOx\text{-}PEI\text{-}BSAGA)_{10}$-Sty-$(LOx\text{-}PEI\text{-}BSAGA)_{10}$-CA is then allowed to dry overnight before use. Throughout this work two concentrations of enzyme are used 1 mg and 100 mg (*see* Section 3.5.3). The 100 mg design was the starting point building from the previous work. A schematic representation of the PEC biosensor is presented in Figure.2.5.

The Polymer/Enzyme Composite (PEC) lactate biosensor showed excellent sensitivity (0.882 ± 0.082 nA / μM, n = 12, R^2 = 0.708) and enzymatic parameters (V_{MAX} = 493 ± 18.8 nA and K_M = 248 ± 15.4 μM), and is compared with neurochemical lactate biosensors reported by other groups Table 4.1. The key to this sensitivity was the application of the BSAGA-PEI-CA layers. When used on its own GA may compromise the enzyme's activity due to its ability to form covalent bonds. To reduce the negative influences of GA, BSA is employed as it is a lysine rich enzyme which preferentially binds to GA helping to reduce the amount of GA interacting with the enzyme's active site and thus increasing substrate turnover. PEI is also incorporated to further enhance the performance by facilitating the neutralisation of electrostatic repulsion between the negatively

charged enzyme and the anionic lactate analyte. The biosensor showed good sensitivity and kinetic parameters, similar to that previously observed in its development work with a sensitivity of 1.06 ± 0.15 nA /µM (n = 8, R^2 = 0.982) and enzymatic parameters V_{MAX} = 639 ± 85 nA and K_M = 286 ± 63 µM[5]. As there was no significant difference between the sensitivities (p = 0.267), V_{MAX} (p = 0.058) and K_M (p = 0.491), we then commenced the characterisation process to determine if the integrity of the signal under *in vitro* conditions indicated suitability for the challenging environment of the brain.

Design	Geometry* / Dimensions (µm)	V_{MAX} (nA.cm^{-2})	K_M (µM)	Sensitivity (nA.cm^{-2}.µM^{-1})
Reference[12]	R, 50 x 150	-	-	119 ± 18
Reference[13]	C, 8 x 50	12.07 ± 0.76	970 ± 140	12.2 ± 0.4
Reference[14]	C, 30 x 500	-	-	9.15 ± 0.91
Reference[15]	C, 350 x 3000	-	-	10.4 – 26.7
PEC (100 mg LOx)	C, 125 x 2000	6163 ± 235	248 ± 15.4	11.03 ± 1.03
(PEC 1 mg LOx)	C, 125 x 2000	1912 ± 175	428 ± 99.0	3.03 ± 0.18

*Geometry R – rectangle, C – cylinder.

Table 4.1 Comparing sensitivities and enzymatic parameters of various lactate biosensor for neurochemical monitoring.

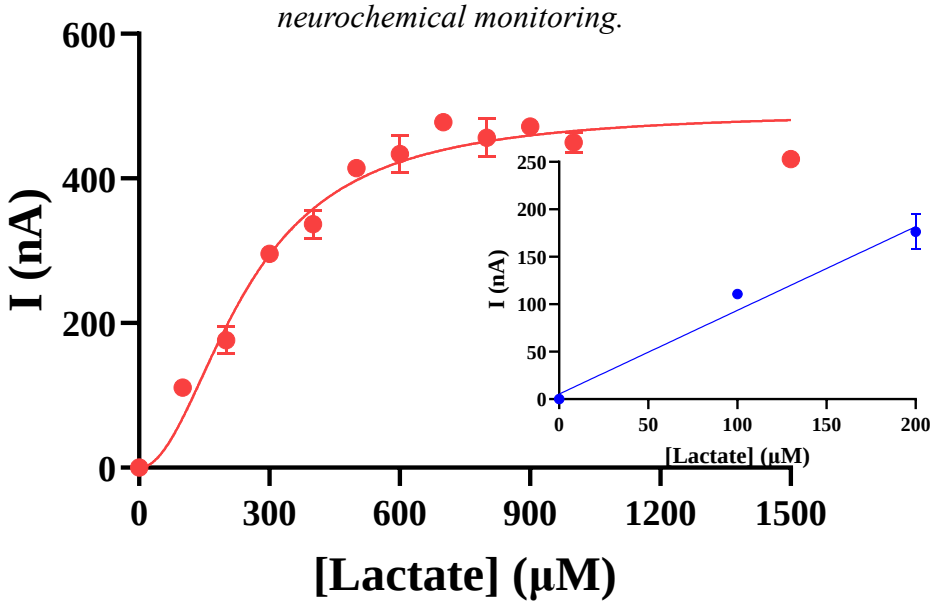

Figure 4.1. Current concentration profiles for lactate calibrations (0-1,500 µM) performed *in PBS (pH 7.4) using CPA at +700mV (vs. SCE) given as mean ± SEM (n = 12). Inset: Linear regression analysis (0-200 µM) used to determine sensitivity (Linear Region Slope, LRS).*

4.2. Interference

One of the crucial factors for successful *in vivo* neurochemical monitoring is selectivity. However, the mammalian brain is a harsh and complex environment consisting of a multitude of electroactive species and electrode poisons such as lipids, glycans and proteins, all of which can alter the response of the biosensor[16]. The principal electroactive interferent in the brain is ascorbic acid (AA), which can be detected at a bare Pt electrode at a sensitivity ca. 600 pA / μM at the potential required for H_2O_2 detection (+700 mV vs SCE)[17] and is present over a relatively large concentration range of 300-500 μM[18] in extracellular fluid (ECF). So, without proper interference rejection strategies the signal from the biosensor will prove unreliable and unusable.

To provide a reliable response free from interference a layer of P*o*PD was electrodeposited onto the surface of the electrode. P*o*PD was chosen due to its superiority with respect to the meta and para isomers[19], ability to improve biocompatibility[20], high permeability to H_2O_2[21,22] coupled with the "self-blocking" phenomenon[23,24] which can be seen in Figure 4.2, resulting in negligible AA interference at concentrations above 200 μM. The $I_{MAX,}$ which is the maximum current value, obtained during the course of an AA calibration on sensors with P*o*PD and I_{LIM} is the current value at the plateau (*see* Section 2.9) for the PEC lactate biosensor are 3.06 ± 0.35 nA and 0.31 ± 0.14 nA (n = 3) respectively. These values indicate minimum interference from AA, and compare well to the literature values of 3.5 ± 0.3 nA ($p = 0.611$) and 1.2 ± 0.2 nA ($p = 0.127$, n = 23) respectively for P*o*PD/BSA electrodes[23]. This suggests that the sensors should provide interference free lactate signals when implanted *in vivo*.

As AA can potentially also interfere with the sensor through a homogeneous mechanism involving H_2O_2 [25-27] a set of sensors were calibrated for lactate in the presence of 500 μM AA. This resulted in an LRS of 0.463 ± .011 nA / μM (n = 3), which was not significantly different to the control LRS obtained from normal calibrations like ones described previously (i.e. without AA) 0.551 ± 0.030 nA / μM (p = 0.052, n = 3). However, interference from the homogeneous mechanism *in-vivo* is highly unlikely due to the lack of ion catalysts in the brain[21].

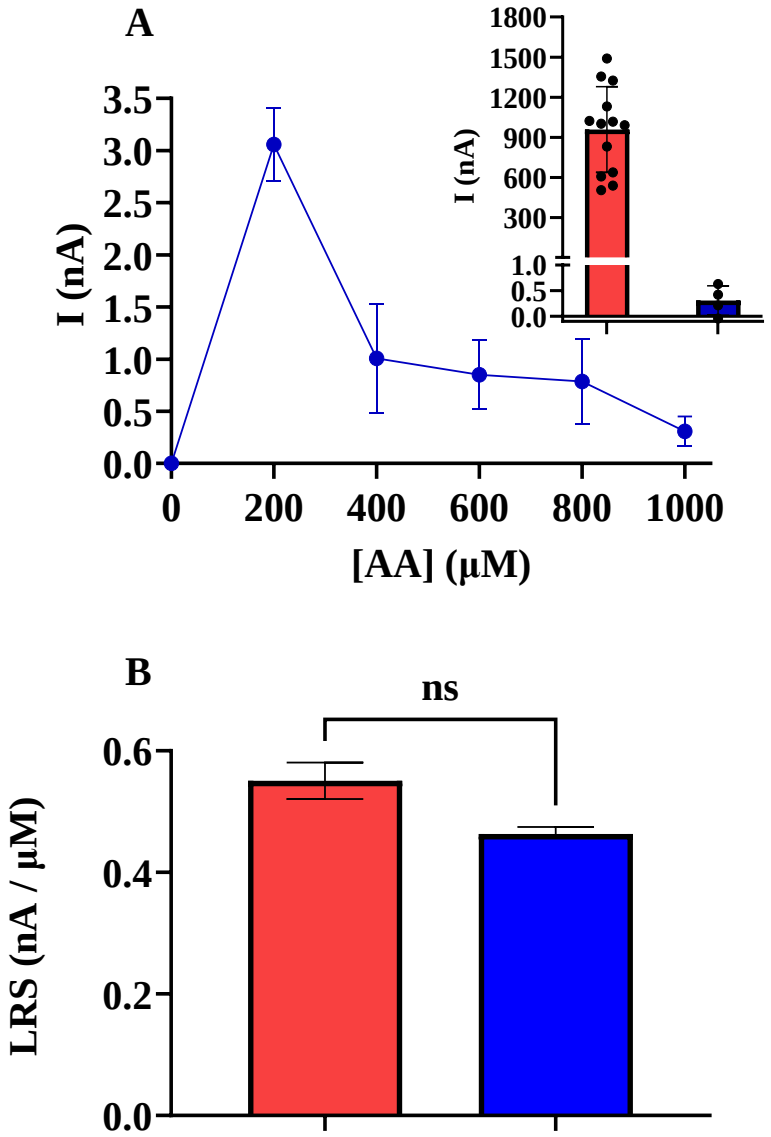

Figure 4.2. A. Current concentration profiles for AA calibrations (0-1,000 µM) performed *in PBS (pH 7.4) using CPA at +700 mV (vs. SCE) given as mean ± SEM (n = 3) Inset. Histogram comparing I_{LIM} values of bare Pt sensors (n = 13, red) and at PEC lactate biosensor (n = 3, blue) B. Comparison of the sensitivity (LRS, mean ± SEM) of control (n = 3, red) and calibration* performed *in the presence of 500 µM AA (n = 3, blue) using 100 mg LOx PEC lactate biosensor.*

4.3. O_2 Dependence

Another form of interference associated with first generation peroxide detecting biosensors is oxygen dependence[28], as oxidase enzymes require molecular oxygen as a co-factor (*see* Section 2.8). As a result, it is necessary when characterising a biosensor to ensure the enzymatic reaction isn't hampered by the levels of O_2 that will be encountered in the brain. Ensuring the sensors signal is reliable across physiological O_2 levels is a crucial step in sensor development. In the mammalian brain the physiological range for O_2 is ca. 40-80 µM[29,30] under normal physiological conditions,

with an average basal level of ca. 50 µM[29,31] Figure 4.3 shows the lactate versus O_2 correlation profile for the PEC biosensor at a fixed lactate concentration of 350 µM. This was chosen as it is close to the concentration of lactate in the ECF which has been reported as ~346 µM[32]. For O_2 dependence testing at the 100 mg PCE lactate biosensor bubbling was used (*see* Section 3.4.1, O_2 Dependence) .In short, the cell was held under a N_2 atmosphere where an aliquot of lactate was added to achieve the desired concentration, when steady-state was reached air was bubbled in and the lactate signal was recorded at the PEC lactate biosensor, with a bare Pt electrode used to monitor [O_2]. At air saturation the [O_2] is 200 µM. At 50 µM [O_2] 38.16 ± 6.63 % (n = 3) of the signal obtained at 200 µM [O_2] was observed, while at 100 µM [O_2] 83.30 ± 15.33 % (n = 3) was observed. This level of drop in sensitivity isn't sufficient for reliable monitoring of lactate *in vivo*; according to Gerhardt *et al.*, at 50 µM [O_2] the biosensor response should be 70-85% of the 200 µM [O_2] signal[12]. As this means the sensor is unsuitable for *in vivo* applications a redesign of the biosensor was required.

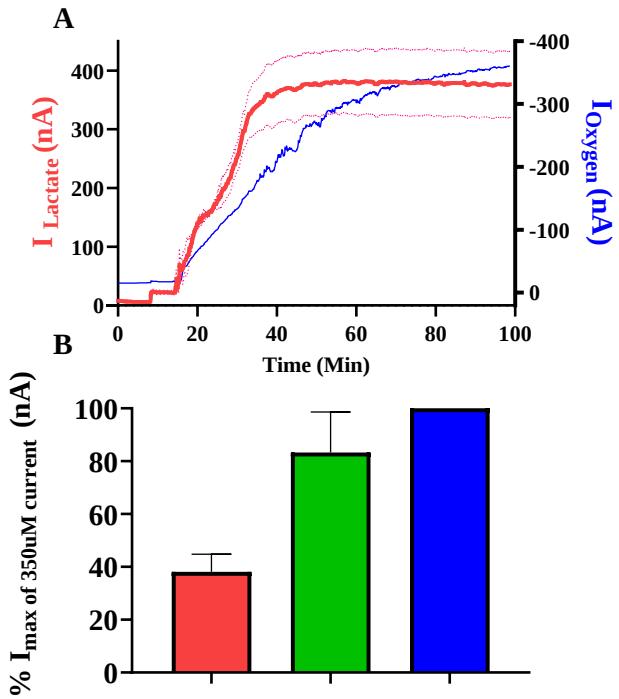

Figure 4.3. A. Typical raw data traces for the simultaneous detection of increasing [O_2] (blue, n = 1, 0-200 µM), in the presence of 350 µM lactate (red , n = 3, pink dashed lines represent SEM) performed *using CPA (+700 mV vs. SCE) in PBS (pH 7.4). B. Comparison of % current*

achieved at 50 (red), 100 (blue) and 200 (green) µM O_2 using 100 mg LOx lactate biosensor. Data normalised to 200 (green) µM response.

There are many ways to address O_2 dependence for first generation biosensors, such as the use of films that limit mass transport[33], or the use of "second-generation" biosensors, i.e. biosensors which replace oxygen with an artificial mediator[34]. A good example of a second-generation biosensor for lactate which incorporates methylene blue as the mediator has recently been reported by Antiochia *et al.*[35]. However, even though second-generation biosensors address the dependence on O_2, they tend not to be suitable for *in vivo* use primarily due to toxicity issues associated with mediator leaching, and interference arising from mediator selectivity[36,37]. As the PEC design already incorporates an outer diffusion limiting CA barrier we decided on an alternative strategy of decreasing the amount of enzyme used in the solution for dip evaporation from 100 to 1 mg/mL, thus reducing the enzyme loading and decreasing the demand for O_2[38,39].

The resultant 1 mg LOx lactate PEC biosensor had the expected drop in sensitivity (*see* Figure 4.4) with a K_M of 428 ± 99 µM, V_{MAX} of 153 ± 14 nA and LRS of 0.242 ± 0.014 nA/µM (n = 23). While these decreases were significant for both parameters (V_{MAX}: $t_{(33)} = 7.06$, $p < 0.001$; LRS: $t_{(33)} = 10.38$, $p < 0.0001$) when compared to the previous design (*see* Table 4.1), the device still retained good and sufficient sensitivity for potential *in vivo* applications.

The K_M showed no significant difference between the two designs ($t_{(33)} = 1.19$, $p = 0.245$) which is consistent with other PEI containing biosensors, and may be explained by reduced electrostatic repulsion resulting from reduced enzyme loading[40].

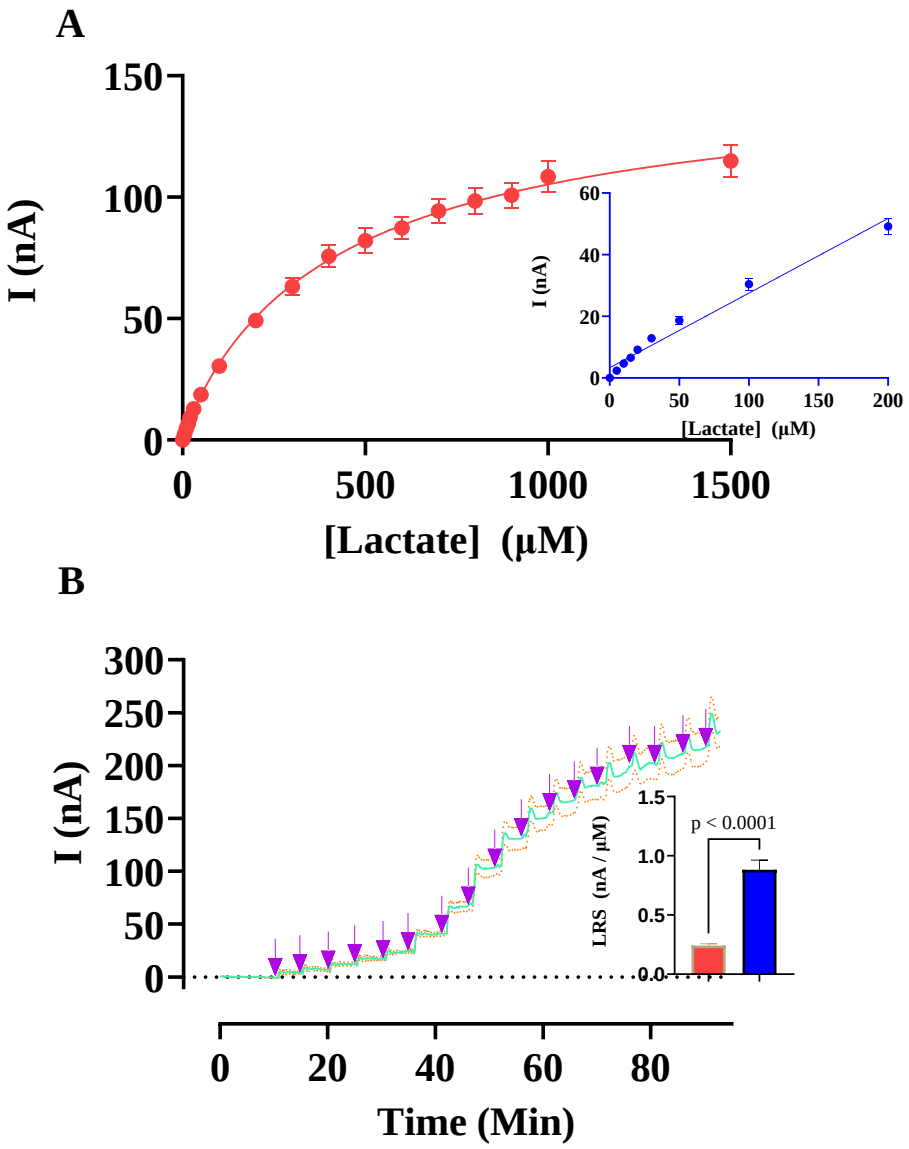

Figure 4.4. A. Current concentration profiles for lactate calibrations (0-1,500 µM) at the 1 mg LOx lactate biosensor performed *in PBS (pH 7.4) using CPA at +700 mV (vs. SCE) given as mean ± SEM (n = 23). Inset: Linear regression analysis (0-200 µM), given as mean ± SEM . B. Typical raw data trace for 1 mg LOx lactate biosensor. Arrows indicate injections yielding concentrations of 5, 10,15, 20, 30, 50, 200, 300, 400, 500, 600, 700, 800, 900, 1,000 and 1,500 µM of Lactate. Inset. Histogram comparing sensitivities (Linear Region Slope, LRS) of 1 and 100 mg LOx lactate biosensors.*

The oxygen dependence of the 1 mg LOx sensor was then tested as before. However, as the experimental protocol of continuous O_2 bubbling is very time consuming, we also used an alternative and more efficient method involving injecting aliquots of O_2-saturated PBS into the cell to produce the desired concentrations of O_2 (*see* Section 3.4.1, O_2 Dependence).

There was no significant difference (Figure 4.5.A) between the 50, 100 and 200 µM current values (*see* Table.4.2) 50 µM – $t_{(4)} = 7.74$, $p = 0.505$, n = 3; 100 µM – $t_{(4)} = 8.87$, $p = 0.650$, n = 3; 200 µM – $t_{(4)} = 8.19$, $p = 0.62$, n = 3) determined using both methods, and as such all values for each concentration were combined (Figure 4.5.B): 50 µM – 76.1 ± 12.1, n = 6; 100 µM – 91.6 ± 13.5, n = 6; 200 µM – 100 ± 14, n = 6.

Method		**50 µM O_2**			**100 µM O_2**			**200 µM O_2**	
	Mean	*SEM*	*n*	*Mean*	*SEM*	*n*	*Mean*	*SEM*	*n*
Bubbling	79.0	14.1	3	91.4	15.3	3	100	14	3
Injections	72.6	22.2	3	91.9	26.2	3	100	28	3
Combined	76.1	12.1	6	91.6	13.5	6	100	14	6

Table 4.2 Showing data obtained from different methods of performingO_2 dependence studies.

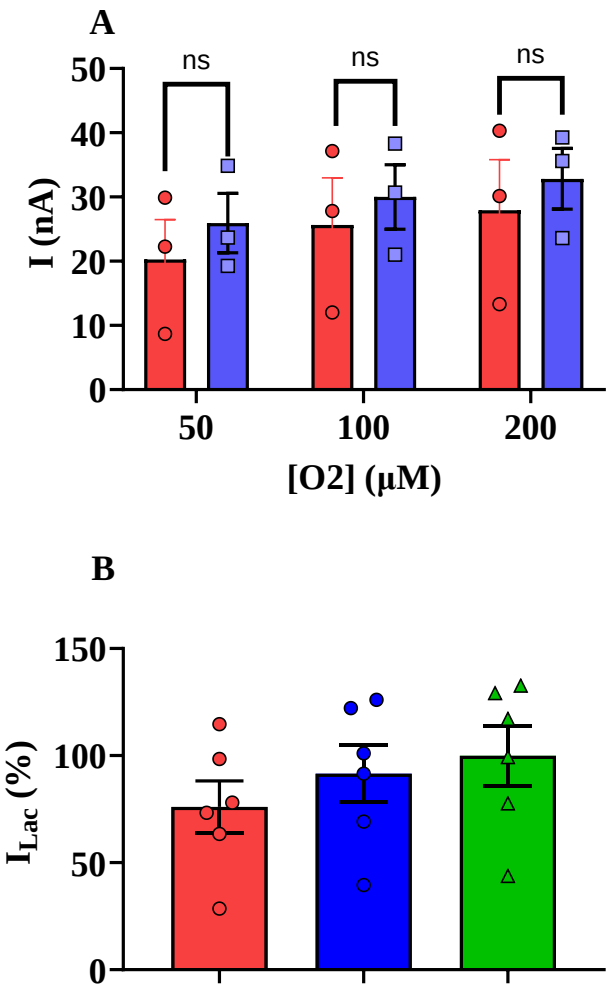

Figure 4.5.A. Comparison of injection (red, n = 3) vs. bubbling (blue, n = 3) for O_2 dependency testing on lactate biosensor using 350 µM lactate. B. Comparison of O_2 dependency combining both methods at 50 µM O_2 (red, n = 6), 100 µM O_2 (blue, n = 6) and 200 µM O_2 (green, n = 6).

The 1 mg LOx lactate biosensor showed a much-improved O_2 dependence; at 50 µM the response was 76.1 ± 12.1 % (n = 6) of that at 200 µM (air-saturated concentration) which is a significant improvement over the previous design prepared using 100 mg LOx, and at the levels appropriate for *in vivo* applications[12].

Given this positive result we also quantified the oxygen dependence by examining the effect of O_2 on basal lactate over an extended range of O_2 levels (Figure 4.6) in order to determine $K_M(O_2)$[1, 2].The smaller the $K_M(O_2)$ value the lower the O_2 dependence as higher O_2 affinity leads to O_2

saturation at lower pO_2, thereby reducing biosensor dependency at higher pO_2 levels. The calculated value of 39.4 ± 17.5 µM (n = 6) suggests minimal dependence on O_2 at basal levels.

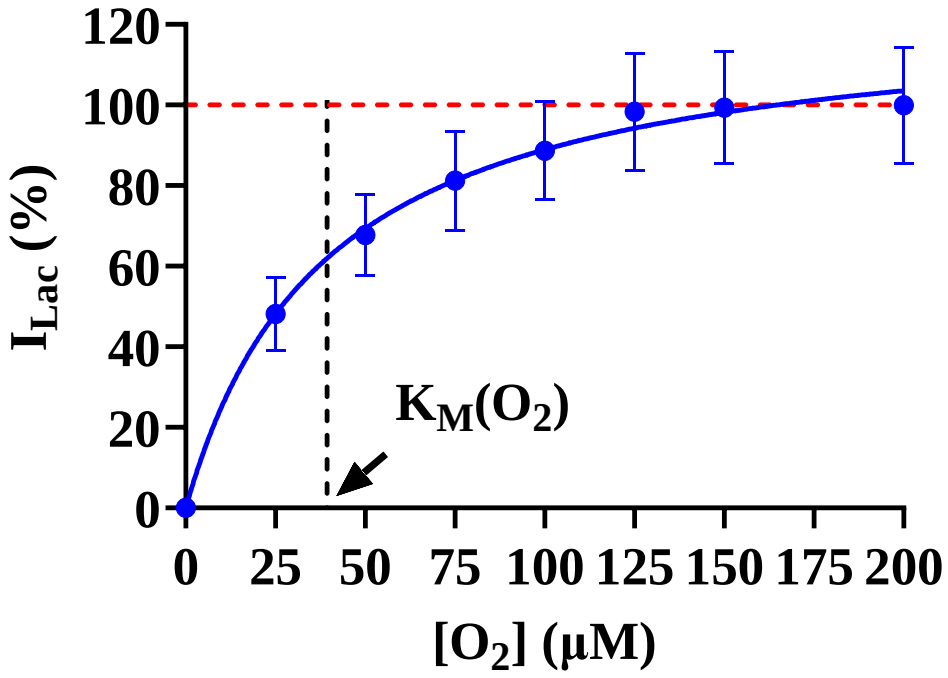

Figure 4.6. The effect of changing oxygen levels (0-200 µM) on the averages normalised lactate biosensor signal for 350 µM lactate (n = 6). Non-linear regression analysis yielded a $K_M(O_2)$ of 39.4 ± 17.5 µM.

In order to understand how *in vivo* changes in both O_2 and lactate would affect the signal we used data for grooming from the literature. This natural behaviour has previously been shown to result in maximum increases of 50 ± 9 % for O_2 (*see* Figure 4.7)[41] and 39 ± 4 % for lactate (*see* Figure 4.8[32]), corresponding to concentrations of 25 µM and 137 µM assuming basal levels of 50 µM and 350 µM respectively.

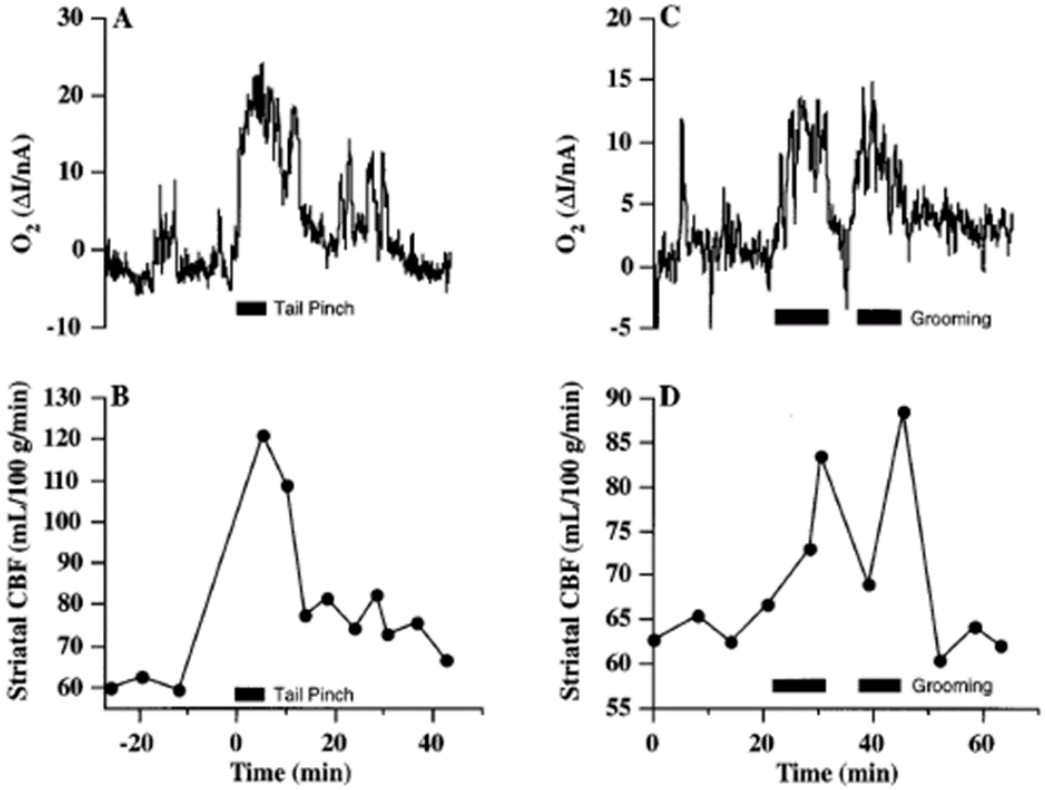

Figure 4.7. Typical examples of the effect of a 5-min tail pinch (dark bar, A and B) and induced grooming (dark bar, C and D) on striatal O_2 and blood flow levels monitored simultaneously with bilaterally implanted carbon paste (O_2) and Pt/Ir (H_2 clearance) electrodes. Absolute currents (ΔI) for O_2 reduction recorded using differential pulse amperometry are shown in each case. Baseline currents of 190 nA (tail pinch) and 165 nA (grooming) have been subtracted. Reproduced from[41] with permission from author.

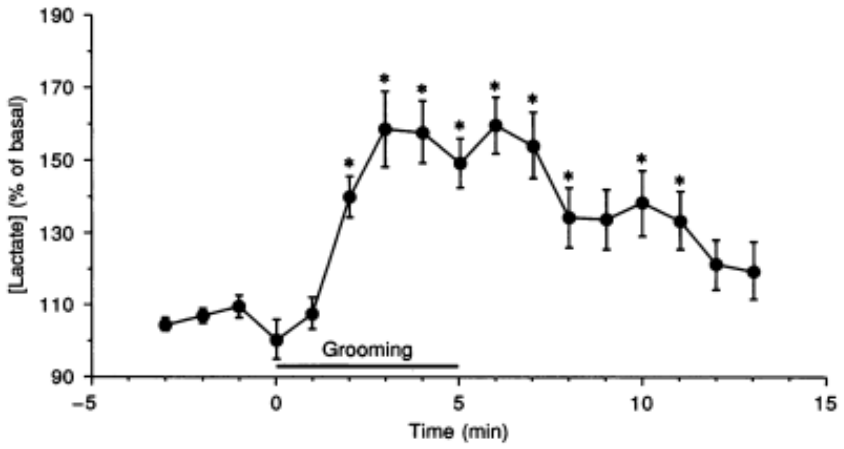

*Figure 4.8. The dialysate lactate concentration is shown as a percentage of basal. Points are means + S.E.M. * P < 0-05, compared with last basal value before stimulus; paired t test using absolute values (n = 16). Reproduced from[32] with permission from author.*

As such, we performed an O_2 profile study for 500 µM lactate (Figure 4.9), the peak concentration observed for grooming. At 75 µM O_2 (peak for grooming) the response was 68.2 ± 4.9 % (n = 9) of that at 200 µM, which is similar to that observed at basal levels of both molecules ($t_{(13)} = 0.689$, $p = 0.5030$).

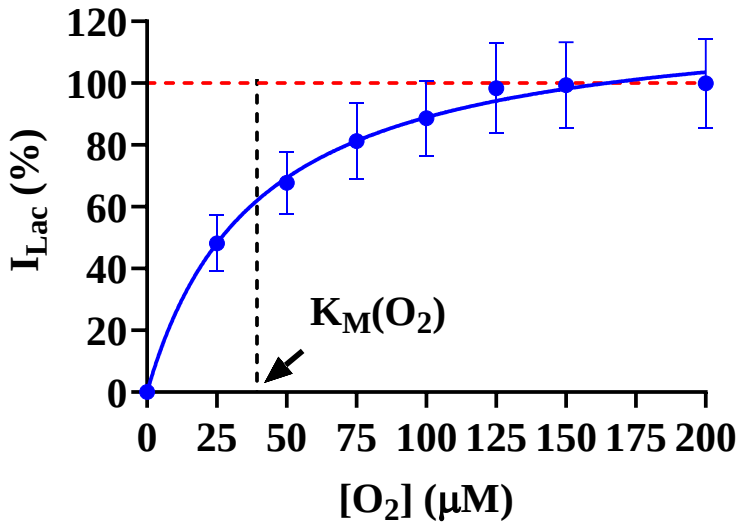

Figure 4.9. The effect of changing oxygen levels (0-200 µM) on the averages normalised lactate biosensor signal for 500 µM lactate (n = 9). Non-linear regression analysis yielded a $K_M(O_2)$ of 40.4 ± 16.1 µM.

This suggests that increases in O_2 and lactate under conditions of normal physiological behaviour compensate to maintain an interference free signal. A conclusion supported by the fact that there was no significant difference ($t_{(13)} = 0.041$, $p = 0.9679$) in the calculated $K_M(O_2)$ values: 40.4 ± 16.1 µM (Peak, n = 9) *vs.* 39.4 ± 17.5 µM (Basal, n = 6). Although *in vitro* studies indicate that O_2 dependence typically becomes more acute at higher concentrations of analyte[2,30,42,43] with $K_M(O_2)$ increasing linearly with concentration, the data presented here suggests that this is not the case for physiological increases in lactate. Noteworthy, is that Shram *et al.*[44] found non-significant O_2 dependence at an LOx-modified carbon fibre biosensor up to concentrations of 1 mM lactate.

4.4. Interference Studies

To ensure there was minimal interference at the 1 mg LOx PEC biosensor it was decided to perform interference testing using several endogenous species known to be potential interferents[2,17,45]. As explained previously, AA is the principal electroactive interferant in the brain and as such this was tested along with its metabolite dehydroascorbic acid. Amino acids were tested such as L-cystine[46], L-tyrosine and L-tryptophan. Uric acid[47] and dopamine were also tested[2,48], for a complete list of compounds tested and their concentrations see Table 4.3. The PEC lactate biosensor showed minimal interference from AA (Figure 4.10 ,ca. 3 % of the lactate signal) as found previously with the 100 mg LOx design, with all other potential interferents showing a response of lesser magnitude then that to AA. In some cases there was no or a negative response, these can be attributed to baseline drift/random noise[17, 49].

Species	n	Concentration (µM)	Current response (nA)	Signal as a % of 350 µM lactate response
Lactate	8	350	35.1 ± 3.82	100 ± 11
Ascorbic acid	20	500	0.998 ± 1.04	2.80 ± 2.92
L-cystine	16	60	-3.27 ± 1.15	-9.18 ± 3.24
L-tyrosine	16	6	0.234 ± 0.556	0.66 ± 1.56
Uric acid	16	10	-1.64 ± 0.662	-4.62 ± 1.86

DOPAC	16	20	0.892 ± 0.421	2.51 ± 1.82
Glutathione	16	50	-0.401 ± 0.480	-1.23 ± 1.35
DHAA	16	100	-2.95 ± 1.40	-8.29 ± 3.93
5-HIAA	16	50	-3.59 ± 0.681	-10.1 ± 1.91
L-tryptophan	16	20	0.036 ± 0.586	0.101 ± 1.65
HVA	16	10	-0.709 ± 0.671	-2.00 ± 1.89
Dopamine	16	0.05	0.328 ± 0.332	0.921 ± 0.932
Serotonin	16	0.01	0.046 ± 0.288	0.128 ± 0.639

Table 4.3. Response of the 1 mg LOx PEC biosensor to physiological lactate and various potential interferents at physiological levels found in vivo, where known.

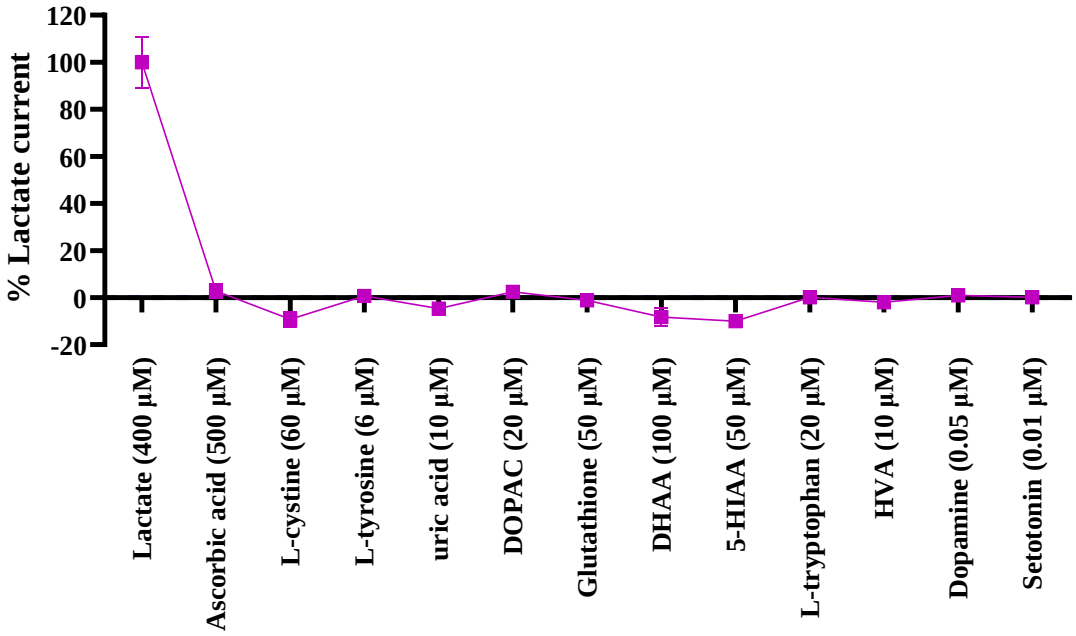

Figure 4.10 Mean (± SEM, n = 8) of normalised PEC lactate biosensor response to 350 µM lactate followed by sequential injections of a series of common potential interfering neurochemicals (see Section 4.4).

4.5. pH and Temperature

The previous calibrations in this body of work have established the 1 mg LOx lactate PEC biosensor's response at pH 7.4 and at room temperature, and the sensors' ability to provide a signal free from interference by endogenous electroactive compounds or changes in [O_2]. As such it is necessary to show that the sensor shows no appreciable changes across other physiological conditions it may experience during implantation. Therefore, it is necessary to characterise the sensor's response to potential fluctuations in pH and temperature associated with behavioural and pharmacological interventions. In freely moving animals, physiological temperature ranges between 35.5 - 38.8 °C[50], with maximum temperature of ~ 40 °C being reached during amphetamine administration[51,52] , and lows of 32-33 °C following administration of pentobarbital[50, 53]. Physiological pH in the brain ranges between 7.2 - 7.6[17]. Figure 4.11 shows the effect of altering the pH on the sensor's performance. There was no significant difference ($F_{(2,45)}$ = 3.12, p = 0.05, one-way ANOVA) in the LRS: pH 7.2 (0.272 ± 0.020 nA/μM, n = 14), pH 7.4 (0.242 ± 0.014 nA/μM, n = 23) and pH 7.6 (0.207 ± 0.012 nA/μM, n = 11).

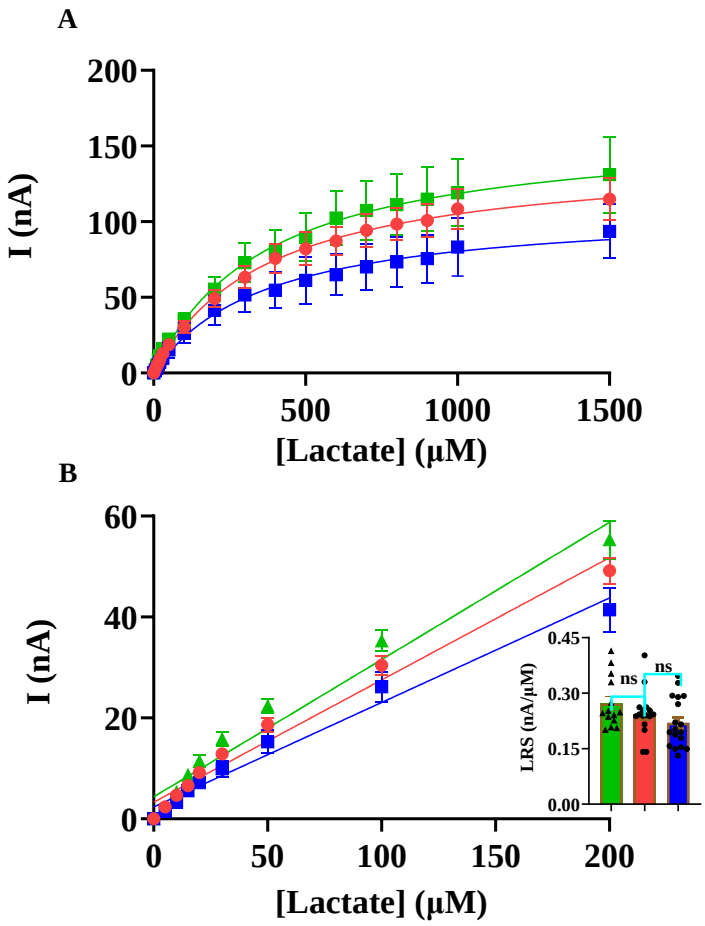

Figure 4.11 A. Current-concentration profile for lactate calibrations (0-1,500 µM) in PBS at different pHs according to those potentially experienced in the brain; pH 7.2 (green, n = 14), 7.4 (red, n = 23) and 7.6 (blue, n = 11). Calibrations performed at room temperature using CPA at +700 mV (vs. SCE) with given as mean ± SEM. B. Linear regression analysis (0-200 µM) used to obtain LRS (sensitivity). Inset. Comparison of sensitivities of PEC lactate biosensor across physiological pH range.

The effect temperature has on the sensor is shown in Figure 4.12. No significant difference ($F_{(3,37)}$ = 1.14, p = 0.027, one-way ANOVA) in sensitivity was observed: room temperature (0.242 ± 0.014 nA/µM, n = 23), 34 °C (0.266 ± 0.010 nA/µM, n = 6), 37 °C (0.301 ± 0.014 nA/µM, n = 4), and 40 °C (0.259 ± 0.015 nA / µM, n = 8). This suggests that the sensor has the ability to measure lactate in freely moving animals without interference from fluctuations in pH and temperature, similar to previously reported lactate biosensors published by Shram *et.al.*[14], Mora *et. al.*[13] and

Wilson *et. al.*, and polymer enzyme composite sensors for other neurochemicals such as choline[17] and glutamate[2].

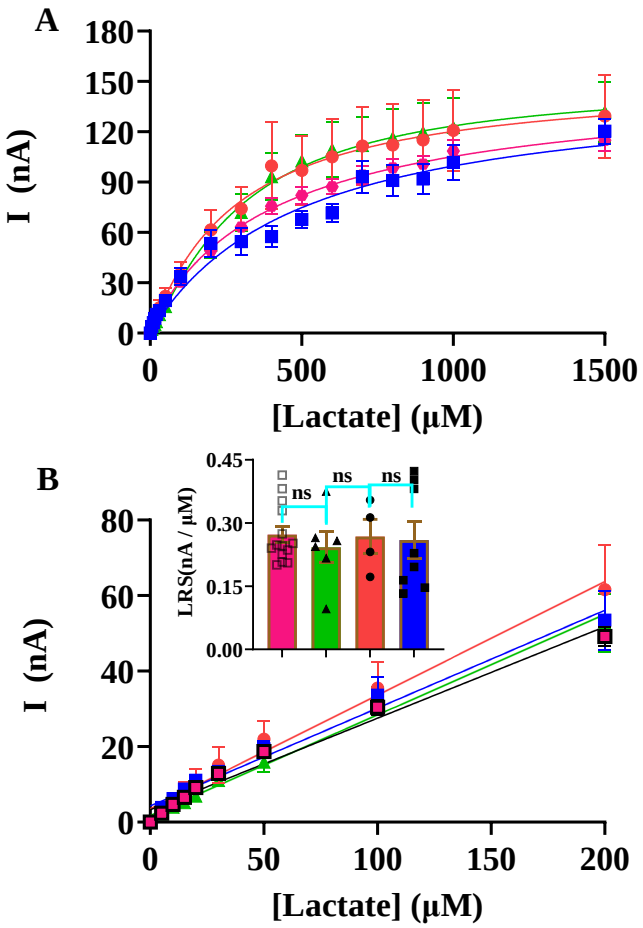

Figure.4.12.A. Current-concentration profile for lactate calibrations (0-1,500 µM) in PBS (pH 7.4) at Room temperature (pink ,n = 23),34 °C (green, n = 6),37 °C (red, n = 4) and 40 °C (blue, n = 8) using CPA at + 700 mV(vs. SCE) given as mean ± SEM. B. Linear regression analysis (0-200 µM) used to obtain LRS (sensitivity). Inset. Comparison of sensitivities of PEC lactate biosensor across various temperatures.

4.6. Stability, biocompatibility, Limit of Detection (LOD) and Response time (Rt)

One of the most important properties to quantify is the interactions between the electrode and its target environment[54,55]. This is of particular importance for sensors intended for harsh environments such as the brain. The brain is a complex chemical matrix, consisting of electrode poisons (proteins), surface modifying agents such as surfactants (lipids) and electrocatalysts such ascorbic acid and glutathione[16]. This may compromise the sensitivity of the implanted biosensor, and as such the biocompatibility of the lactate biosensor was tested. Each set of sensors was calibrated, stored in moist brain tissue for a period of 14 days, and a second calibration performed. A small non-significant change of + 0.002 ± 0.004 nA/µM in the LRS (Figure 4.13A) was observed ($t_{(5)}$ = 0.739, p = 0.934, n = 6) between the pre (0.185 ± 0.011 nA/µM, n = 6) and post (0.187 ± 0.015 nA/µM, n = 6)) calibrations. This suggests potential reliable monitoring of lactate *in vivo*.

A critical characteristic that also needs to be considered for a biosensor is the time over which the sensor will be expected to operate. Stability is the parameter used to measure the longevity of the sensor[2,17]. While repeated calibrations have been shown to decrease the sensitivity of some biosensors (e.g. for choline[56]), it was not observed for the lactate biosensor, with no significant decrease in sensitivity found (Figure 4.13B). Sensors calibrated on day one (0.386 ± 0.029 nA/µM, n = 5), seven (0.339 ± 0.030 nA/µM, n = 5) and fourteen (0.289 ± 0.015 nA/µM, n = 5) days after fabrication showed no significant change ($F_{(2,12)}$ = 3.66, p = 0.057, n = 5) across the three calibrations.

Limit of detection (LOD) was determined from three times the standard deviation of the baseline signal divided by the LRS[2,17,22]. The LOD determined for the lactate biosensor is 0.153 ± 0.098 µM (n = 8), which is an improvement compared to the LODs reported for other lactate biosensors by Smith *et. al.*, (7.0 ± 0.7 µM)[48] and Mora *et. al.* (1,200 µM) intended for neurochemical monitoring. This suggests that this sensor has sufficient sensitivity to measure lactate changes *in vivo* and to allow such changes to be correlated to behaviour.

The response time for a biosensor is defined as the time taken for the response to raise from 10 % to 90 %. In classical electrochemical studies, such as the ones performed here, it is a challenge to separate the mixing time from the response time. A typical raw data trace for the lactate biosensor is shown in Figure 4.13C. The response time obtained for this sensor was ~ 18 seconds with a ten-

second mixing time used (*see* Section 3.4.1, Response time). However, *in-vitro* response times aren't necessarily representative of response times of implanted devices. Similar PEC biosensors have been reported with response times close to or less than the mixing time *in vitro*. These demonstrated sub-second response times when characterised *in vivo*[43], and as such it is not unreasonable to expect a similar case for this (lactate) biosensor[42,57,58].

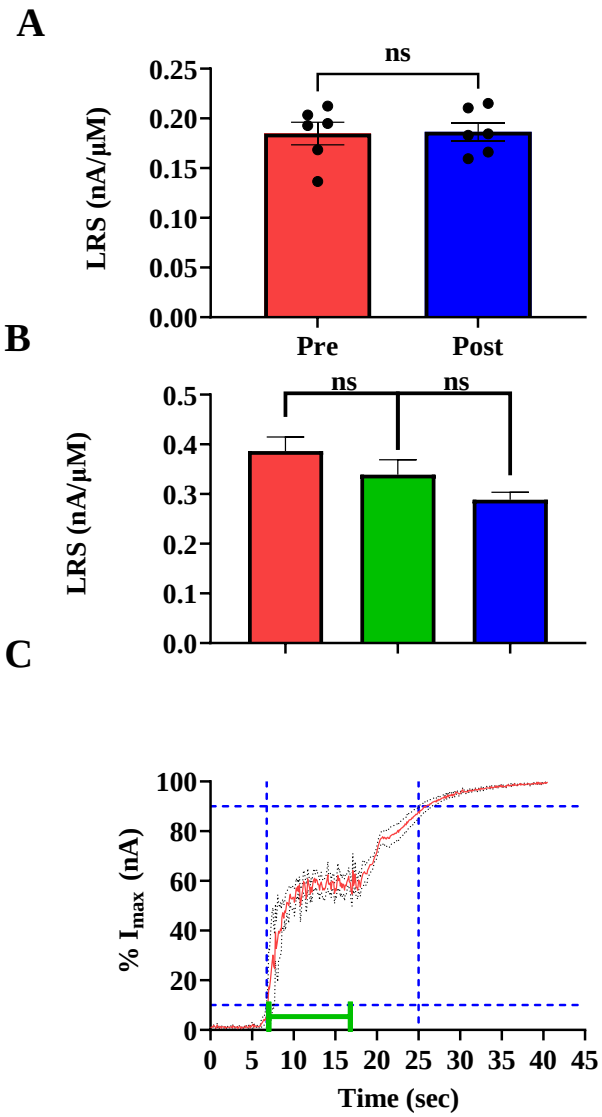

Figure 4.13.A. The effect of two weeks storage in ex-vivo rodent brain tissue at 4 °C on the 1 mg PEC lactate biosensor sensitivity (LRS, Mean ± SEM, n = 6). B. Comparison of sensitivities (n =5) for a batch of biosensors measured following dry storage at 4 °C between initial calibration on Day 1, and repeated calibrations on Days 14 and 28. C. A typical example of the average (n

= 4, black dashed lines represent the SEM) normalised current change (response time, $t_{10–90\,\%}$) for a lactate injection (5 μM, red line) performed at room temperature. Green bar represents stirring period.

4.7. Dialdehyde starch investigation

In an attempt to extend the K_M and therefore the LRS of the PEC lactate biosensor it was decided to lower the amount of GA and replace it with dialdehyde starch (DAS), similar to work done with a choline biosensor by Xin and Wightman[59]. They had shown that using the larger crosslinking agent (DAS) allowed less GA to be used which resulted in a higher enzyme activity. As DAS is a larger molecule it was concluded that it didn't affect the 3-D structure of the enzyme resulting in an increased K_M. As such, it was decided to see if DAS might increase the K_M of the lactate sensor allowing it to have an increased linear range. The sensors were constructed using the dip adsorption method as described in Section 3.5, however instead of using the usual GA solution DAS/GA solutions were made up according to Table 3.2, and then BSA was added to create the biosensors shown in Table 4.4. The enzymatic parameters and sensitivity (LRS) resulting from lactate calibrations performed with the DAS-modified biosensor are presented in Table 4.1, and graphically in Figure 4.14.

As can be seen in Figure 4.14.B. there was no significant increase in the K_M for the different concentrations of GA in DAS ($F_{(5,44)} = 23$, $p = 0.999$). This was not what we were hoping for, however there were improvements in the V_{MAX} and the LRS of the lactate biosensors (*see* Figure.4.10A and Figure 4.14C respectively). There was an ~300 % increase in the LRS and V_{max} for the design that incorporated the lowest amount of GA in saturated DAS. While the overall goal of increasing the K_M of the biosensor wasn't achieved, these results showed a good improvement in the sensitivity of the biosensor which warrants more investigation to see if the LRS and V_{Max} will continue to increase with decreasing the amount of GA in saturated DAS. This increase in

sensitivity also opens up methods that would increase the K_M of the sensor by reducing the sensitivity, e.g. the addition of diffusional barriers[60].

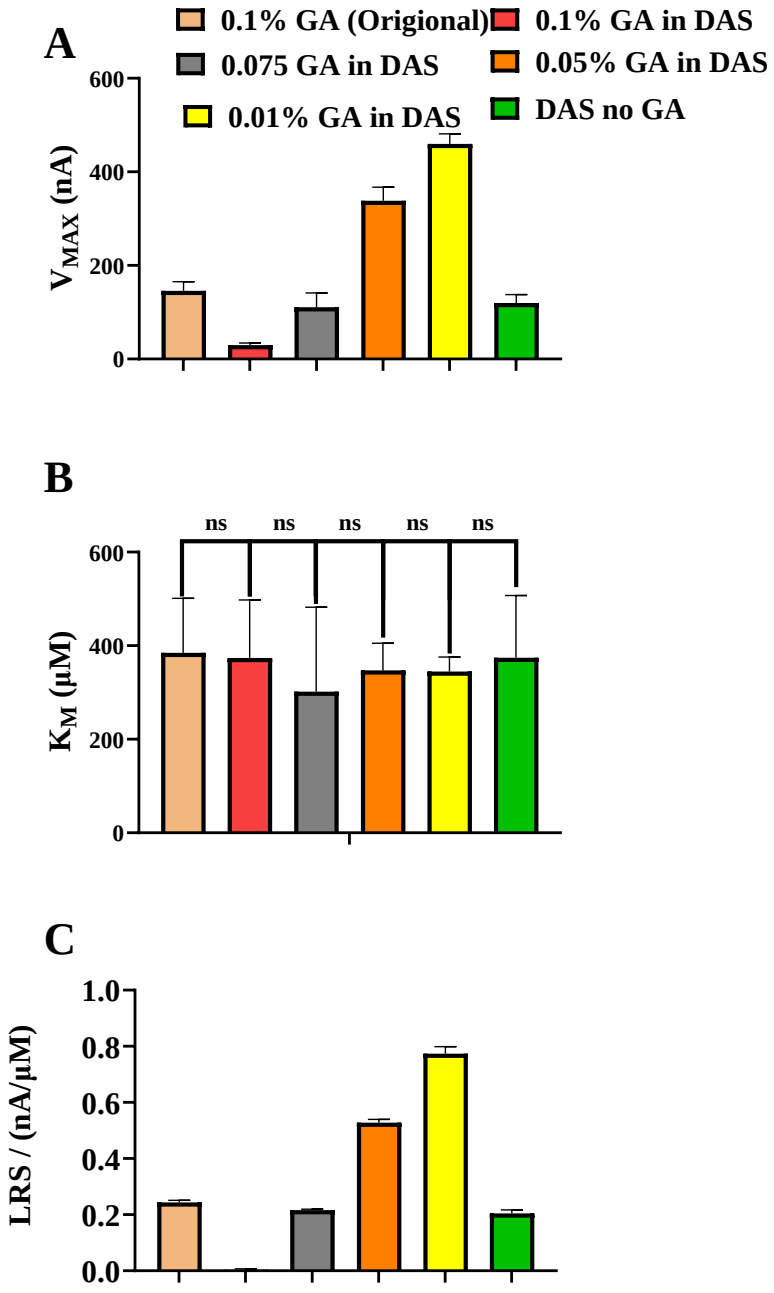

Figure 4.14. Histograms comparing the A. V_{MAX} B. K_M and C. LRS of biosensors incorporating different amounts of GA in DAS, all resulting from calibrations performed *in PBS (pH 7.4) at room temperature using CPA at +700 mV (vs. SCE).*

Design	n	V_{MAX} (nA)	K_M (µM)	LRS (nA/µM)
0.1% GA (original design)	23	146 ± 19.7	385 ± 116	0.224 ± 0.007
0.1% GA in DAS	7	29.7 ± 4.8	374 ± 124	0.004 ± 0.004
0.075% GA in DAS	4	110 ± 30	302 ± 181	0.216 ± 0.004
0.05% GA in DAS	4	338 ± 29	347 ± 58	0.528 ± 0.012
0.01% GA in DAS	8	460 ± 22	345 ± 31	0.773 ± 0.025
DAS (0% GA)	4	120 ± 18	374 ± 133	0.204 ± 001

Table 4.4. Comparison of enzymatic parameters (K_M and V_{MAX}) and sensitivity (LRS) of lactate biosensor designs incorporating different amounts of GA in saturated DAS .

4.8. Conclusions

This chapter described the *in vitro* characterisation of a LOx microelectrode biosensor for the real-time neurochemical monitoring of lactate. The original design which included 100 mg of LOx showed good sensitivity and selectivity but was hampered by its dependence on [O_2]. This was overcome by reducing the amount of LOx used from 100 mg to 1 mg. This design was then retested to ensure sufficient sensitivity and selectivity. The sensor displayed minimal interference from a range of potential endogenous electroactive interferents found in the brain. It also showed little oxygen dependence for basal and levels of lactate associated with physiological stimulation *in vivo*. Additionally, the sensor showed minimal change in response when tested over physiologically relevant pH and temperature ranges, which suggests this composite biosensor may be able to reliably monitor lactate in freely-moving animals. This is examined in the next chapter. Reducing the amount of glutaraldehyde and the addition of dialdehyde starch showed promise for increasing the sensitivity of the sensor. This will be investigated further in the future.

4.9. References

(1) Baker, K. L.; Bolger, F. B.; Lowry, J. P. Development of a microelectrochemical biosensor for the real-time detection of choline. Sensors and Actuators B: Chemical **2017**, 243, 412-420.

(2) Bermingham, K. P.; Doran, M. M.; Bolger, F. B.; Lowry, J. P. Design optimisation and characterisation of an amperometric glutamate oxidase-based composite biosensor for neurotransmitter l-glutamic acid. Analytica Chimica Acta **2022**, 1224, 340205.

(3) Doran, M. M.; Finnerty, N. J.; Lowry, J. P. In–Vitro Development and Characterisation of a Superoxide Dismutase-Based Biosensor. Chemistry Select **2017**, 2 (14), 4157-4164.

(4) O'Riordan, S. L.; Lowry, J. P. In vivo characterisation of a catalase-based biosensor for real-time electrochemical monitoring of brain hydrogen peroxide in freely-moving animals. Analytical Methods **2017**, 9 (8), 1253-1264.

(5) Bolger, F. B. The in-vitro and in-vivo characterisation and application of real-time sesnors and biosesnor for neurochemical studies of brain metabolism PhD, Maynooth University, Maynooth 2007.

(6) Ryan, M. R.; Lowry, J. P.; O'Neill, R. D. Biosensor for neurotransmitter L-glutamic acid designed for efficient use of L-glutamate oxidase and effective rejection of interference. Analyst **1997**, 122 (11), 1419-1424.

(7) Baker, K. L.; Bolger, F. B.; Lowry, J. P. A microelectrochemical biosensor for real-time in vivo monitoring of brain extracellular choline. Analyst **2015**, 140 (11), 3738-3745.

(8) P. Lowry, J.; R. Ryan, M.; D. O'Neill, R. Behaviourally induced changes in extracellular levels of brain glutamate monitored at 1 s resolution with an implanted biosensor. Analytical Communications **1998**, 35 (3), 87-89.

(9) Dash, M. B.; Bellesi, M.; Tononi, G.; Cirelli, C. Sleep/wake dependent changes in cortical glucose concentrations. Journal of Neurochemistry **2013**, 124 (1), 79-89.

(10) Hu, Y.; Wilson, G. S. A temporary local energy pool coupled to neuronal activity: fluctuations of extracellular lactate levels in rat brain monitored with rapid-response enzyme-based sensor. Journal of Neurochemistry **1997**, 69 (4), 1484-1490.

(11) Hu, Y.; Mitchell, K. M.; Albahadily, F. N.; Michaelis, E. K.; Wilson, G. S. Direct measurement of glutamate release in the brain using a dual enzyme-based electrochemical sensor. Brain Research **1994**, 659 (1-2), 117-125.

(12) Burmeister, J. J.; Palmer, M.; Gerhardt, G. A. L-lactate measures in brain tissue with ceramic-based multisite microelectrodes. Biosensensors and Bioelectronics **2005**, 20 (9), 1772-1779.
(13) Martin, M.; O'Neill, R. D.; Roche, R.; Gonzalez-Mora, J. L. Biosensors Based On Prussian Blue Modified Carbon Fibers Electrodes for Monitoring Lactate in The Extracellular Space of Brain Tissue. International Journal of Electrochemical Science **2012**, 7 (7), 5910-5926.
(14) Shram, N. F.; Netchiporouk, L. I.; Martelet, C.; Jaffrezic-Renault, N.; Bonnet, C.; Cespuglio, R. In vivo voltammetric detection of rat brain lactate with carbon fiber microelectrodes coated with lactate oxidase. Analitical Chemistry **1998**, 70 (13), 2618-2622.
(15) Yang, Q.; Atanasov, P.; Wilkins, E. Needle-type lactate biosensor. Biosensensors and Bioelectronics **1999**, 14 (2), 203-210.
(16) O'Neill, R. D. Sensor–tissue interactions in neurochemical analysis with carbon paste electrodes in vivo. Analyst **1993**, 118 (4), 433-438.
(17) Baker, K. L.; Bolger, F. B.; Doran, M. M.; Lowry, J. P. Characterisation of a Platinum-based Electrochemical Biosensor for Real-time Neurochemical Analysis of Choline. Electroanalysis **2019**, 31 (1), 129-136.
(18) Brown, F. O.; Lowry, J. P. Microelectrochemical sensors for in vivo brain analysis: an investigation of procedures for modifying Pt electrodes using Nafion®. Analyst **2003**, 128 (6), 700-705.
(19) Killoran, S. J.; O'Neill, R. D. Characterization of permselective coatings electrosynthesized on Pt–Ir from the three phenylenediamine isomers for biosensor applications. Electrochimica Acta **2008**, 53 (24), 7303-7312.
(20) Lowry, J. P.; Miele, M.; O'Neill, R. D.; Boutelle, M. G.; Fillenz, M. An amperometric glucose-oxidase/poly(o-phenylenediamine) biosensor for monitoring brain extracellular glucose: in vivo characterisation in the striatum of freely-moving rats. Journal of Neuroscience Methods **1998**, 79 (1), 65-74.
(21) Lowry, J. P.; McAteer, K.; El Atrash, S. S.; Duff, A.; O'Neill, R. D. Characterization of Glucose Oxidase-Modified Poly(phenylenediamine)-Coated Electrodes in vitro and in vivo: Homogeneous Interference by Ascorbic Acid in Hydrogen Peroxide Detection. Analytical Chemistry **1994**, 66 (10), 1754-1761.

(22) Ford, R.; Quinn, S. J.; O'Neill, R. D. Characterization of Biosensors Based on Recombinant Glutamate Oxidase: Comparison of Crosslinking Agents in Terms of Enzyme Loading and Efficiency Parameters. Sensors **2016**, 16 (10), 1565.
(23) Craig, J. D.; O'Neill, R. D. Comparison of simple aromatic amines for electrosynthesis of permselective polymers in biosensor fabrication. Analyst **2003**, 128 (7), 905-911.
(24) McMahon, C. P.; Killoran, S. J.; Kirwan, S. M.; O'Neill, R. D. The selectivity of electrosynthesised polymer membranes depends on the electrode dimensions: implications for biosensor applications. Chemical Communications **2004**, (18), 2128-2130.
(25) Rothwell, S. A.; Kinsella, M. E.; Zain, Z. M.; Serra, P. A.; Rocchitta, G.; Lowry, J. P.; O'Neill, R. D. Contributions by a Novel Edge Effect to the Permselectivity of an Electrosynthesized Polymer for Microbiosensor Applications. Analytical Chemistry **2009**, 81 (10), 3911-3918.
(26) Lowry, J. P.; O'Neill, R. D. Strategies for reducing ascorbate interference at glucose oxidase modified conducting organic salt electrodes. Journal of Electroanalytical Chemistry **1992**, 334 (1), 183-194.
(27) O'Neill, R. D.; Rocchitta, G.; McMahon, C. P.; Serra, P. A.; Lowry, J. P. Designing sensitive and selective polymer/enzyme composite biosensors for brain monitoring in vivo. TrAC Trends in Analytical Chemistry **2008**, 27 (1), 78-88.
(28) Dixon, B. M.; Lowry, J. P.; O'Neill, R. D. Characterization in vitro and in vivo of the oxygen dependence of an enzyme/polymer biosensor for monitoring brain glucose. Journal of Neuroscience Methods **2002**, 119 (2), 135-142.
(29) Nair, P. K.; Buerk, D. G.; Halsey, J. H., Jr. Comparisons of oxygen metabolism and tissue PO2 in cortex and hippocampus of gerbil brain. Stroke **1987**, 18 (3), 616-622.
(30) McMahon, C. P.; O'Neill, R. D. Polymer-enzyme composite biosensor with high glutamate sensitivity and low oxygen dependence. Analitical Chemistry **2005**, 77 (4), 1196-1199.
(31) Murr, R.; Berger, S.; Schürer, L.; Peter, K.; Baethmann, A. A novel, remote-controlled suspension device for brain tissue PO2 measurements with multiwire surface electrodes. Pflügers Archiv: European Journal of Physiology **1994**, 426 (3), 348-350.
(32) Demestre, M.; Boutelle, M.; Fillenz, M. Stimulated release of lactate in freely moving rats is dependent on the uptake of glutamate. Journal of Physiology **1997**, 499 (Pt 3), 825-832.

(33) Qin, S.; Van der Zeyden, M.; Oldenziel, W. H.; Cremers, T. I. F. H.; Westerink, B. H. C. Microsensors for in vivo Measurement of Glutamate in Brain Tissue. Sensors **2008**, 8 (11), 6860-6884.

(34) Scheller, F. W.; Schubert, F.; Neumann, B.; Pfeiffer, D.; Hintsche, R.; Dransfeld, I.; Wollenberger, U.; Renneberg, R.; Warsinke, A.; Johansson, G.; et al. Second generation biosensors. Biosensensors and Bioelectronics **1991**, 6 (3), 245-253.

(35) Bollella, P.; Sharma, S.; Cass, A. E. G.; Antiochia, R. Minimally-invasive Microneedle-based Biosensor Array for Simultaneous Lactate and Glucose Monitoring in Artificial Interstitial Fluid. Electroanalysis **2019**, 31 (2), 374-382.

(36) Murugaiyan, S.; Ramasamy, R.; Gopal, N.; Kuzhandaivelu, V. Biosensors in clinical chemistry: An overview. Advanced Biomedical Research **2014**, 3 (1), 67-67, Review Article.

(37) Mayorga Martinez, C. C.; Treo, E. F.; Madrid, R. E.; Felice, C. C. Real-time measurement of glucose using chrono-impedance technique on a second generation biosensor. Biosensensors and Bioelectronics **2011**, 29 (1), 200-203.

(38) Burmeister, J. J.; Davis, V. A.; Quintero, J. E.; Pomerleau, F.; Huettl, P.; Gerhardt, G. A. Glutaraldehyde Cross-Linked Glutamate Oxidase Coated Microelectrode Arrays: Selectivity and Resting Levels of Glutamate in the CNS. American Chemical Sciences Chemical Neuroscience **2013**, 4 (5), 721-728.

(39) McMahon, C. P.; Killoran, S. J.; O'Neill, R. D. Design variations of a polymer–enzyme composite biosensor for glucose: Enhanced analyte sensitivity without increased oxygen dependence. Journal of Electroanalytical Chemistry **2005**, 580 (2), 193-202.

(40) McMahon, C. P.; Rocchitta, G.; Serra, P. A.; Kirwan, S. M.; Lowry, J. P.; O'Neill, R. D. The efficiency of immobilised glutamate oxidase decreases with surface enzyme loading: an electrostatic effect, and reversal by a polycation significantly enhances biosensor sensitivity. Analyst **2006**, 131 (1), 68-72.

(41) Lowry, J. P.; Boutelle, M. G.; Fillenz, M. Measurement of brain tissue oxygen at a carbon past electrode can serve as an index of increases in regional cerebral blood flow. Journal of Neuroscience Methods **1997**, 71 (2), 177-182.

(42) Rothwell, S. A.; Killoran, S. J.; O'Neill, R. D. Enzyme Immobilization Strategies and Electropolymerization Conditions to Control Sensitivity and Selectivity Parameters of a Polymer-Enzyme Composite Glucose Biosensor. Sensors **2010**, 10 (7), 6439-6462.

(43) O'Riordan, S. L.; Mc Laughlin, K.; Lowry, J. P. In vitro physiological performance factors of a catalase-based biosensor for real-time electrochemical detection of brain hydrogen peroxide in freely-moving animals. Analytical Methods **2016**, 8 (42), 7614-7622.
(44) Shram, N. F.; Netchiporouk, L. I.; Martelet, C.; Jaffrezic-Renault, N.; Bonnet, C.; Cespuglio, R. In Vivo Voltammetric Detection of Rat Brain Lactate with Carbon Fiber Microelectrodes Coated with Lactate Oxidase. Analytical Chemistry **1998**, 70.
(45) Ganesana, M.; Trikantzopoulos, E.; Maniar, Y.; Lee, S. T.; Venton, B. J. Development of a novel micro biosensor for in vivo monitoring of glutamate release in the brain. Biosensors and Bioelectronics **2019**, 130, 103-109.
(46) Kulagina, N. V.; Shankar, L.; Michael, A. C. Monitoring glutamate and ascorbate in the extracellular space of brain tissue with electrochemical microsensors. Analitical Chemistry **1999**, 71 (22), 5093-5100.
(47) Chatard, C.; Meiller, A.; Marinesco, S. Microelectrode Biosensors for in vivo Analysis of Brain Interstitial Fluid. Electroanalysis **2018**, 30 (6), 977-998.
(48) Smith, S. K.; Gosrani, S. P.; Lee, C. A.; McCarty, G. S.; Sombers, L. A. Carbon-Fiber Microbiosensor for Monitoring Rapid Lactate Fluctuations in Brain Tissue Using Fast-Scan Cyclic Voltammetry. Analytical Chemistry **2018**, 90 (21), 12994-12999.
(49) Burmeister, J. J.; Davis, V. A.; Quintero, J. E.; Pomerleau, F.; Huettl, P.; Gerhardt, G. A. Glutaraldehyde Cross-Linked Glutamate Oxidase Coated Microelectrode Arrays: Selectivity and Resting Levels of Glutamate in the CNS. American Chemical Society Chemical Neuroscience **2013**, 4 (5), 721-728.
(50) Kiyatkin, E. A.; Wakabayashi, K. T.; Lenoir, M. Physiological Fluctuations in Brain Temperature as a Factor Affecting Electrochemical Evaluations of Extracellular Glutamate and Glucose in Behavioral Experiments. American Chemical Society Chemical Neuroscience **2013**, 4 (5), 652-665.
(51) Brown, P. L.; Wise, R. A.; Kiyatkin, E. A. Brain hyperthermia is induced by methamphetamine and exacerbated by social interaction. Journal of Neuroscience **2003**, 23 (9), 3924-3929.
(52) Arora, H.; Owens, S. M.; Brooks Gentry, W. Intravenous (+)-methamphetamine causes complex dose-dependent physiologic changes in awake rats. European Journal of Pharmacology **2001**, 426 (1), 81-87.

(53) Kiyatkin, E. A.; Brown, P. L. Brain and body temperature homeostasis during sodium pentobarbital anesthesia with and without body warming in rats. Physiology & Behavior **2005**, 84 (4), 563-570.
(54) Phillips, P. E. M.; Wightman, R. M. Critical guidelines for validation of the selectivity of in-vivo chemical microsensors. TrAC Trends in Analytical Chemistry **2003**, 22 (8), 509-514.
(55) Soto, R. J.; Hall, J. R.; Brown, M. D.; Taylor, J. B.; Schoenfisch, M. H. In Vivo Chemical Sensors: Role of Biocompatibility on Performance and Utility. Analytical Chemistry **2017**, 89 (1), 276-299.
(56) Ganesana, M.; Trikantzopoulos, E.; Maniar, Y.; Lee, S. T.; Venton, B. J. Development of a novel micro biosensor for in vivo monitoring of glutamate release in the brain. Biosensors and Bioelectronics **2019**, 130, 103-109.
(57) Calia, G.; Rocchitta, G.; Migheli, R.; Puggioni, G.; Spissu, Y.; Bazzu, G.; Mazzarello, V.; Lowry, J. P.; O'Neill, R. D.; Desole, M. S.; et al. Biotelemetric Monitoring of Brain Neurochemistry in Conscious Rats Using Microsensors and Biosensors. Sensors **2009**, 9 (4), 2511-2523.
(58) Lowry, J. P.; Fillenz, M. Evidence for uncoupling of oxygen and glucose utilization during neuronal activation in rat striatum. Journal of Physiolgy **1997**, 498 (Pt 2), 497-501.
(59) Xin, Q.; Wightman, R. M. Enzyme modified amperometric sensors for choline and acetylcholine with tetrathiafulvalene tetracyanoquinodimethane as the electron-transfer mediator. Analytica Chimica Acta **1997**, 341 (1), 43-51.
(60) Bilitewski, U.; Rüger, P.; Schmid, R. D. Glucose biosensors based on thick film technology. Biosensors and Bioelectronics **1991**, 6 (4), 369-373.

Chapter 5 - In-vivo Lactate

Chapter 5. In-vivo Lactate.

5.1. Lactate response studies

To characterise a sensor signal *in vivo* specific criteria must be met: the sensor must be sensitive, selective, and stable for the intended time-course of use[1-4]. The first task here was to validate the 1 mg LOx PEC biosensor's response to lactate. The first experiment performed was a control injection of normal saline (0.9% NaCl).

A typical example of the observed change in signal is shown in Figure 5.1A. Saline resulted in an increase in signal from 18.1 ± 1.7 nA to a maximum of 21.8 ± 2.6 nA at 19 ± 2 seconds (n = 4), representing a 20 ± 3 % increase (p = 0.0013) . The pre- and post-injection baseline levels were not significantly different (p = 0.1697, 18.0 ± 1.6 nA at 8.2 ± 1.6 min, n = 4). Short-lived injection stress effects have also been observed for choline[1], glucose[5], O_2[6] and NO[7]. To test the sensor's ability to respond to changes in extracellular levels of lactate an i.p. injection of lactate was given and compared to that of the saline treatment. A typical example of the effect of the lactate administration (0.45 g/kg) is shown in Figure 5.1B. Once again there was an injection stress response which was observed over a similar time course as that for saline, and again there was no significant difference (p = 0.1858) in baseline pre- and post-treatment (9.5 ± 2.5 nA vs. 9.3 ± 2.4 nA, n = 4).

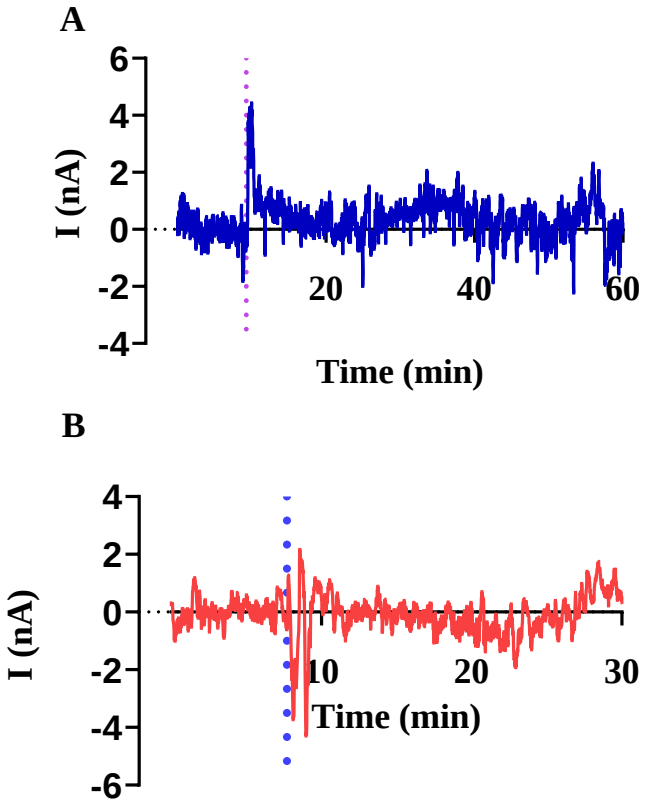

Figure 5.1 Typical examples of the effect of intraperitoneal injection of normal saline (A, 0.9 % NaCl), and lactate (B, 0.45 g/kg in 1.5 mL) on the signal recorded from the lactate biosensor implanted the striatum of a freely moving rat. Hashed lines indicate the point of injection. Baselines of 19.15 ± 0.02 nA (saline) and 10.85 ± 0.38 nA (lactate) were subtracted.

The lack of response to systemic administration of lactate is not overly surprising given that peripherally the body treats it as a by-product which needs to be eliminated. We have also previously observed a lack of response to systemic administration of glucose for an implanted glucose biosensor[2]. For a biosensor to not be responding to systemic administration of its target analyte there are two possibilities: i) the substrate isn't reaching the biosensor; or ii): the biosensor is not functioning in the *in vivo* environment. As lactate has slow kinetics crossing the blood brain barrier[8,9], we suspected that the reason for the failed response was most likely the former. Additionally, under resting conditions the amount of lactate produced in the periphery is normally

equal to that consumed, resulting in a blood level of *ca.* 0.5 to 1 mM[10] Lactate is transported across the blood-brain barrier by Monocarboxylate Transporters (MCT1s) *via* facilitated diffusion, and while the concentration injected (*ca.* 500 μM) was comparable to baseline levels, and chosen so as not to significantly alter metabolism/normal physiology, the combined effects of slow kinetics and dilution in periphery and brain are mostly likely the cause of the lack of response observed. Thus, to confirm that the biosensor could reliably monitor lactate *in-vivo* it was decided to use retro-microdialysis (*see* Section 3.3.4) to deliver the substrate to the immediate area surrounding the implanted biosensor, and thus avoid unwanted alterations in metabolism/physiology potentially associated with peripheral injection of higher concentrations.

A solution of lactate (1 mM) was locally perfused via a co-implanted microdialysis probe, following a protocol previously validated for glucose[2]. There was an immediate increase following the beginning of the perfusion reaching a maximum of 27.2 ± 2.7 nA (n = 8, $p < 0.01$, a typical example is shown in Figure 5.2) before returning to baselineon cessation of perfusion. This shows that the sensor does respond to changes in the concentration of ECF lactate when implanted. Initial perfusion with aCSF resulted in a decrease in signal of 4.4 ± 0.62 nA (n = 5) (Figure 5.2, *Inset*) from the pre-perfusion baseline associated with removal of analyte from the local environment of the sensor.

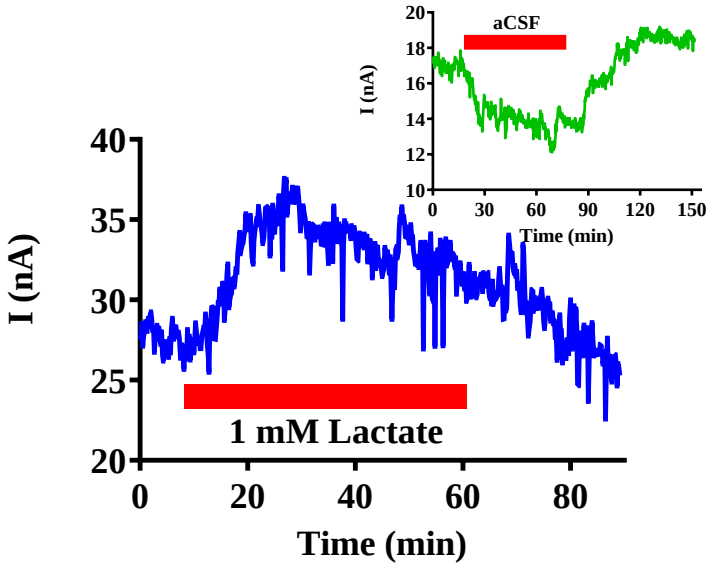

Figure 5.2. Typical example of the effect of a local perfusion (reverse micro-dialysis) of lactate (1 mM, 2.0 µL min^{-1}) on the response of an adjacent PEC lactate biosensor implanted into the striatum of a freely moving rat. Shaded area indicates period of perfusion. Inset: Typical effect of local perfusion of aCSF on the PEC lactate biosensor response.

5.2. Interference Studies

As AA is the principal electroactive interferant in the brain (*see* Section 4.2) it is important to ensure that the biosensor's response *in-vivo* is free from any potential AA contribution. In terms of interference testing we would typically co-implant (bilaterally) the biosensor with a carbon paste electrode for simultaneous monitoring of AA, and perform systemic administration of AA (2 g/kg, i.p.)[2] Figure 5.3 shows data for both AA and glucose reproduced from[2].

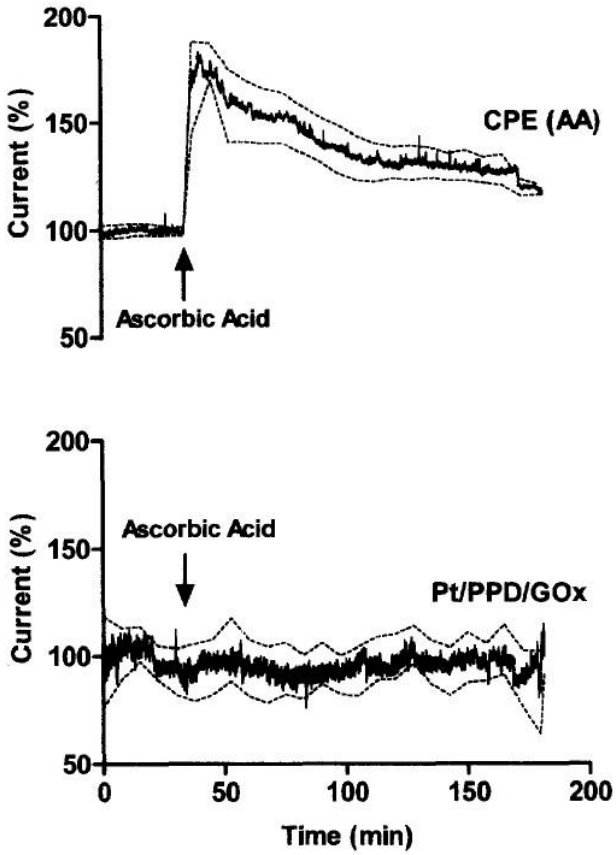

Fig 5.3. The effect of intraperitoneal injection of ascorbic acid (AA; 2 g/ kg) on the amperometric response of carbon paste (CPE, top) and Pt:PoPD:Gox (bottom) sensors implanted bilaterally in the striatum of freely-moving rats.The CPEs monitored AA at a constant potential of +250 mV. Taken from[2] with permission from author.

Being mindful of the ANLS (*see* Section 1.3.1), where increases in extracellular glutamate lead to the downstream production of lactate, and an older model suggesting that changes in extracellular glutamate levels are coupled, via a heteroexchange mechanism involving the glutamate transporter proteins, to fluctuations in extracellular AA levels[11-13], we redesigned the experimental protocol (*see* Figure 5.4A) to include a carbon paste electrode and a blank biosensor (often called a sentinel electrode[14,15]) prepared using an identical protocol to the biosensor with the exception of the LOx enzyme.

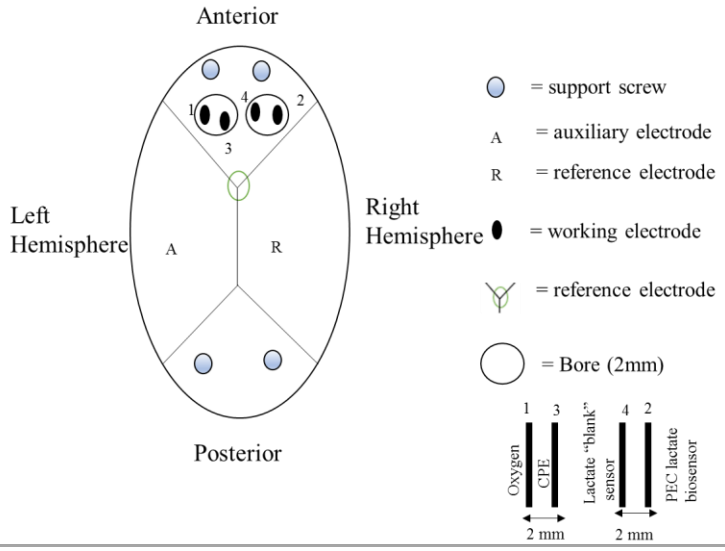

	A-P	M-L	D-V
O_2	+1	+2.5	5
PEC lactate biosensor	+1	-2.5	5
AA	+1	+2.5	5
Lactate "blank" sensor	+1	-2.5	5

Figure 5.4. Schematic representation of the implantation procedure and stereotaxic co-ordinates used in interference studies. Note: applying 3R principles, the O_2 sensor (bare Pt electrode) was implanted for later O_2 studies (see Section 5.2) and was not used in the interference testing.

A typical example of the time course of the signal changes observed following i.p. injection of AA is shown in Figure 5.5. There is a clear response to the AA administration at the CPE confirming that AA crosses the blood-brain barrier as previously reported; there was an immediate and significant increase of 4.0 ± 1.0 nA (n = 8, $p < 0.01$) from baseline, corresponding to 77 ± 14 %, which started to decrease within 1-2 hours, and continued to gradually return to baseline over 11 ± 2 hours (n = 8). The lactate biosensor signal also increased but with a different time course and trend; the signal slowly increased to an initial peak of 4.1 ± 1.5 nA (n = 8, $p < 0.05$) after 1.3 ± 0.6 hours, before decreasing and subsequently increasing to a second peak (maximum) of 10.1 ± 2.7 nA (n = 8, $p < 0.01$) at 4.9 ± 1.3 hours. Return to baseline occurred 15.0 ± 1.3 hours following initial injection.

Interestingly, this biphasic change was also observed at the blank biosensor with a similar time course and trend for all biosensor/blank pairings, but with smaller signal changes and the two peaks having similar amplitudes; the average difference between the two signals at the maximum

increase was 7.6 ± 2.2 nA (n = 8). Return to baseline was also similar to that for the biosensor, occurring 14.5 ± 1.4 (n = 8) hours after injection.

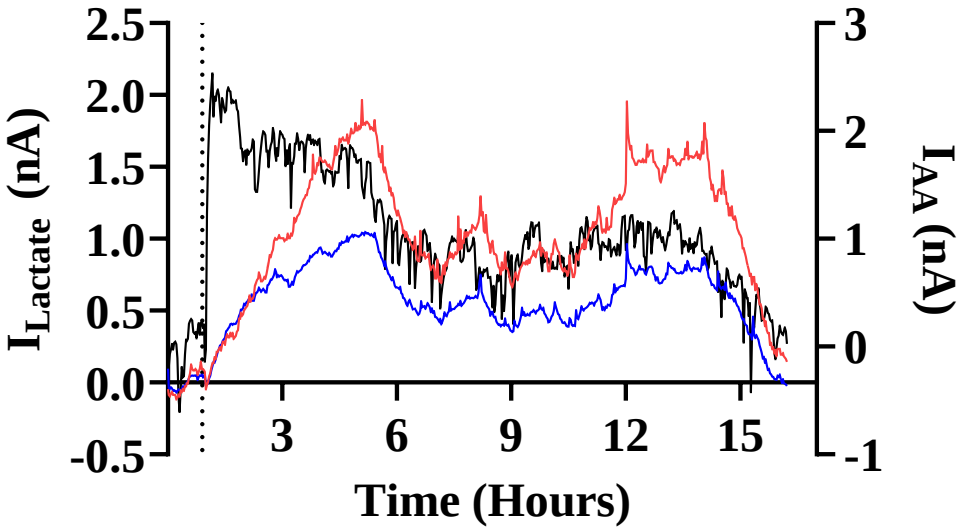

Figure 5.5. Comparison of the effect of an intraperitoneal injection of ascorbate (2 g/kg) on the currents recorded from a lactate biosensor (red), CPE AA sensor (black) and lactate "blank" sensor (blue) recorded in the striatum of a freely moving rat. Dashed line indicates point of injection. Lactate and "blank" currents on left axis, ascorbate current on right axis. Baselines normalised to 0 to facilitate direct comparison.

The different time course and trend for the CPE (AA) and biosensor (lactate) signal changes, coupled with the excellent interference rejection properties of the P*o*PD layer[16-19] (*see* Sections 4.2 and 4.3), suggests that the increase in current observed at the lactate biosensor represents physiological changes in lactate and is not due to AA interference. This is supported by evidence that AA can act as metabolic switching molecule by modulating glucose and lactate metabolism in the brain[20]. However, rather than finishing our interference studies here we felt that the observed response at the blank electrode warranted further investigation. This was primarily motivated by the fact that blank signals are normally subtracted from the biosensor signal to (i) eliminate any residual interference signals that might be present following permselective polymer rejection, and (ii) more importantly in this case where almost identical trends were observed, remove background

or capacitance current thus facilitating baseline and signal changes to be more accurately converted to concentration.

We suspected crosstalk as the cause of the almost identical signal dynamics observed at the biosensor and blank, and if proven correct this would negate any possibility of taking advantage of the blank signal to successfully address (i) and (ii) above. As the signal producing H_2O_2, which is not impeded by P*o*PD[20] is a surface generated molecule (from the enzyme-substrate reaction, see Equation 2.3) there is equal probability that it will diffuse towards or away from the electrode surface[22].

In order to test this hypothesis and develop a practical solution if found to be the case, we performed a series of *in-vitro* experiments in tandem with targeted *in-vivo* work. We started by carrying out lactate calibrations (Figure 5.6A) on the following combination of electrodes/sensors in our (four electrode) electrochemical cell; Bare Pt, Pt-P*o*PD, lactate biosensor and blank. As can be seen in Figure 5.6A the lactate biosensor displayed the anticipated sensitivity and enzyme kinetic parameters: LRS, 0.236 ± 0.010 nA/μM; $V_{Max,}$ 178 ± 4 nA; and $K_{M,}$ 331 ± 13 μM . However, similar kinetic-type responses were also recorded at the bare Pt, Pt-P*o*PD and blank sensor indicating that H_2O_2 from the lactate biosensor is producing crosstalk signals at these devices when they are located in close proximity and calibrated in the same electrochemical cell. This was validated by performing separate calibrations of each electrode type where no crosstalk effect was observed (Figure 5.6B).

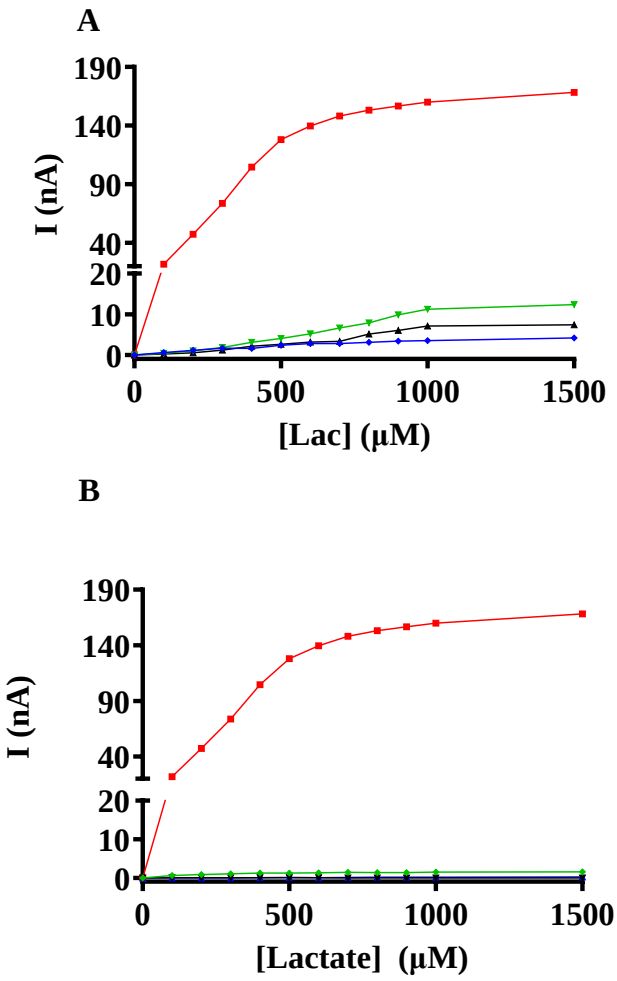

*Figure 5.6. Comparison of lactate calibrations (0 – 1,500 µM) for A. Combined calibrations of PEC lactate biosensor (red), Bare-Pt (black), Pt-PoPD (green) and Blank lactate sensor (blue) B. Separate calibrations of PEC lactate biosensor (red), Bare-Pt (black), Pt-*PoPD *(green) and Blank lactate sensor (blue)* performed *in PBS (pH 7.4) using CPA at +700mV (vs. SCE) given as mean.*

AA calibrations performed on the same combination of electrodes/sensors showed the expected linear response (0.901 ± 0.039 nA/µM, n=3, R^2 = 0.993) at bare Pt, and confirmed interference rejection at the P*o*PD-modified devices(Figure 5.7.)

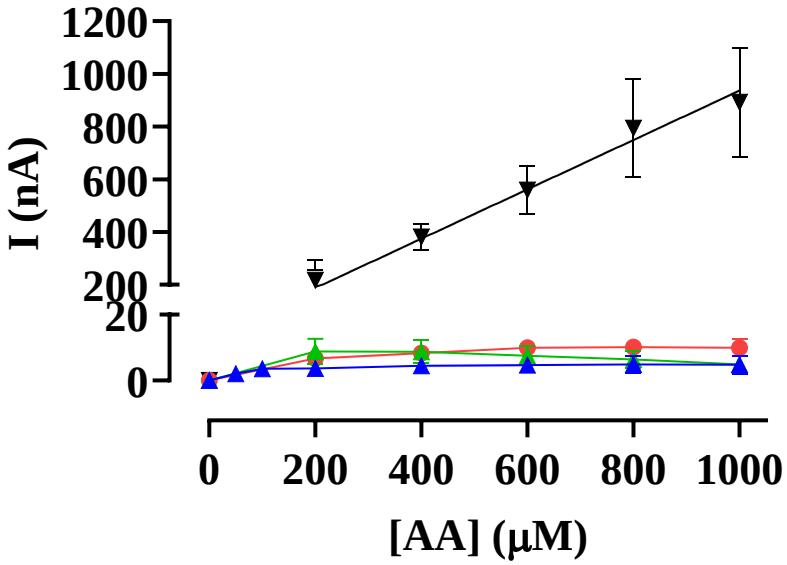

Figure 5.7. AA calibrations (0 – 1,000 µM) for Bare-Pt (black, n = 3, current shown on right y-axis), PEC lactate biosensor (red, n = 2), Pt-PoPD (green, n = 3) and Blank lactate sensor (blue, n = 3) performed in PBS (pH 7.4) using CPA at +700mV (vs. SCE) given as mean ± SEM.

Based on the *in vitro* results presented above we modified our *in vivo* surgical protocol to increase the spacing between the different implanted electrodes/sensors. The new stereotaxic coordinates used are given in Figure 5.8. We also changed the types implanted so that they mimicked the electrodes used in the *in-vitro* tests, i.e. we replaced the CPE with a Pt-P*o*PD electrode and used the bare Pt electrode (previously used as an oxygen sensor by applying a negative reduction potential) to monitor AA (by applying a positive oxidation potential).

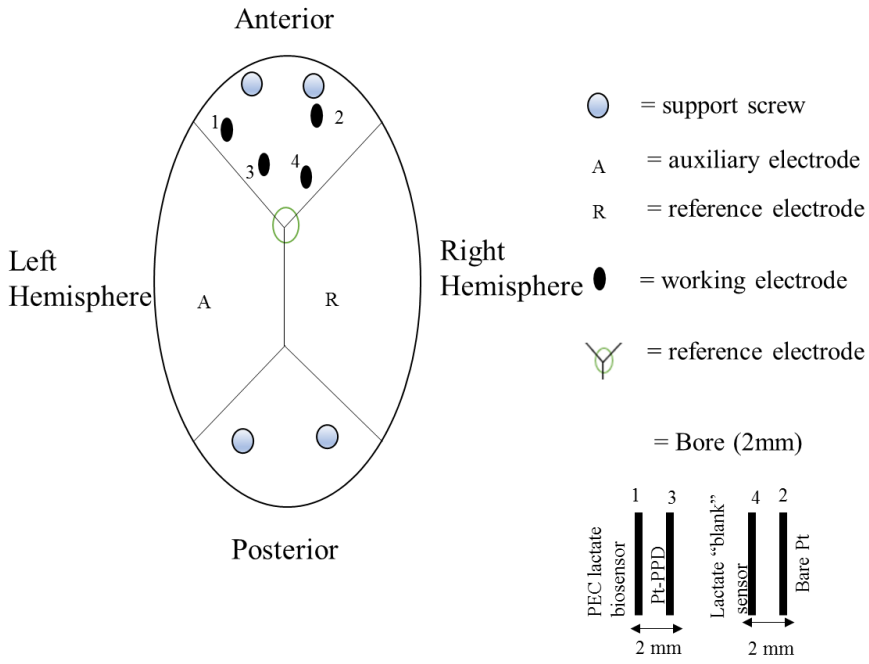

	A-P	M-L	D-V
PEC lactate biosensor	+1.68	+2.5	-5.8
Bare Pt	+1.68	-2.5	-5.8
Pt-P*o*PD	+0.36	+2.5	-6.0
Lactate "blank" sensor	+0.36	-2.5	-6.0

Figure 5.8. Schematic representation of the updated implantation procedure and stereotaxic co-ordinates used in interference studies.

We then repeated the AA (2 g/kg i.p.) treatment to see if separation of the electrodes reduced what we previously observed, and suspected was crosstalk. This resulted in the data presented in Figure.5.9. An immediate increase in current was observed at the bare Pt electrode, similar to what was previously observed at the CPE, and confirming that the systemically administered AA has crossed the blood brain barrier. The lactate biosensor showed good interference rejection properties with a different time course and response from that observed at the "lactate blank" sensor. With a slight increase following the administration of AA.

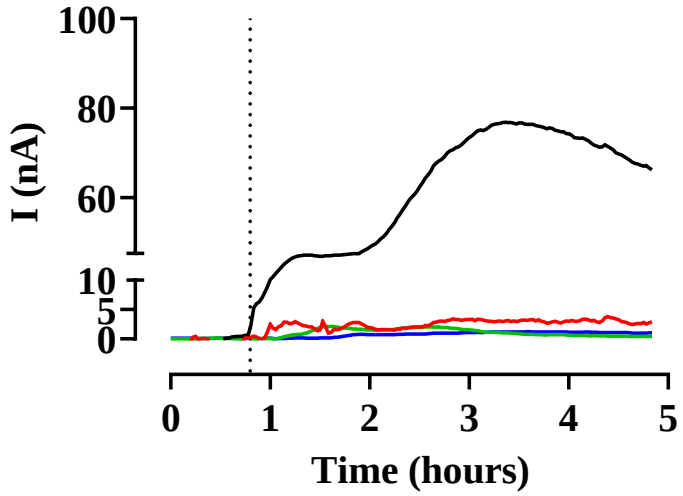

Figure 5.9 Comparison of the effect of an intraperitoneal injection of ascorbate (2 g/kg) on the signals recorded with a PEC lactate biosensor (red, n = 3), bare Pt electrode (black, n =3), Pt-PoPD (green, n = 3) and lactate blank (blue n =3) implanted in rat striatum. Dashed line indicates point of injection. Pre-injection baselines have been subtracted to facilitate comparison. .

The previously observed similar time course and trend recorded at the blank sensor did not occur, with both it and the Pt-P*o*PD electrode showing no response to AA. This supports the *in vitro* data presented above and confirms that the previously observed blank sensor signal was due to H_2O_2 crosstalk. The blank sensor is usually used to remove any interference present in the signal and is used in calculations for basal levels of analytes as it allows the subtraction of any capacitance current. However, this can't be done when crosstalk is present between the sensor and blank.

Oxygen interference *in vivo* was also tested using the non-volatile anaesthetic chloral hydrate which is known to change cerebral blood flow and thus tissue oxygenation (Figure 5.10). Previous reports have shown that an anaesthetic dose (350 mg/kg) causes parallel increases in both regional cerebral blood flow (rCBF) and O_2 (*see* Figure 5.10), and as such is an ideal agent for examining the O_2 dependence of a biosensor exposed to increased physiological O_2 levels.

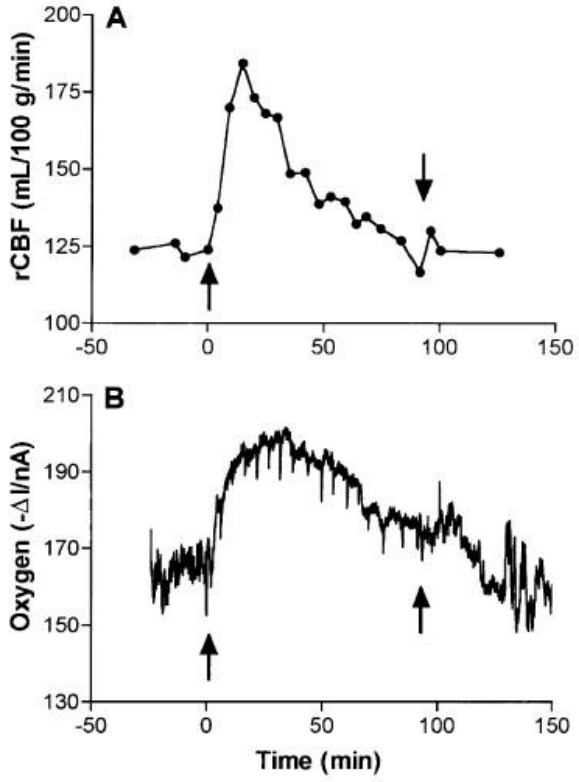

Figure 5.10 A typical example of the effect of intraperitoneal injection of chloral hydrate (350 mg/kg) on (A) regional cerebral blood flow (rCBF), (B) tissue oxygen, monitored in rat striatum. Arrows indicate the points of injection, and recovery from, the anaesthetic. Taken from[5] with authors permission.

While O_2 and rCBF both increase in response to the anaesthetic, lactate (*see* Figure 5.11) in contrast decreased reaching a minimum of 2.38 ± 0.89 nA ($p < 0.05$, n = 9) after 112 ± 11 min (when both O_2 and rCBF are back at baseline) and took a further 164 ± 23 min to return to baseline levels. The different time course and direction of change support the *in vitro* O_2 interference results presented in Section 4.3, confirming that the LOx PEC biosensor is not affected by changes in O_2 over physiologically relevant concentration ranges for the brain.

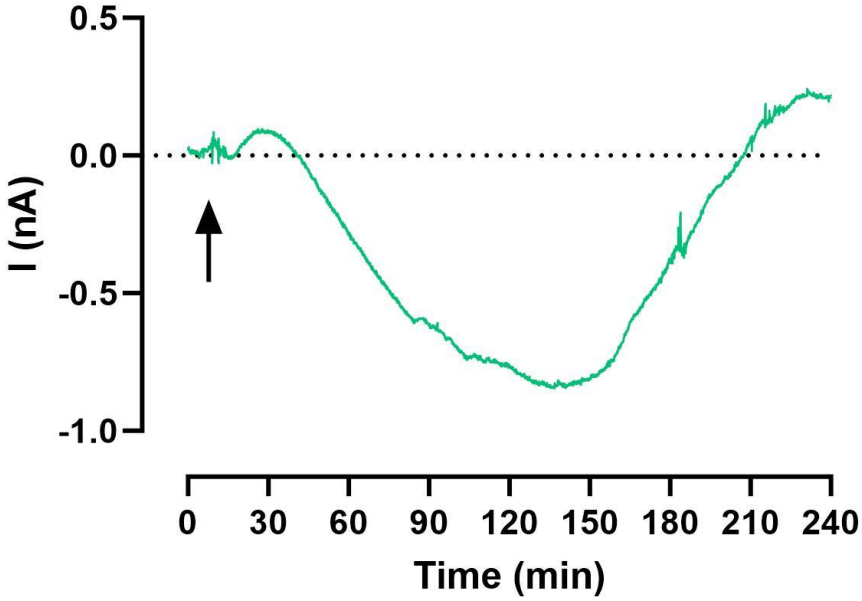

Figure 5.11 A typical example of the effect of an injection of chloral hydrate (350 mg/kg, i.p.) on extracellular lactate (background subtracted), monitored with the LOx PEC biosensor implanted in the striatum of a freely-moving rat. Arrow indicates the point of injection.

5.3. Circadian changes

As all *in-vivo* experiments were performed in the animal's home bowl with a 12 h light/dark cycle (lights on at 07:00, *see* Section 3.6.1), continuously monitored basal lactate signals were examined to investigate endogenous lactate dynamics over consecutive light-dark phases. As can be seen from Figure 5.12A diurnal oscillations in rat striatum occurred across repetitive light-dark cycles, with transitioning levels increasing into the dark phase and decreasing into the light phase. Recorded lactate current was significantly higher ($p < 0.0001$) during the dark phase compared to the light phase (Figure 5.12B). A review of the literature yielded two publications using biosensors which support this finding of increased lactate during wakefulness (night) and decreased levels during sleep (day)[23,24]; measurements were performed in the cortex and attributed to decreased lactate production and increased efflux during sleep with the opposite occurring when the animals were awake and active. A microdialysis study in mice found similar cortical trends[25].

Interestingly, there does not appear to be a correlation with locomotor activity despite the fact that rats are a nocturnal species, and as such are predominantly active during the dark phase, spending more time asleep during the light phase. However, we had limited recording of movement data in our experiments and further studies would need to be performed to validate this observation.

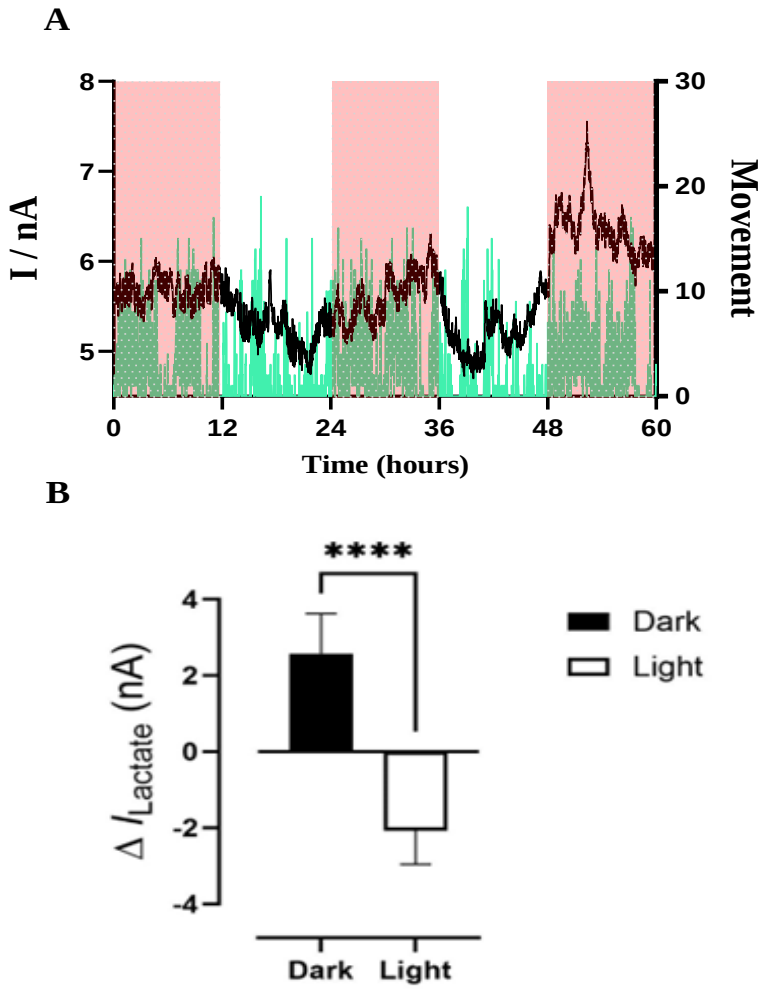

Figure 5.18. A typical example of the striatal lactate current obtained over the course of 60 hours recording from a freely-moving rat. Shaded regions represent the night period. B. Comparison of mean (± SEM) lactate current changes for dark (n = 6) and light periods (n = 5).

5.4. Tail pinch

Finally, physiological stimulation, in the form of tail pinch, was used to investigate the effects of neuronal activation on ECF levels of lactate. This is a well established behavioural paradigm which produces a stereotypical behavioural pattern consisting primarily of gnawing and licking, and a general increase in locomotor activity[26-28]. We began by looking at the effects of the traditionally used 5 min tail pinch (Figure 5.13A); following an initial brief decrease of 2.5 ± 0.03 nA, which lasted ca. 2 min, the signal increased to a maximum of 5.8 ± 0.04 nA ($p < 0.05$, n = 10) before returning to baseline, typically within 20 min of removal of the stimulus. A typical example is shown in Figure 5.13A. In Figure 5.13B we have combined a lactate recording with previously obtained glucose data[28] to facilitate a comparison of the two signals (details on the glucose changes are provided in the legend).

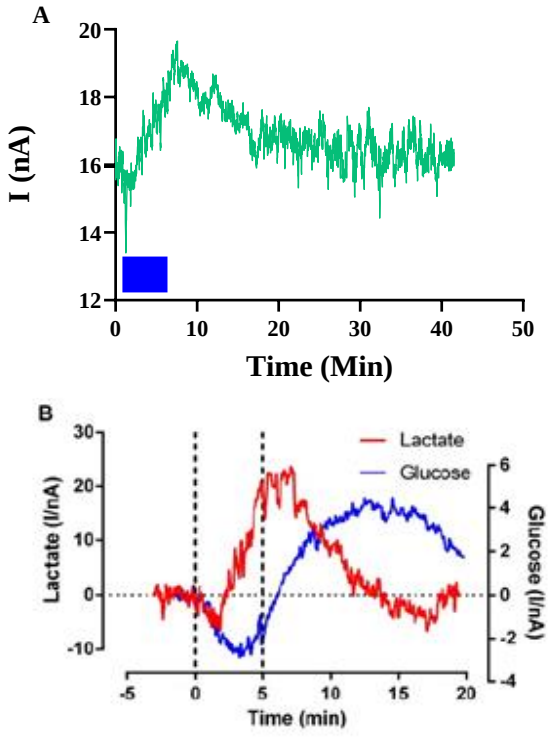

Figure 5.13. A. Typical example of the lactate current obtained from the striatum of a feeling moving rat following a 5-min tail pinch. Blue box represents duration of tail pinch. B. Typical examples of combined raw data obtained for the measurement of lactate and glucose, monitored

with implanted biosensors in rat striatum, in response to a 5-min tail pinch (hashed lines). Glucose decreases by ca. 5% over the period of the stimulus.

As the 5 min tail pinch can be quite stressful on the animal (a piece of wood is held in front of the animal's snout to distract attention from the paper clip and to encourage gnawing actions) we decide to look at trying to refine (in line with the 3Rs) the protocol by reducing the duration of the pinch. As such, we investigated 1.5 min and 1 s pinches (Figure 5.14), the former retaining the use of a paperclip, while the latter was applied using a surgical tweezers.

The 1.5 min pinch (Figure 5.14A) produced a signal change trend that was similar to that observed for the 5 min pinch but with a shorter time course; application of the paper clip resulted in an immediate decrease in the lactate current of 2.9 ± 0.7 nA which was short-lived (lasting ca. 30 s) before increasing by a maximum of 3.0 ± 0.2 nA ($p < 0.05$, n = 3) before returning to baseline levels ca. 11 min after the removal of the paperclip. In contrast, the 1 s pinch (Figure 5.14B), resulted in a maximum increase of 1.45 ± 0.04 nA (n = 2) 83 s after the application of the tail pinch before returning to baseline over a period of ca. 8 min.

It is interesting to note that microdialysis data for 5 min tail pinch also shows increased dialysate lactate, but in contrast to the real-time data reported here failed to pick up the initial decrease associated with the stimulus[30,31] due to the 5 min sampling used and typically associated with the technique. Also, as tail pinch (5 min) has also been reported to increase extracellular levels of glutamate[32], it is most likely that this stimulates the observed release of lactate found here, as proposed by the ALNSH theory and supported by microdialysis data for stimulated grooming[33].

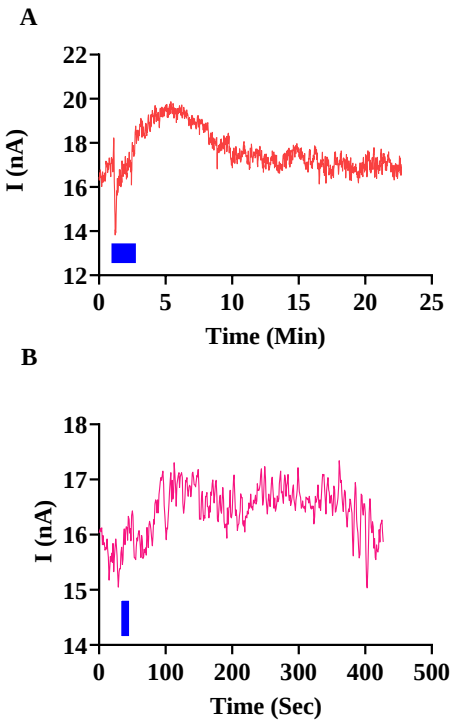

Figure.5.14. Typical examples of the lactate current obtained from the striatum of a feeling-moving rat following a1.5-minute tail pinch (A) and a 1 second tail pinch (B). Blue boxes represent duration of tail pinch.

5.5 Stability

As already outlined in Section 4, contact of biosensors with brain tissue can result in a decrease in sensitivity due to surface fouling by biological consituents such as lipids and proteins. As such we investigated the stability of the PEC lactate biosensor by examining the baseline *in vivo* data for 12 days following implantation (day 0). As can be seen from Figure 5.15, the baseline decreased over the first two days following implantation before settling at 68 % of the initial signal measured on Day 1 of recording. This is in line with decreases reported for other biosensors *in vivo* where drops of between 20 and 50 % have been reported[34,35].

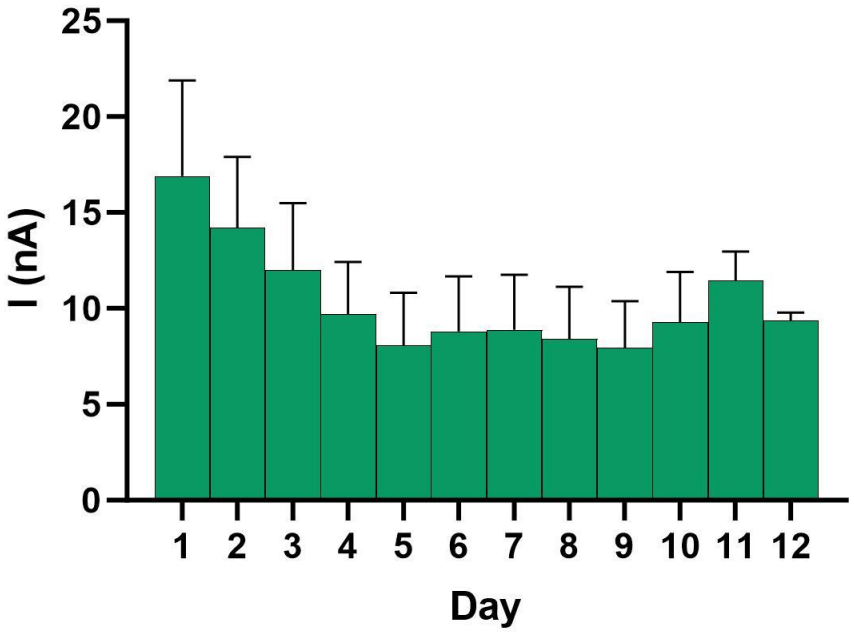

Figure 5.15. Baseline in vivo data (± SEM, n = 5) for the lactate PEC biosensor recorded from striatum using CPA at +700 mV over a 12-day period. All data taken from the same daily 1-h (8–9 a.m.) period when the animals were mostly inactive.

5.6. Conclusions

This chapter details the *in vivo* characterisation of the lactate PEC biosensor. The sensor showed no response to an injection of lactate, which is expected as this has been shown to be the case with other biosensors[2], but did respond to local perfusion demonstrating that the sensor is capable of responding to lactate *in vivo*. Systemic administration of ascorbate did not result in interference but did cause an increase in the signal recorded at a co-implanted blank sensor. This was subsequently shown to be due to H_2O_2 crosstalk as the response was mitigated once the implanted sensors were separated. The circadian rhythm of lactate matched what has previously been published, and neuronal activation caused by tail pinch was similar to that previously observed using microdialysis. However, it is more advantageous to use biosensors for monitoring physiological activation given the better temporal-spatial resolution of microelectrodes *vs.* microdialysis, and pinch application can be reduced from the traditionally used 5 min period to 1.5 min thus improving animal welfare. A drop in sensitivity occurs over the first four days following implantation before the signal settles. This should be factored into concentration changes

determined using *in vitro* calibration data. Future work will involve using this biosensor to monitor changes associated with pharmacological agents with the hope this will increase our understanding of energy metabolism and its role in neurodegenerative disorders such as Alzheimer's disease.

5.7. References

(1) Baker, K. L.; Bolger, F. B.; Lowry, J. P. A microelectrochemical biosensor for real-time in vivo monitoring of brain extracellular choline. Analyst **2015**, 140 (11), 3738-3745.

(2) Lowry, J. P.; Miele, M.; O'Neill, R. D.; Boutelle, M. G.; Fillenz, M. An amperometric glucose-oxidase/poly(o-phenylenediamine) biosensor for monitoring brain extracellular glucose: in vivo characterisation in the striatum of freely-moving rats. Journal Neuroscience Methods **1998**, 79 (1), 65-74.

(3) Phillips, P. E. M.; Wightman, R. M. Critical guidelines for validation of the selectivity of in-vivo chemical microsensors. TrAC Trends in Analytical Chemistry **2003**, 22 (8), 509-514.

(4) Xu, C.; Wu, F.; Yu, P.; Mao, L. In Vivo Electrochemical Sensors for Neurochemicals: Recent Update. American Chemical Society Sensors **2019**, 4 (12), 3102-3118.

(5) Lowry, J. P.; Fillenz, M. Real-time monitoring of brain energy metabolism in vivo using microelectrochemical sensors: the effects of anesthesia. Bioelectrochemistry **2001**, 54 (1), 39-47.

(6) Kealy, J.; Bennett, R.; Lowry, J. P. Simultaneous recording of hippocampal oxygen and glucose in real time using constant potential amperometry in the freely-moving rat. Journal of Neuroscience Methods **2013**, 215 (1), 110-120.

(7) Finnerty, N. J.; Bolger, F. B.; Pålsson, E.; Lowry, J. P. An Investigation of Hypofrontality in an Animal Model of Schizophrenia Using Real-Time Microelectrochemical Sensors for Glucose, Oxygen, and Nitric Oxide. American Chemical Society Chemical Neuroscience **2013**, 4 (5), 825-831.

(8) Knudsen, G. M.; Paulson, O. B.; Hertz, M. M. Kinetic analysis of the human blood-brain barrier transport of lactate and its influence by hypercapnia. Journal of Cereberal Blood Flow and Metabolism **1991**, 11 (4), 581-586.

(9) Cremer, J. E.; Cunningham, V. J.; Pardridge, W. M.; Braun, L. D.; Oldendorf, W. H. Kinetics of blood-brain barrier transport of pyruvate, lactate and glucose in suckling weanling and adult rats. Journal of Neurochemistry **1979**, 33 (2), 439-445.

(10) Riske, L.; Thomas, R. K.; Baker, G. B.; Dursun, S. M. Lactate in the brain: an update on its relevance to brain energy, neurons, glia and panic disorder. Therapeutic Advances in Psychopharmacology **2017**, 7 (2), 85-89.

(11) Cammack, J.; Ghasemzadeh, B.; Adams, R. N. The pharmacological profile of glutamate-evoked ascorbic acid efflux measured by in vivo electrochemistry. Brain Research **1991**, 565 (1), 17-22.

(12) Rebec, G. V.; Wang, Z. Behavioral Activation in Rats Requires Endogenous Ascorbate Release in Striatum. The Journal of Neuroscience **2001**, 21 (2), 668-675.

(13) Kulagina, N. V.; Shankar, L.; Michael, A. C. Monitoring Glutamate and Ascorbate in the Extracellular Space of Brain Tissue with Electrochemical Microsensors. Analytical Chemistry **1999**, 71 (22), 5093-5100.

(14) Burmeister, J. J.; Gerhardt, G. A. Self-referencing ceramic-based multisite microelectrodes for the detection and elimination of interferences from the measurement of L-glutamate and other analytes. Analitical Chemistry **2001**, 73 (5), 1037-1042.

(15) Rutherford, E. C.; Pomerleau, F.; Huettl, P.; Strömberg, I.; Gerhardt, G. A. Chronic second-by-second measures of L-glutamate in the central nervous system of freely moving rats. Journal of Neurochemistry **2007**, 102 (3), 712-722.

(16) Kirwan, S. M.; Rocchitta, G.; McMahon, C. P.; Craig, J. D.; Killoran, S. J.; O'Brien, K. B.; Serra, P. A.; Lowry, J. P.; O'Neill, R. D. Modifications of Poly(o-phenylenediamine) Permselective Layer on Pt-Ir for Biosensor Application in Neurochemical Monitoring. Sensors (Basel) **2007**, 7 (4), 420-437.

(17) Baker, K. L.; Bolger, F. B.; Lowry, J. P. Development of a microelectrochemical biosensor for the real-time detection of choline. Sensors and Actuators B: Chemical **2017**, 243, 412-420.

(18) Bermingham, K. P.; Doran, M. M.; Bolger, F. B.; Lowry, J. P. Design optimisation and characterisation of an amperometric glutamate oxidase-based composite biosensor for neurotransmitter l-glutamic acid. Analytica Chimica Acta **2022**, 1224, 340205.

(19) Zain, Z. M.; O'Neill, R. D.; Lowry, J. P.; Pierce, K. W.; Tricklebank, M.; Dewa, A.; Ab Ghani, S. Development of an implantable D-serine biosensor for in vivo monitoring using mammalian D-amino acid oxidase on a poly (o-phenylenediamine) and Nafion-modified platinum-iridium disk electrode. Biosensenors and Bioelectronics **2010**, 25 (6), 1454-1459..

(20) Castro, M. A.; Beltrán, F. A.; Brauchi, S.; Concha, I. I. A metabolic switch in brain: glucose and lactate metabolism modulation by ascorbic acid. Journal of Neurochemistry **2009**, 110 (2), 423-440.

(21) Lowry, J. P.; O'Neill, R. D. Partial characterization in vitro of glucose oxidase-modified poly(phenylenediamine)-coated electrodes for neurochemical analysis in vivo. Electroanalysis **1994**, 6 (5-6), 369-379.

(22) Bartlett, P. N.; Whitaker, R. G. Electrochemical immobilisation of enzymes: Part II. Glucose oxidase immobilised in poly-N-methylpyrrole. Journal of Electroanalytical Chemistry and Interfacial Electrochemistry **1987**, 224 (1), 37-48.

(23) Naylor, E.; Aillon, D. V.; Barrett, B. S.; Wilson, G. S.; Johnson, D. A.; Johnson, D. A.; Harmon, H. P.; Gabbert, S.; Petillo, P. A. Lactate as a biomarker for sleep. Sleep **2012**, 35 (9), 1209-1222.

(24) Shram, N.; Netchiporouk, L.; Cespuglio, R. Lactate in the brain of the freely moving rat: voltammetric monitoring of the changes related to the sleep-wake states. European Journal of Neuroscience **2002**, 16 (3), 461-466.

(25) Lundgaard, I.; Lu, M. L.; Yang, E.; Peng, W.; Mestre, H.; Hitomi, E.; Deane, R.; Nedergaard, M. Glymphatic clearance controls state-dependent changes in brain lactate concentration. Journal of Cereberal Blood Flow and Metabolism **2017**, 37 (6), 2112-2124.

(26) Antelman, S. M.; Szechtman, H.; Chin, P.; Fisher, A. E. Tail pinch-induced eating, gnawing and licking behavior in rats: dependence on the nigrostriatal dopamine system. Brain Research **1975**, 99 (2), 319-337.

(27) Fellows, L. K.; Boutelle, M. G. Rapid changes in extracellular glucose levels and blood flow in the striatum of the freely moving rat. Brain Research **1993**, 604 (1-2), 225-231.

(28) Lowry, J. P.; Boutelle, M. G.; Fillenz, M. Measurement of brain tissue oxygen at a carbon paste electrode can serve as an index of increases in regional cerebral blood flow. Journal of Neuroscience Methods **1997**, 71 (2), 177-182.

(29) Lowry, J. P.; Fillenz, M. Evidence for uncoupling of oxygen and glucose utilization during neuronal activation in rat striatum. Journal of Physiology **1997**, 498 (Pt 2), 497-501.

(30) Fellows, L. K.; Boutelle, M. G.; Fillenz, M. Physiological stimulation increases nonoxidative glucose metabolism in the brain of the freely moving rat. Journal of Neurochemistry **1993**, 60 (4), 1258-1263.

(31) Fray, A. E.; Forsyth, R. J.; Boutelle, M. G.; Fillenz, M. The mechanisms controlling physiologically stimulated changes in rat brain glucose and lactate: a microdialysis study. Journal of Physiology **1996**, 496 (Pt 1), 49-57.
(32) Albery, W. J.; Boutelle, M. G.; Galley, P. T. The dialysis electrode—a new method for in vivo monitoring. Journal of the Chemical Society, Chemical Communications **1992**, (12), 900-901.
(33) Demestre, M.; Boutelle, M.; Fillenz, M. Stimulated release of lactate in freely moving rats is dependent on the uptake of glutamate. Journal of Physiology **1997**, 499 (Pt 3), 825-832.
(34) Garguilo, M. G.; Michael, A. C. Quantitation of choline in the extracellular fluid of brain tissue with amperometric microsensors. Analitical Chemistry **1994**, 66 (17), 2621-2629.
(35) Hu, Y.; Mitchell, K. M.; Albahadily, F. N.; Michaelis, E. K.; Wilson, G. S. Direct measurement of glutamate release in the brain using a dual enzyme-based electrochemical sensor. Brain Research **1994**, 659 (1-2), 117-125.

Chapter 6 – Conclusions

Chapter 6 – Conclusions

6.1. Conclusions

As previously discussed, the aim of this research project was to characterise a composite biosensor for the real time neurochemical monitoring of lactate. A sensor that will be of particular importance due to lactate's complex and controversial role as an energy metabolite in the brain. Lactate has been shown to play a role in long-term potentiation and as a signalling molecule. However, it's role as an energy substrate in the brain still isn't fully appreciated as highlighted by the controversy surrounding the astrocyte lactate neuron shuttle hypothesis proposed in 1994 by Pellerin and Magistretti[1], which is still highly controversial today[2,3].

In this work the enzyme lactate oxidase (LOx) was immobilised onto the surface of a Pt cylinder electrode using dip adsorption. First P*o*PD was electropolymerised onto the surface of the electrode acting as in interference rejection layer as it has been well characterised in the literature for its ability to block AA, the principal electroactive interferent in the brain[4,5]. The other components of the composite design were also added using dip adsorption. Styrene (Sty) was used to immobilise the enzyme and as it is a liquid at room temperature it allows for a simple method of entrapment of the enzyme[6,7]. The sensor was then dipped into a solution containing the enzyme LOx which allows the electrochemical detection of lactate by producing H_2O_2. This was followed by dipping into a solution of polyethylenimine (PEI) which has been shown to increase enzyme immobilisation[8,9] by reducing the electrostatic repulsion between the enzyme substrate and biosensor components[10]. After which, the sensor was dipped in a mixed solution of bovine serum albumin and glutaraldehyde (BSAGlu), the glutaraldehyde acting as a crosslinking agent that is regularly applied in biosensor design[11]. The incorporation of the lysine rich BSA prevents the GA from over crosslinking the enzyme and increases the sensitivity of the sensor[7] by retaining more active enzyme. Finally, a layer of cellulose acetate (CA) was added, which acts as a diffusional barrier increasing the K_M and as a result the linear range (sensitivity) of the biosensor. This dip adsorption process resulted in the following biosensor design:

Pt-P*o*PD-Sty-(LOx-PEI-BSAGa)$_{10}$-Sty-(LOx-PEI-BSAGa)$_{10}$-CA

The design originally used 100 mg of LOx and showed high sensitivity (0.88 ± 0.08 nA/μM). The calculated kinetic parameters were V_{MAX} = 493 ± 18.8 nA and K_M = 248 ± 15.4 μM, indicating sufficient sensitivity for reliable lactate detection *in vivo*. As the brain has a wide range of potential electroactive interferents, with ascorbic acid being the one of most concern due to its high μM concentrations[12], AA calibrations were performed to ensure the P*o*PD layers ability to eliminate interference. To further prove the biosensors signal was free from any ascorbate initiated homogeneous interference lactate calibrations were performed in 500 μM AA and showed no significant difference compared to normal lactate calibrations. However, the 100 mg LOx had a fatal flaw, due to the large amount of enzyme used to fabricate the biosensor it was found to be compromised by O_2 interference and consequently was unlikely to function reliably in the brain.

This problem was overcome by reducing the amount of enzyme used in the solution for dip adsorption from 100 mg to 1 mg. This solved the problem of O_2 dependence while still maintaining sufficient sensitivity (0.24 ± 0.01 nA/μM) and good enzyme kinetic parameters (V_{MAX} = 153 ± 14 nA and K_M = 428 ± 99 μM). This sensor was then tested against a comprehensive range of potential interferents found in the brain. It showed excellent interference rejection against the range of species tested with AA showing the highest response of ca. 3 % of the lactate signal. Once the sensor had shown the ability to provide an interference free signal it was then tested to ensure signal integrity over a variety of biological conditions that it would be exposed to in the brain. Physiologically relevant pH (7.2, 7.4 and 7.6) and temperature (34 - 40 °C) changes had minimal effect on the biosensor performance. As previously mentioned, the brain is a harsh environment filled with electroactive interferents, however, it also consists of electrode poisons, and surface modifying agents such as surfactants and electrocatalysts[13]. In order to test the effect of these on the sensor's signal it was placed in wet brain tissue and stored at 4 °C for two weeks. This had no effect on the sensitivity (LRS) of the biosensor. There was also no significant decrease in sensor response following dry storage at 4 °C. The biosensor showed a low μM limit of detection and a slightly longer than expected response time. However, *in vitro* response times have been shown to not be indicative of those found *in vivo* and this was validated for the lactate biosensor in subsequent *in vivo* experiments. DAS was investigated as a potential means of increasing the K_M

of the biosensor but was not successful. It did however result in a significant increase in sensitivity which warrants further investigation.

Given that the sensor maintained signal integrity across the variety of target environment physiological conditions tested it was decided to characterise the biosensor *in vivo*. Initial testing with vehicle (0.9 % normal saline) showed a brief increase which was attributable to injection stress. Systemic administration of lactate resulted in no change in signal, presumably due to lactate having slow kinetics crossing the blood brain barrier under basal conditions[14]. Reverse microdialysis was then employed to increase lactate concentrations in the local area surrounding the biosensor to confirm its ability to monitor lactate changes *in vivo*. This resulted in a clear response to lactate. Systemic administrations of ascorbic acid and chloral hydrate suggest minimal interference from physiological levels of potential endogenous electroactive interferents, and changing O_2 concentrations, although appropriate spacing of implanted sensors is important to eliminate H_2O_2 crosstalk, particularly when using blank sensors. While analysis of baseline stability over several days following implantation revealed an initial drop in sensitivity which subsequently stabilises, it was found that the biosensor does respond rapidly to behavioural activation and offers significant advantages over microdialysis.

In summary, this body of work reports the successful *in vitro* and *in vivo* validation of a lactate biosensor developed to monitor neurochemical levels of lactate. Future work will include further investigation into the effect of dialdehyde starch on the biosensor's performance factors, and targeted pharmacological studies to investigate brain metabolism and the ALNSH.

6.2. References

(1) Pellerin, L.; Magistretti, P. J. Glutamate uptake into astrocytes stimulates aerobic glycolysis: a mechanism coupling neuronal activity to glucose utilization. Proceedings of the National Academy of Sciences **1994**, 91 (22), 10625-10629.

(2) Chih, C. P.; Roberts, E. L., Jr. Energy substrates for neurons during neural activity: a critical review of the astrocyte-neuron lactate shuttle hypothesis. Journal Cereberal Blood Flow and Metabolism **2003**, 23 (11), 1263-1281.
(3) Pellerin, L.; Magistretti, P. J. Sweet sixteen for ANLS. Journal Cereberal Blood Flow and Metabolism **2012**, 32 (7), 1152-1166.
(4) Killoran, S. J.; O'Neill, R. D. Characterization of permselective coatings electrosynthesized on Pt–Ir from the three phenylenediamine isomers for biosensor applications. Electrochimica Acta **2008**, 53 (24), 7303-7312.
(5) Ryan, M. R.; Lowry, J. P.; O'Neill, R. D. Biosensor for neurotransmitter L-glutamic acid designed for efficient use of L-glutamate oxidase and effective rejection of interference. Analyst **1997**, 122 (11), 1419-1424.
(6) O'Brien, K. B.; Killoran, S. J.; O'Neill, R. D.; Lowry, J. P. Development and characterization in vitro of a catalase-based biosensor for hydrogen peroxide monitoring. Biosensensors and Bioelectronics **2007**, 22 (12), 2994-3000.
(7) Baker, K. L.; Bolger, F. B.; Lowry, J. P. Development of a microelectrochemical biosensor for the real-time detection of choline. Sensors and Actuators B: Chemical **2017**, 243, 412-420.
(8) Reybier, K.; Zairi, S.; Jaffrezic-Renault, N.; Fahys, B. The use of polyethyleneimine for fabrication of potentiometric cholinesterase biosensors. Talanta **2002**, 56 (6), 1015-1020.
(9) McMahon, C. P.; Rocchitta, G.; Serra, P. A.; Kirwan, S. M.; Lowry, J. P.; O'Neill, R. D. The efficiency of immobilised glutamate oxidase decreases with surface enzyme loading: an electrostatic effect, and reversal by a polycation significantly enhances biosensor sensitivity. Analyst **2006**, 131 (1), 68-72.
(10) McMahon, C. P.; Rocchitta, G.; Kirwan, S. M.; Killoran, S. J.; Serra, P. A.; Lowry, J. P.; O'Neill, R. D. Oxygen tolerance of an implantable polymer/enzyme composite glutamate biosensor displaying polycation-enhanced substrate sensitivity. Biosensensors and Bioelectronics **2007**, 22 (7), 1466-1473.
(11) Rothwell, S. A.; Killoran, S. J.; O'Neill, R. D. Enzyme immobilization strategies and electropolymerization conditions to control sensitivity and selectivity parameters of a polymer-enzyme composite glucose biosensor. Sensors **2010**, 10 (7), 6439-6462.

(12) Brown, F. O.; Lowry, J. P. Microelectrochemical sensors for in vivo brain analysis: an investigation of procedures for modifying Pt electrodes using Nafion®. Analyst **2003**, 128 (6), 700-705.
(13) O'Neill, R. D. Sensor–tissue interactions in neurochemical analysis with carbon paste electrodes in vivo. Analyst **1993**, 118 (4), 433-438.
(14) Knudsen, G. M.; Paulson, O. B.; Hertz, M. M. Kinetic analysis of the human blood-brain barrier transport of lactate and its influence by hypercapnia. Journal of Cerebral Blood Flow and Metabolism **1991**, 11 (4), 581-586.